UV Photoinduced Dynamics of Conformer-Resolved Aromatic Peptides

Satchin Soorkia, Christophe Jouvet, Gilles Grégoire

UV Photoinduced Dynamics of Conformer-Resolved Aromatic Peptides

Satchin Soorkia,[1] Christophe Jouvet[2] and Gilles Grégoire[1,]*

[1] Institut des Sciences Moléculaires d'Orsay (ISMO), CNRS, Univ. Paris-Sud, Université Paris-Saclay, F-91405 Orsay, France

[2] CNRS, Aix Marseille Université, PIIM UMR 7345, 13397, Marseille, France

ABSTRACT

A detailed understanding of radiative and nonradiative processes in peptides containing an aromatic chromophore requires the knowledge of the nature and energy level of low-lying excited states that could be coupled to the bright $^1\pi\pi^*$ excited state. Isolated aromatic amino acids and short peptides provide benchmark cases to study, at the molecular level, the photoinduced processes that govern their excited state dynamics. Recent advances in gas phase laser spectroscopy of conformer-selected peptides have paved the way to a better, yet not fully complete, understanding of the influence of intramolecular interactions on the properties of aromatic chromophores. This review aims at providing an overview of the photophysics and photochemistry at play in neutral and charged aromatic chromophore containing peptides, with a particular emphasis on the charge (electron, proton) and energy transfer processes. A significant impact is exerted by the experimental progress in energy- and time-resolved spectroscopy of protonated species, which leads to a growing demand for theoretical supports to accurately describe their excited state properties.

CONTENTS

1. Introduction

Photochemistry and photophysics are at the heart of the interaction between light and molecules, and reveal a particular importance for biological systems, as evidenced for instance in the photosynthesis of green plants or the photostability of DNA. Fascinating developments in this field is fueled by applications for biomedical imaging based on fluorescent proteins (FP). The unique properties of green fluorescent protein (GFP)[1–4] have revolutionized many areas in the life sciences by enabling in vivo observations of proteins localization and interactions. The field of fluorescent proteins of GFP family is covered by excellent recent reviews and we shall refer the interested reader to them.[5–11] The photoinduced process is initiated by the absorption of a single photon by a UV chromophore, allowing the promotion of the system from the ground, stable state to an electronic excited state. Regarding applications in biology, it is worth mentioning that the knowledge of the initial dynamics of the excited chromophore is crucial to the possible control of a chemical reaction. It has generally been accepted that the photolytic degradation of peptides and proteins proceeds by interaction involving residues of cysteine and the aromatic amino acids and support for this has been deduced from studies of ultraviolet spectra. It is indeed the aim of this review to provide the description of the photochemistry and photophysics involved in the nonradiative deactivation processes at play at the molecular level in amino acid building blocks and short peptides. In comparison to the ground state reactions, excited state processes are much more complex with many competitive deactivation pathways such as radiative and non-radiative transitions, intersystem crossing (ISC), charge (electron/proton) transfer, energy transfer and photofragmentation. One of the most fascinating

aspect of the photochemistry of biomolecules is the high sensitivity of the chromophore subunit upon the local environment, where intra- and inter molecular interactions can drastically disturb its intrinsic properties. At the molecular level, a good description of the excited states Potential Energy Surfaces (PESs) is the starting key point for the understanding of the photoinduced processes. We won't specifically address in this review all the challenges of the computation photochemistry. Among them, the multi configurational character and non-adiabatic behavior of the excited state dynamics have very recently been reviewed in this journal.[12–14] It should be stressed here that while many theoretical works have been devoted to the electronic properties and nonradiative deactivation processes in nucleic acids and DNA strands,[15–17] computational studies focusing on the excited state properties of amino acids and peptides containing aromatic residues have attracted less attention. We have restricted this review to gas phase spectroscopic studies of relatively small molecular species. A deep understanding of the photophysics of peptides indeed requires an optimal degree of control of the initial and final states of the reaction, which can be achieved in the gas phase through the combination of mass spectrometry with laser spectroscopy on conformer-selected molecular systems.

The study of biomolecular conformation in the gas phase has attracted great attention thanks to the advent of matrix-assisted laser desorption ionization (MALDI)[18] and electrospray ionization (ESI)[19] sources coupled to mass spectrometer. Mass spectrometry has indeed many attractive features for studying peptides, such as isolation of bare, unsolvated ions, mass- and charge-selection, and a set of methods available for obtaining conformational information. Some methods can be considered as passive: hydrogen-deuterium exchange,[20–22] (non)-covalent tagging of biomolecules based on surface accessibility of specific moieties,[23,24] ion mobility mass spectrometry which indirectly measures the cross section that relies upon the global shape of the peptide.[25–27] Other techniques are active, in which an external excitation such as collisions with rare buffer gas[28,29] or electron attachment[30–32] lead to fragmentation.

More recently, optical spectroscopy has emerged both in the infrared[33–35] and ultraviolet[36–39] ranges. One of the great advantages of such optical methods is the control of the deposited energy and the localization of the initial excitation.

We will restrict our review on relatively small systems following a bottom-up approach, in which the parameters of the photochemistry are, preferably and ideally, controlled. As in any photoreaction, the entrance, exit channels and the energetic must be properly defined. Among these parameters, the charge state, the initial internal energy, the UV wavelength and the number of absorbed photons can be accurately determined. Ideally, the investigated molecules should adopt a well-defined 3-D structure in order to reveal the influence of the local interactions upon the photophysical properties. This is clearly one of the most challenging experimental conditions to fulfill, even in the gas phase. For these floppy biomolecules with low-frequency modes, cooling techniques as supersonic expansion for neutral and cryogenic ion traps for ionic species coupled with laser spectroscopy are required to record well-resolved spectroscopic data that can thus be directly compared to quantum chemistry calculations. In time domain, when several time constants are observed, it is crucial to know that only one well defined species is excited to differentiate between conformers having specific properties or if the different time constants are associated to separate relaxation pathways.

In this review, we will focus on fundamental concepts in excited state properties of aromatic chromophores at play in the photoinduced processes in peptides. Starting from the bare UV chromophores of the amino acid building blocks (section 2), we will underline the role of the coupling of different electronic excited states with the locally excited $^1\pi\pi^*$ state on the deactivation mechanisms. We will show how the basic picture of the photodynamics could be transposed to neutral amino acids and short peptides (section 3). This will serve as ground for investigating chemical processes as photodissociation triggered by electron and proton transfer of protonated molecules (section 4) and protonated peptide chains (section 5). We finally focus

on electronic energy transfer processes in bi-chromophore systems (section 6). We conclude with general remarks and an overview of future prospects.

2. The $^1\pi\sigma^*$ state: a paradigm for nonradiative decay in aromatic chromophores

The excited state dynamics of the aromatic amino acid chromophores (benzene, phenol and indole) has been investigated in great detail and the main outcomes are summed up in this chapter. As it will be seen, the excited state dynamics of the aromatic amino acids is governed both by its chromophore properties and by the interaction of the locally excited chromophore with the side chain amino acid. The overall description of the model (see Figure1) can be found in the paper of Sobolewski, Jouvet and coworkers.[40] The authors state that "*The combined results of ab initio electronic-structure calculations and spectroscopic investigations of jet-cooled molecules and clusters provide strong evidence of a surprisingly simple and general mechanistic picture of the nonradiative decay of biomolecules such as nucleic bases and aromatic amino acids. The key role in this picture is played by excited singlet states of $\pi\sigma^*$ character, which have repulsive potential-energy functions with respect to the stretching of OH or NH bonds. The $^1\pi\sigma^*$ potential-energy functions intersect not only the bound potential-energy functions of the $^1\pi\pi^*$ excited states, but also that of the electronic ground state*". The S_1 surface typically exhibits a local minimum of $^1\pi\pi^*$ character in the vicinity of the equilibrium geometry of the ground state. The second excited state is a dissociative $^1\pi\sigma^*$, which induces a barrier on the S_1 surface, which separates the local $^1\pi\pi^*$ minimum from the Conical Intersection (CI) with the $^1\pi\sigma^*$ state. The excited state lifetime is governed by the tunneling through the barrier from the $\pi\pi^*$ to $\pi\sigma^*$ states.[41,42] This barrier is also responsible for pronounced isotope effects on the fluorescence lifetime and quantum yield.[40,43,44] The $\pi\sigma^*$ state crosses at longer distance the ground state leading to a second CI. Classically, at this point, the H atom can pursue on the $\pi\sigma^*$

potential curve and will have quite high kinetic energy, or be trapped on the ground state surface leading to a hot molecule which undergoes statistical evaporation of the H atom. From the theoretical point of view, the potential energy surfaces calculated by different methods are quite similar and vary only on details.[40,45–49]

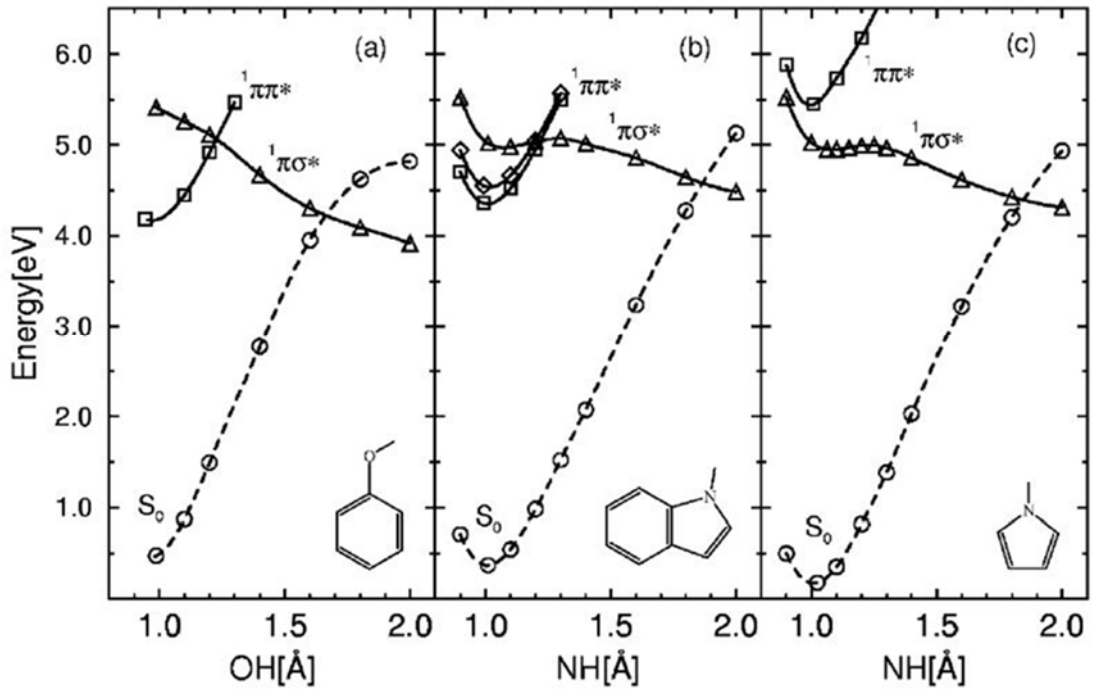

Figure 1. Potential Energy (PE) profiles of the lowest $^1\pi\pi^*$ states (squares and diamonds), the lowest $^1\pi\sigma^*$ state (triangles) and the electronic ground state (circles) as a function of the OH stretch (phenol) or NH stretch (indole, pyrrole) reaction coordinate. Geometries have been optimized in the excited electronic states at the CASSCF level; the PE profiles have been obtained with the CASPT2 method. Reproduced with permission from ref 40. Copyright 2002 The Royal Society of Chemistry.

2.1. Phenol chromophore

The H atom loss dissociation in photo excited phenol has been well characterized by the measurements of the kinetic energy of the H atom. A bimodal distribution is observed. For the

fast H atoms, the kinetic energy reflects the vibrational progression in the remaining PhO• along the out of plane vibration (out of plane vibrations are necessary in order to couple the ππ* and the πσ* states which have a different symmetry).[50–52] Such a well-defined and structured kinetic energy distribution is characteristic of bond rupture on a dissociative potential. The detection of the PhO• radical by VUV ionization is also a demonstration of the H loss process.[53] The second component of the distribution, the slow H atoms, is assigned to a statistical fragmentation which occurs after Internal Conversion (IC) following the crossing of the πσ* and ground states. By measuring both the picosecond transients of parent and fragment and the total translational energy distribution of products as a function of the reaction time, it was evidenced that both the slow and fast components of the H fragment have the same tunneling origin and that the ground state is populated at the second πσ*-S_0 crossing and not through a direct ππ*-S_0 IC process.[54]

Using picosecond laser, a complete survey of the evolution of the excited lifetime of phenol as a function of the excess energy has shown that the lifetime changes from 2 ns at the band origin 0_0^0 to 600 ps at 3500 cm^{-1} above.[54,55] These surveys show that the excitation of A" symmetry vibrational levels in the S_1 state shortens the lifetime, mainly through S_1-S_2 vibronic coupling. At high energy, the direct excitation of the πσ* state leads to a very fast dynamics of about 150 fs at 207 nm (excess energy of 12 000 cm^{-1}).[56,57]

Basically the whole concept developed in 2002 by Sobolewski and coworkers has been shown to be correct. An alternative model neglecting the tunneling mechanism, proposed by Ashfold and collaborators[58] has been dismissed since. Experimentally, the H-atom transfer mechanism was somehow fortuitously evidenced by trying to characterize the excited state proton transfer in Phenol-$(NH_3)_n$ clusters.[59–63] It was found that the reaction was indeed an H transfer by detection of NH_4 radical clusters[64–66] and supported by ab-initio calculations.[67] It appears only

very recently that the excited state proton transfer was in fact responsible for the lowering of the barrier height and for the acceleration of the H transfer as the size of the ammonia cluster increases.[68,69]

The role of the initial excitation of the OH vibration has been investigated by looking at the energy distribution of the fragments.[70] Dissociation of phenol with an initially excited O–H stretching vibration produces significantly more fragments with low recoil energies than does one-photon dissociation at the same total energy, implying that one quantum in the OH stretch mode induces more fragmentation through the statistical fragmentation in the ground state.

This system has become a textbook example to test different theoretical methods for the excited state dynamics such as quantum wave packet propagation method[45,71] or multistate semi classical trajectory method.[49] Xu clearly confirms that hydrogen tunneling is the main reaction mechanism of phenol photodissociation at the 0_0^0 band origin and agrees with experiments for the bimodal nature of the kinetic energy spectra for the photodissociation of phenol. They also show that the low kinetic energy release is due to both statistical dissociation to ground state and direct dissociation to the first excited state of the phenoxyl radical. Experimentally, the translational energy distributions and branching ratio of the phenoxyl radicals produced in the different electronic states have been reported.[72] It should be noticed that at very high energy (193 nm), the other channels such as OH, CO and H_2O losses have been detected, which are issued from statistical fragmentation occurring in the ground state.[73]

The excitation of phenol with a side chain reveals interesting side-chain size-dependent dissociation properties.[73,74] At 248 nm (5.17 eV), the photoexcitation of p-methylphenol, p-ethylphenol, and p-(2-aminoethyl) phenol shows that the decay of the excited phenyl ring is very different between these three molecules. For both p-methylphenol and p-ethylphenol, the major relaxation channel is through the coupling between the $\pi\pi^*$ and $\pi\sigma^*$ states leading to H atom elimination from a repulsive state. As the side chain changes from H, CH_3 or C_2H_5 to

$C_2H_4NH_2$, the dissociation properties change drastically implying a new channel, the C_α-C_β bond rupture (*vide infra*). The effect of the side chain is the increase of the S_1-S_0 IC rate and/or S_1-T_1 ISC rate which competes with the predissociation from the repulsive potential energy surface.

2.2. Benzene and phenyl chromophores

Radiationless processes from the $^1B_{2u}$ state of benzene in the range 245-260 nm involves ISC.[75–77] Predissociation (CH dissociation) does not seem to play a role in the nonradiative decay of the excited state. At higher energy (< 244 nm), the so called "channel 3" opens.[78] The fluorescence quantum yield is about 30% below the opening of "channel 3" and just below it, isomerization has been suggested.[79] At the opening of "channel 3", the excited state lifetimes become very short, in the order of hundreds of fs.[80,81] This is due to IC which occurs through a CI between the ground and first excited states in a geometry that lies along the reaction coordinate linking benzene and prefulvene biradical species with a non-planar geometry.[82,83]

More appropriate systems to the amino acids discussion is provided by substituted benzene such as toluene or alkyl benzene. Photoexcitation of alkylbenzenes at 248 nm (5 eV) leads to fragmentation, the main fragment coming from the C_α-C_β bond rupture leading to the benzyl radical $C_6H_5CH_2$ and its counterpart.[74] The translational energy distribution of the fragments were measured. Two distinct components have been observed. A slow one is due to dissociation after IC to the ground state and a fast component. The later one implies a late barrier and dissociation from a triplet state with an exit channel barrier following a two-step mechanism $S_1 \rightarrow T_1 \rightarrow S_0$. *Ab initio* calculations showed that the lowest triplet state is dissociative along the C_α-C_β bond through a barrier of 1.3 eV (~30 kcal/mol). Then, dissociation from the triplet state was the reasonable explanation for the $C_\alpha - C_\beta$ bond breaking with the fast kinetic energy component. In ethylbenzene and n-propylbenzene, the dissociation via the triplet channel characterized by the fast translational energy represents around 75% of the fragmentation

processes.[84] For larger molecules such as phenylethylamine, N-methyl-phenylethylamine, and N-acetyl phenylalanine methyl ester, the main fragmentation channel is still the C_α–C_β bond cleavage. However, as the size of the molecule increases, the contribution of the fast component in the translational energy distribution decreases, indicating that IC begins to dominate, due probably to the increase of the state density in S_0.[74]

2.3. Indole chromophore

Excited state dynamics of the indole chromophore is probably one of the most studied systems due to the strong variation of its fluorescence lifetime and emission wavelength with the environment, which is used to get information on the protein structure.[85–88] The electronic relaxation of the chromophore is governed by the interplay of at least three singlet electronic states along with the ground state: S_1 (L_b ππ*), S_2 (L_a ππ*), and S_3 (πσ*) (L_a and L_b from the Platt notations).[89] The oscillator strength from the ground to the ^1L_b state is weak with the transition dipole moment parallel to the long-axis. For the ^1L_a state, the transition moment is large and along the short-axis of the molecule. The (^1L_b ππ*) state has a low dipole moment (1.55 D), similar to the ground state (1.81 D), while the (^1L_a ππ*) one is high (6.07 D), more than three times larger with respect to the former.[90] In the gas phase, the ^1L_b state is the adiabatic minimum but due to its high dipole moment, the ^1L_a state becomes the fluorescent state in condensed phase.

Number of experimental[91–99] and theoretical[90,100–103] papers have studied the coupling and the relaxation of the L_a/L_b states. The L_b state is the first electronic state, its band origin being at 35 231 cm^{-1} (283.8 nm) with many vibronic bands observed up to ~271 nm (+1700 cm^{-1}). At shorter excitation wavelengths, the spectrum becomes increasingly unstructured due to the onset of excitation to the L_a state, its origin seems to be located close to 273 nm (+1500cm-1) although it has not been observed directly. The lack of observable vibronic structure in the L_a state may be attributed to its short lifetime due to the L_a/L_b relaxation.[96,97] A CI connecting the

L_b and L_a states, which can be accessed via different Herzberg–Teller active modes, is found approximately 2000 cm^{-1} above the L_b minimum.[97] Using time resolved dynamics,[98,99,104] the ultrafast IC of the L_a state toward the lower L_b minimum is detected at threshold energies, in the range of 1000/1500 cm^{-1} above the origin of the L_b. The 40 fs time constant measured points out the involvement of a CI, as predicted by calculations. At excitation wavelengths shorter than 263 nm (2800 cm^{-1} above the L_b minimum), the relaxation through the πσ* state in the hundreds of fs time scale is observed.

The role of the dissociation on the NH bond along the πσ* state has been evidenced both theoretically[90,101] and experimentally.[95,98,105–108] In stark contrast to phenol, the tunneling effect does not seem to be important in this molecule since the fast H atoms are not observed on the 0_0^0 band. The onset of a structured, high kinetic energy H atom elimination channel, attributed to direct dissociation on the πσ* state along the N-H coordinate, was observed at excitation wavelengths shorter than 263 nm (+2800 cm^{-1}).[107] However, it will be seen later that these nonradiative pathways does not seem to be the dominant processes in tryptophan (Trp).

3. Neutral aromatic amino acids and conformer-selected peptides

3.1. Tryptophan fluorescence: the rotamer model

The knowledge of the photophysical properties of fluorophores has become crucial in biochemical research by virtue of the extensive use of fluorescence spectroscopy to monitor unfolding transitions in proteins.[109,110] Among the three fluorescent amino acid constituents of proteins, tryptophan (Trp), and in a less extent tyrosine (Tyr), is the most popular probe, the contribution of phenylalanine (Phe) being negligible due to its very low absorption yield. The analysis of fluorescence decay of protein has been long and difficult especially in proteins with more than one Trp.[111,112] The spectroscopic properties of Trp are indeed quite complex, in particular the high sensitivity of the indole chromophore to the local environment. It is currently

admitted that in most of the proteins, Trp emission originates from the ^1L_a state of the indole chromophore.[113,114] Its large excited state dipole moment and ionic character result in large shifts due to electric field imposed by the protein and the solvent. Not only the magnitude but also the field direction determine the sign of the shifts relative to in vacuo experiments.[86] Fluorescence quenching by electron transfer to the backbone amide group has been invoked in Trp because it can easily donate an electron, which is directly related to its low ionization potential as compared to the other aromatic amino acids.[115] The coupling of the ^1L_a state with weakly emitting charge transfer (CT) states is highly sensitive to the electrostatic field imposed by the environment, which causes the large variability of fluorescence quantum yield, emission wavelength and lifetime.[116–118] In addition to fluorescence emission, the variation of the Trp fluorescence quantum yield (from nearly 0 to 0.35)[87,119,120] points out to the complex photophysics and nonradiative processes that compete with emission for deactivation of the excited state. These nonradiative processes include IC, ISC,[121] solvent quenching,[122] excited state proton transfer[123] and excited state electron transfer[121] with common quenchers of Trp fluorescence which are water molecules, peptide bonds and acid/basic amino acids.[85] For zwitterionic Trp in water, the protonated amino group seems to be key side chain group for excited state deactivation involving intramolecular proton transfer from NH_3^+ to the indole chromophore.[124,125]

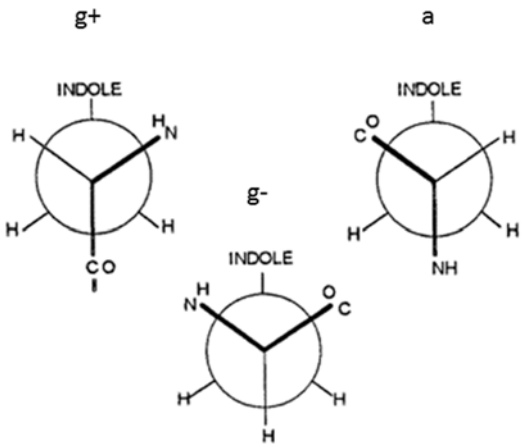

Figure 2. $\chi 1$ rotamers of the indole chain of Trp. The projections indicates the rotation of the indole group about the C_α-C_β bond. The χ_1=-60° (g-) is assigned to a lifetime component τ ranging from 2.7 to 5.5 ns, the χ_1=180° (a) rotamer with τ=0.5 ns.[126]

Although these processes are responsible for the dramatic variation of the Trp lifetime, they do not explain the existence of multiple lifetimes for a single residue. The most often suggested origin of the multi-exponential decay relies on the rotamer model of Trp, which states that ground state heterogeneity leads to different conformations with specific properties that do not interconvert on the time scale of the fluorescence lifetime.[127] These rotamers correspond to $2\pi/3$ rotation around the C_α-C_β bond, leading to different configurations of the alanyl side chain in reference to the indole chromophore (see Figure 2). Because the local environment of Trp can be disordered and quite complex in proteins with multiple ground state populations, Barkley and coworkers[126,128] have used a series of cyclic hexapeptides with rigid backbone to assign the three fluorescence lifetimes to the corresponding rotamers of the Trp side chain. Since in these cyclic peptides, the peptide bond is the only efficient quenching group,[121] a straight correlation can thus be made between Trp rotamers, excited state electron transfer rates and fluorescence lifetimes.

3.2. Intrinsic properties of gas-phase neutral aromatic amino acids and short peptides

3.2.1. The locally excited $^1\pi\pi^*$ state

As stated above, the complex photochemistry of Trp has been the subject of extensive investigations in the condensed phase, pointing out the role of solvent and local interactions which are still difficult to properly model. Understanding the behavior of isolated species in the gas phase, from single amino acids to short peptide chains, should in fact highlight their intrinsic properties without the effects due to the solvent. Besides, by studying cold molecules streamed in a cold molecular beam through laser spectroscopy techniques, one should be able to decipher the electronic properties of each individual conformers. However, only a few studies have focused on the electronic spectroscopy of neutral species, mainly due to the difficulties to evaporate these fragile molecules without degradation. The combined use of laser-desorption techniques with a supersonic expansion[129–131] leads to an efficient cooling that nevertheless enables conformational relaxation towards the lowest energy structures of the system but remains limited in size to few hundreds Dalton (Da).[132,133]

Levy and coworkers[134] first reported the dispersed fluorescence of cold, isolated Trp in the gas phase. Several conformers were observed that do not interconvert in the excited state during the fluorescence lifetime, in perfect agreement with the rotamer model. The different fluorescence patterns, in particular a broad, red-shifted emission observed only for a specific conformer, were qualitatively explained by relaxation of the locally excited state (^1L_b) towards a dark, low-lying state not accessible from the ground state. Besides, this particular conformer has the shortest fluorescence lifetime (10.4 ns) among all the conformers (12.9 ns).[135] The assignment of the broad, red-shifted emission has been subject to a long debate. Levy first suggested that this could be an indication of exciplex formation following charge transfer from the indole ring to the amino acid backbone. In the excited state, the zwitterionic form would result from proton transfer from the carboxylic to the amino groups through a small energy

barrier. This model was tested by looking at the deuterated species, which indeed exhibits a less extensive exciplex formation by a factor of 1.8, consistent with a slower tunneling rate upon deuteration. Several Trp derivatives were further investigated showing that both the amine and acid groups are necessary for the observation of the red-shifted emission.[136,137] However, the existence of a zwitterionic form in the excited state of bare Trp, in absence of solvent environment, raised several issues, in particular the large amount of energy required to stabilize this state. It was proposed an alternative mechanism based on an excited state perturbation through a dipole-dipole interaction between the amino acid backbone and the indole ring, switching the ordering of the ^1L_a and ^1L_b states.[138] Such interaction depends on the amplitude, distance and relative orientation of the dipole moments that varies from one conformer to the others, leading to relative shifts of the dipolar S_2 (^1L_a) state compared to the S_1 (^1L_b) state. Ten years later, Snoek et al.[139] provided a qualitative evaluation of the dipole-dipole interactions between the glycine side chain and the indole ring that did not support the initial suggestion of the $^1L_a/^1L_b$ state switching. The authors finally proposed that the broad, red-shifted emission reflects the unresolved vibronic activity of one specific conformer.

Ab initio calculations[140,141] confirm that the locally excited ^1L_b state has the lowest vertical excitation energy. However, to the best of your knowledge, geometry optimization of the excited states ($^1\pi\pi^*$, $^1\pi\sigma^*$, $^1n\pi^*$) of bare Trp has never been reported. More experimental and theoretical works have been devoted to tryptamine (Tryp), a close analogue of Trp by decarboxylation. High-resolution ultraviolet spectroscopy along with *ab initio* excited state geometry optimization have unequivocally demonstrated that the ^1L_b state is the adiabatic S_1 state for all the conformers, the origin of the ^1L_a state being predicted few hundreds wavenumbers higher in energy.[142–144] However, the close vicinity of the two excited states causes an efficient mixing with a CI not far above the minima of the two states.

3.2.2. The $^1\pi\sigma^*$ state of the heteroaromatic chromophores

According to the seminal work of Sobolewski and Jouvet,[40] the photophysical properties of these heteroaromatic amino acids containing an O-H/N-H bond should be influenced by a third, dissociative $^1\pi\sigma^*$ excited state (see section 2.3). In tryptamine,[136,145] tryptophan[131] and tyrosine,[146] the electronic spectra of all conformers are sharp, extend at least one thousand wavenumbers above the band origin with no sign of efficient deactivation process in the vicinity of the minimum of the locally excited $^1\pi\pi^*$ state. The first experimental evidence for the existence of the $^1\pi\sigma^*$ state was provided by the complete absence of indole NH stretch band in the IR spectrum of the S_1 state in tryptamine.[95] Instead, a broad absorption appeared, ascribed to the strong coupling of the ^1L_b state NH stretch (v=1) level to the $^1\pi\sigma^*$ state, dissociative along the NH bond. H-atom elimination dynamics from tyrosine, p-ethylphenol and tyramine following excitation at 200 nm, almost 2 eV above the band origin, was investigated by Iqbal and Stavros.[147] The analysis of the total kinetic energy release (TKER) spectra of these three molecules derived from the time-resolved H^+ velocity map images confirms that H-atom elimination is mediated by the $^1\pi\sigma^*$ state of the phenolic O-H site rather than from the O-H/N-H groups of the amino acids backbone. At this excitation energy, the time constants associated to the H-atom release were found on the order of 100 fs or less. Ovejas et al.[148] reported the relaxation channels of Trp using fs pump-probe ionization at different excitation energies, from the band origin up to 220 nm (see Figure 3). The signal transients showed different time scales that depend on the excitation wavelength. At the band origin (287 nm), a nanosecond relaxation time is observed, ascribed to the ^1L_b lifetime. At 280 nm, an ultrafast time constant of about 50 fs was assigned to ^1L_a-^1L_b IC while at wavelengths shorter than 272 nm, a third time constant of 200-300 fs was extracted and assigned to the dynamics on the $^1\pi\sigma^*$ potential energy surface along the indole N-H coordinate, as already observed in the bare indole chromophore.[104]

Finally, excitation at wavelengths shorter than 250 nm revealed an ultrafast sub-50 fs lifetime not present in indole which was thus ascribed to relaxation via excited states localized on the amino acid backbone.

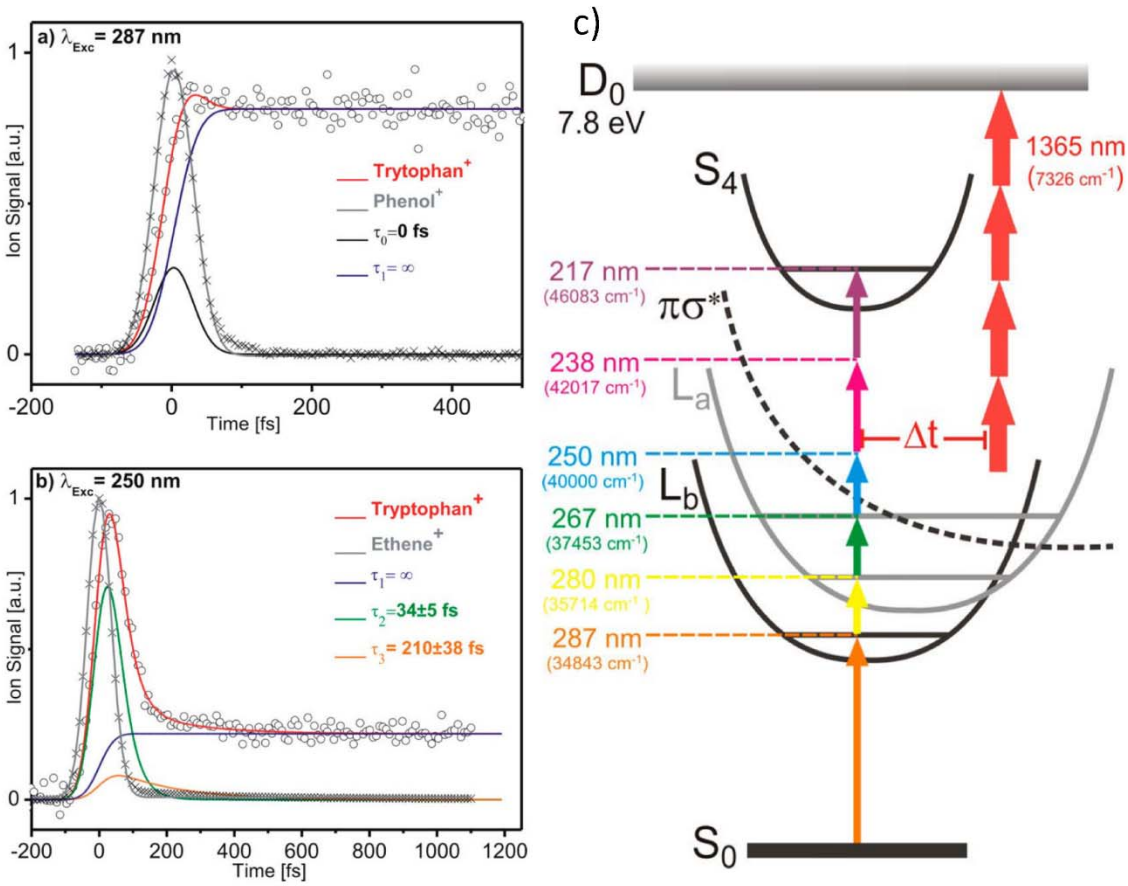

Figure 3. a) and b) Trp photoionization transients recorded at two different excitation wavelengths with individual exponential components of the fitting. c) Schematic representation of the pump-probe wavelengths used by Ovejas et al.[148] together with the electronic structure of Trp. Adapted with permission from ref 148. Copyright 2013 American Chemical Society.

3.2.3. The influence of locally excited states of the peptide backbone

Capped aromatic amino acids provide the simplest molecular systems to highlight the role of excited states localized on the peptide backbone on the photophysics of aromatic amino acids

containing peptides.[149] N-acetyl tryptophan amide (NATA) and N-acetyl tryptophan methyl amide (NATMA) were studied by Zwier and coworkers through laser-induced fluorescence[150] and fluorescence-dip infrared spectroscopy.[95] These peptide mimics can adopt two kinds of conformation, an extended, β-like peptide backbone structure (C_5) or a folded, γ-turn type (C_7 H-bond between the amide NH and CO carbonyl).[151] In such systems, the H-bonding interaction between the amide NH group of one residue and the carbonyl CO group of another residue not only dictates the conformational preferences but also influences the photophysical properties of the peptides. First, the excitation spectrum of the C_5 structures show well-resolved vibronic transitions while the C_7 conformers are characterized by a highly congested spectra involving a long progression of low frequency modes extending several hundred wavenumbers to the red of the band origin, suggesting that the locally excited $^1\pi\pi^*$ state decays towards a second, low-lying state. Second, in all conformers are missing the indole NH stretch transition in the IR spectra of the locally excited $^1\pi\pi^*$ state, as already observed for tryptamine. This finding points out to the coupling of the $^1\pi\pi^*$ NH_{ind} (v=1) state with the predissociative $^1\pi\sigma^*$ state. Finally, for the C_7 conformers, all the infrared transitions are washed out in the excited state, replaced by a broad, unresolved background absorption. The authors suggested that the broad congested spectra of the γ-turn conformers are indicative of a switch in the ordering of the ^1L_b with the $^1L_a/^1\pi\sigma^*$ states. Without theoretical support, it was rather difficult at that times to decipher the exact nature of the low-lying excited states.

In order to theoretically investigate the role of hydrogen bonds on the electronic properties of short peptides, the photochemistry of small polyglycines was first studied by Sobolewski and Domcke.[152] Small polyglycine peptides (trimer and pentamer) provide the smallest molecular models of β-turn (C_{10} type HB) and α-helix (C_{13} type HB), respectively. The authors showed that two electronically excited states are at play in the photophysics of these peptides. First, a

locally excited (^{1}LE,^{1}nπ^*) state involves the excitation from the nonbonding (n) orbital of the hydrogen-bonded carbonyl group to an antibonding molecular orbital localized on the same branch of the backbone. Second, a charge transfer (^{1}CT) state, which corresponds to electronic excitation from the amide to the carbonyl involved in the H-bond. This ^{1}CT state is strongly stabilized by proton transfer from the amide to the carbonyl and crosses the ^{1}LE state and the S_0 ground state in the course of the proton transfer reaction. Such photoinduced electron-driven proton transfer has also been invoked (CASSCF/PT2) in a model glycine dimer mimicking a β-turn motif found in protein.[153]

This nonradiative deactivation model has been proposed to explain the different excited state properties of the extended and folded conformers of NATMA.[154] The authors found that geometry optimizations (at the ADC2 level) of the lowest excited $^1\pi\pi^*$ states reversed the ordering of the ^1L_b and ^1L_a state, and that the C_7 conformer has the largest energy gap. The authors also locate the dissociative $^1\pi\sigma^*$ state along the indole NH stretch, which crosses the ^1L_b state not far above the indole NH stretching energy level, in agreement with the experimental findings. Besides, while the vertical excitation energies of the electronic states of the backbone are rather high in energy, they are strongly stabilized upon geometry optimization, becoming the adiabatic energy minimum of the S_1 state. The locally excited state of the backbone (^{1}LE) corresponds to an excitation from the nonbonding orbital to the π^* orbital of the peptide backbone (^{1}nπ^* transition) and lies only 1.7 eV or 1.2 eV above the ground state in the C_5 and C_7 conformers, respectively. In the γ-turn conformer, the barrier on the $^1\pi\pi^*/^1$LE reaction path is smaller by 0.1 eV compared to the extended conformer, which might thus explain the conformer selectivity experimentally observed. Finally, an additional reaction channel is energetically open from the ^{1}LE state only for the folded conformer that involves a proton transfer along the N-H···O=C C_7 H-bond triggered by the electron transfer to the

carbonyl. The proton transfer strongly stabilizes the charge transfer state (^{1}CT), in a structure with a small ^{1}CT/S_0 energy gap allowing efficient IC.

Short peptides containing a Trp residue (TrpGly, GlyTrp, TrpGlyGly)[129,155] or a phenylalanine residue (PheGlyGly, GlyPheAla)[156,157] were investigated by laser spectroscopy. As explained above, the photophysics of the indole chromophore by itself complicates the understanding of the nonradiative decays at play in peptides containing Trp. In phenylalanine, neither the ^1L_a/^1L_b state switching nor the $^1\pi\sigma^*$ state of the indole NH group are relevant to the photophysics, so the influence of the hydrogen bonds and secondary structure of the peptide backbone on the deactivation mechanism of the Phe residue can be investigated in an easier way. The vibronic spectra of these peptides can change drastically, showing either weak or dense vibrational progressions, as already observed in NATMA. Interestingly, all conformers which exhibit a strong hydrogen bond between the carboxylic acid group and the carbonyl of the peptide bond (γ-turn type) were not detected although being among the lowest energy structures. This raises the question of the potentially efficient radiationless decay processes which render the lifetime of the excited $^1\pi\pi^*$ states too short (sub-ps) to be probed through ns multiphoton ionization scheme (REMPI). This pitfall has already been documented in case of DNA bases for instance, for the first three lowest energy tautomers of guanine[158,159] or for selected conformations of DNA base pairs such as the Watson-Crick guanine-cytosine structure.[160] It could be stressed here that in the latter case, an electron-driven proton transfer process was already thought to be at play as proposed for the polyglycines.[152] Shemesh et al.[161] suggested that the same electron/proton transfer process could explain the unobserved conformer γ_L of GlyPheAla that exhibits a strong intramolecular H-bond.

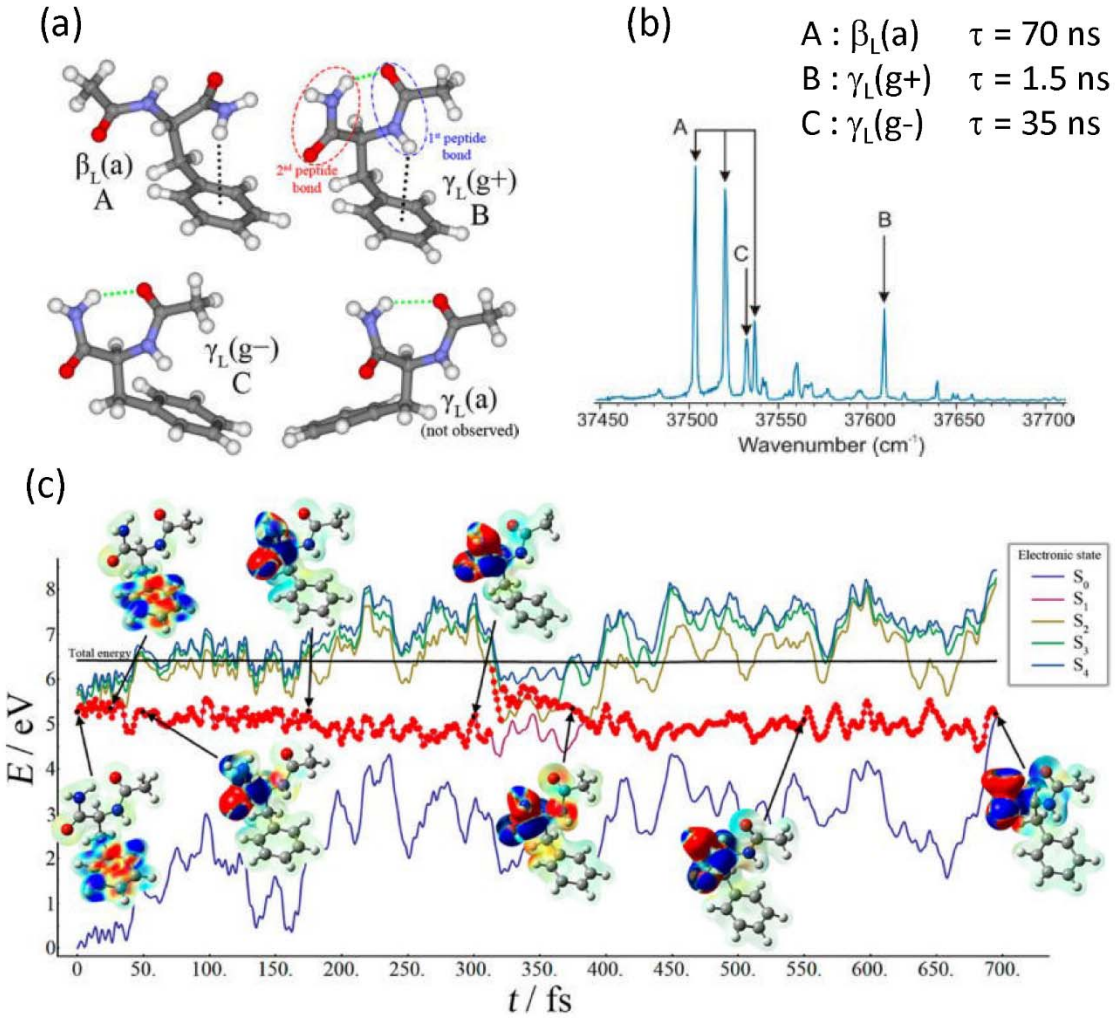

Figure 4. (a) Most stable conformer of NAPA. The label a/g-/g+ refer to the Phe χ_1 rotamer of the benzyl chromophore. (b) R2PI spectrum of NAPA in the region of the band origin of the first ππ* transition of the three observed conformers. (c) Time dependence of the potential energy of the ground (blue) and the excited states along a nonadiabatic trajectory involving nπ* excitation of the second peptide bond. Adapted with permission from ref 162. Copyright 2012 American Chemical Society.

In the tripeptides PheGlyGly and GlyPheAla mentioned above, the conformational heterogeneity is already quite large and some conformers are suspected to have too short excited

state lifetimes to be probed through ns laser spectroscopy. According to the previous study of Zwier et al. on NATA,[150] Mons and Ljubic[162–164] chose an isolated peptide chain model containing a Phe residue, N-Acetyl Phenylalanine Amide (NAPA) to explore the dynamics of the deactivation processes through a joint experimental and theoretical collaboration (see Figure 4). $^1\pi\pi^*$ excited state lifetimes were measured for the three lowest energy conformers through ns and ps REMPI spectroscopy. Interestingly, the folded γ_L(g+) conformer with a strong C_7 H-bond between the amide group and carbonyl group of the peptide bond has its lifetime (1.5 ns) reduced by a factor of 50 compared to the extended β_L(a) conformer (70 ns). The third conformer γ_L(g-), with the same C_7 H-bond but with another orientation of the benzyl residue (no NH-π bond between the amide peptide and the π cloud of the aromatic ring), has an intermediate lifetime of 35 ns.

Two main deactivation mechanisms have been deduced from the nonadiabatic simulations performed at the TD-DFT level to account for this conformer selected shortening of the excited state lifetimes and efficient IC to the ground state. The first one implies an H-transfer from the Phe NH to the ring triggered by an electron transfer from the ring. A rather large barrier of 0.48 eV is estimated at the CC2 level for the H-transfer, which might be compensated by the large zero point energy of the NH stretch mode. However, the absence of significant deuteration effect (Phe NH *vs* ND) in the lifetime of all conformers, in stark contrast to the phenol case (see section 2.1), dismisses such process. In the second mechanism, a nonadiabatic transition occurs from the initial $\pi\pi^*$ state to the $n\pi^*$ states of the first (localized on the N-acetyl group) or second (the $CONH_2$ group) peptide bonds. It should be noted that the $\pi\pi^*/n\pi^*$ CI is reminiscent of the first step of the seminal mechanism introduced by Soboleswki and Domcke for NATMA.[154] Geometry optimizations of the two $n\pi^*$ states have been performed at the CC2 level. These $n\pi^*$ states are found about 0.7 eV below the $\pi\pi^*$ minimum and are separated from the ground state

through small energy barriers, providing an efficient way for nonradiative processes. The barrier for the $^1\pi\pi^*/n\pi^*$ transition was predicted slightly lower for the γ_L conformers, in good agreement with the experimental findings. However, the question remained on which peptide bond is responsible for the efficient nonradiative deactivation of the initially excited $\pi\pi^*$. This has been disclosed by the same group of authors[165,166] by comparing the excited state properties of the vibrationless level (adiabatic transition) of NAPA and NAPMA (methyl amide). Experimentally, the excited state lifetime of γ_L(g+) NAPMA, in which the second peptide bond is methylated, is much longer (48 ns) than in NAPA (1.5 ns), which clearly does not support the involvement of the first peptide bond in the rapid deactivation process. Besides, they demonstrated that the accessibility to the $^1\pi\pi^*/n\pi^*$ CI of the second peptide bond strongly depends on the molecules, pointing out the effect of the zero point energy and enhanced rigidity of the terminal amide group of the $\pi\pi^*/n\pi^*$ transition. These experimental results and nonadiabatic dynamics simulations clearly emphasize the high sensitivity of the nonradiative deactivation processes to the backbone environment of the aromatic ring. Such rapid radiationless decay processes may be essential to rationalize the photostability of larger peptides and proteins under UV irradiation.[167]

4. Protonated aromatic amino acids: Charge does matter

While thermal or matrix assisted laser desorption (MALD) source cannot vaporize large neutral biomolecules without degradation, the advent of soft and efficient vaporization techniques such as electrospray ionization (ESI) has undeniably opened new opportunities for gas phase studies of fragile biomolecules. UV photofragmentation has become the most efficient method for studying the photochemistry of electronically excited biologically relevant molecules, according to the fact that fluorescence detection within an ion trap is much harder to set up (see section 6). The principle of the photofragment spectroscopy is rather simple: the

(resonant) absorption of a UV photon by the aromatic chromophore is detected by the apparition of photofragments at lower masses. While, from a spectroscopic point of view, the only adjustable and important parameter would be the laser wavelength, the full description and understanding of the photofragmentation mechanism should provide insights into the underlying photophysics of the deactivation process.

4.1. Protonated aromatic amines: the H loss, specific photofragmentation channel

Protonated tryptamine, an intermediate derived by decarboxylation of Trp, has provided a benchmark system for the understanding of the photoinduced process at play in this protonated aromatic molecules. Following 266 nm excitation, protonated tryptamine ($TrypH^+$ m/z 161) fragments by loss of H atom (m/z 160) along with its two secondary fragments at m/z 130 and 131 (C_α-C_β bond break) and ammonia loss (m/z 144). The excited state dynamics of $TrypH^+$ was recorded through a fs pump-probe photodissociation scheme.[168] The striking result was the ultrafast transient recorded only on the H loss channels (m/z 160, 130 and 131) with a time constant of 250 ± 50 fs, within the experimental time resolution of the fs lasers. The excited state potential energy surfaces (PESs) of protonated tryptamine were calculated at the coupled-cluster level CC2.[169] The excited state calculations have pointed out the role of the πσ* state dissociative along the NH stretch of the protonated ammonium group. This πσ* notation is somewhat not strictly exact since $TrypH^+$ doesn't have a Cs symmetry. If the π orbital refer to the plane of the chromophore, the σ* orbital is located on the NH_3^+ group and has a σ symmetry in the amino acid part. The coupling between the optically excited ππ* state and the πσ* state induces an electron transfer from the aromatic ring to the NH_3^+ group, resulting in the formation of a hypervalent, neutral radical species C_α-$NH_3^\bullet$, dissociative along the C_α-N and the N-H coordinates. The Minimum Energy Path (MEP) for the detachment of the hydrogen atom and for the elimination of ammonia directly in the excited state have been calculated at the CC2

level. For both cases, a small energy barrier in the excited state of 0.05 eV and 0.25 eV for H loss and ammonia loss, respectively, is predicted. Although the ammonia loss has a larger exothermicity than the H loss reaction, the higher energy barrier and the larger mass of the ammonia compared to the hydrogen atom is in agreement with the experimental observation of the H loss reaction in the excited state following 266 nm excitation. In the course of the H loss reaction, the πσ* energy surface crosses the electronic ground state, point where competition between direct dissociation in the excited state and hydrogen recombination and ammonia loss following IC occurs.

It should be stressed here that the H loss reaction channel, mediated by the dissociative $^1\pi\sigma_{NH3}$* state, was initially developed for substituted aromatic molecules such as phenol and indole (see sections 2.1 and 2.3). In protonated amino species, the dissociative $^1\pi\sigma$* state involves an electron transfer from the aromatic ring toward the protonation site (the NH_3^+ group of the amino acid) leading to an hypervalent (NH_4 like) moiety dissociative along the NH coordinate. So the main difference between protonated and neutral species is the coordinate of the dissociation asymptote of the ππ, ππ* and πσ* states. For the neutrals, the reaction leads to the $M^\bullet$ (radical) + H and for the protonated species, it leads to M^++H, as depicted in Figure 5.

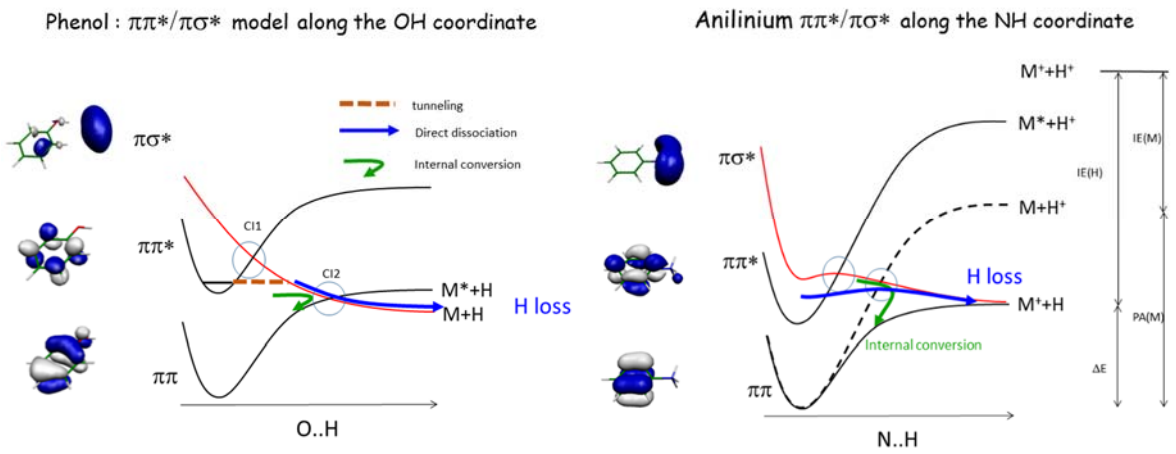

Figure 5. Comparison between the dissociation driven by the πσ* state in neutral molecule (phenol) and protonated one (anilinium).

A model based on the πσ*/ππ* energy gap has been proposed to explain the excited state dynamics of other protonated aromatic amines.[170] Depending on the length of the alkyl chain bearing the ammonium group, the photofragmentation pattern of protonated aniline, benzylamine and phenylethylamine drastically changes. In anilinium, the H loss channel is detected along with the ammonia loss at the band origin of the ππ*, while only the ammonia loss channel is open in protonated benzylamine. The competition between the H and NH_3 loss channels is determined by the ππ*/πσ* coupling and the crossing of the dissociative πσ* along the N-H stretch with the electronic ground state. The H and NH_3 loss reactions are related to the dynamics on the πσ* state reached from the locally excited state through a barrier. When the dissociation limit of the H loss reaction (M^+ + H) is lower than the 0_0^0 energy, then the H loss fragmentation channel is open, as observed and predicted for aniline and para-aminophenol. Otherwise, due to the exit barrier along the N-H stretch, an aborted H loss reaction occurs at the second πσ*/S_0 curve crossing resulting in IC and fragmentation in the ground state leading to the NH_3 loss.

For protonated phenylethylamine, the fragmentation channel changes abruptly within 500 cm^{-1} from the band origin, which clearly evidences that two competitive deactivation processes in the excited state exist. The C_α-C_β bond break channel is first open up to 500 cm^{-1} and then the fragmentation channel shifts to the NH_3 loss to be the only one 700 cm^{-1} above the 0_0^0 transition. By substituting the benzyl by a phenol chromophore, the overall picture of the photochemistry of protonated tyramine remains the same.[171] In these cases, the C_α-C_β bond break is triggered by a proton transfer to the ring, which can only occur when the length of the alkyl chain is long enough to insure an efficient overlap of the molecular orbitals centered on the ammonium and π cloud. The proton transfer reaction is further confirmed by the mass of the ionic fragments associated to the C_α-C_β bond cleavage, which bears an extra hydrogen as compared to the simple bond cleavage. This proton transfer reaction happens through a small barrier and competes with the ππ*/πσ* electronic coupling leading to the NH_3 loss channel after IC.

4.2. Protonated aromatic amino acids

4.2.1. Protonated tryptophan

Among the three naturally occurring aromatic amino acids, tryptophan has been the most studied owing to its high fluorescence yield and extreme sensitivity to the environment. The first photofragmentation experiments on protonated aromatic amino acids have thus been performed on protonated tryptophan ($TrpH^+$) almost at the same time by five independent groups. In the special issue "*bio-active molecules in the gas phase*" of PCCP in 2004,[172] Andersen et al.,[173] Kang et al.[174] and Nolting et al.[140] report the first UV photoinduced dissociation experiments on $TrpH^+$, followed by Talbot et al.[175] in 2005 and Boyarkin et al.[176] in 2006. The outcomes of the photophysics of $TrpH^+$ were indeed much more complex than expected. IC to the ground state was initially supposed to be the main deactivation mechanism

in competition with fluorescence. Indeed, the resonant photo fragmentation spectrum of $TrpH^+$, cooled at liquid nitrogen temperature in a Paul ion trap, is very similar to the absorption spectrum of the neutral, with the band origin around 285 nm, but somehow broader than expected at this temperature.[140] Interestingly, the electronic spectroscopy of $TrpH^+$ cooled at much lower temperature (6K) still shows a broad band origin although a well-resolved vibronic spectrum could be recorded for protonated tyrosine ($TyrH^+$) in the same conditions.[176] Complementary photo fragmentation results were obtained at 266 nm with the observation of a new fragmentation channel not detected at the band origin, the H atom loss leading to the formation of radical cation Trp^+.[174] The photo specific H loss channel, never detected in collision induced dissociation (CID) experiments where fragmentation occurs in the ground electronic state, points out the role of dissociative excited states in the deactivation mechanism of photo excited $TrpH^+$. A comprehensive photodissociation spectroscopy study done by Talbot et al.[175] confirmed that the branching ratio between the different fragmentation channels changes with the excitation energy in the excited state. In particular, the H loss channel opens 10 nm to the blue of the band origin and has a maximum intensity at 250 nm.

One of the unexpected results is the rather large number of fragmentation channels for such simple molecule within this given excess energy, around 4-5 eV: H loss (m/z 204), the C_α-C_β bond break (m/z 130 and m/z 132), NH_3 loss (m/z 188) and the formation of immonium ion m/z 159 ($CO + H_2O$ loss) are the primary fragmentation channels in competition. Other detected photofragments are secondary or tertiary fragmentation channels: m/z 130 from the radical cation Trp^+, m/z 170, m/z 146, m/z 144 and m/z 118 from m/z 188. A comprehensive understanding of the photochemistry of $TrpH^+$ has indeed been quite challenging, in part because these different primary fragmentation channels in competition are related to several deactivation pathways involving excited states of different electronic characters. Besides, the

solely detection of the ionic fragment of a given m/z is not unambiguously associated to a unique deactivation process, as revealed by the ion/neutral coincidence experiment.

Detecting in coincidence the ionic and neutral fragments using position and time sensitive detectors is a powerful means for a comprehensive understanding of the fragmentation mechanisms. The multi coincidence analysis allows to differentiate between direct (two fragments) or sequential (more than two fragments) fragmentation processes. In the case of a two-step process, the sequential order can also be precisely determined. Contrary to conventional mass spectrometry techniques based on the sole identification of the mass-to-charge ratio of the ionic fragments, this technique allows an additional indirect identification of the neutral fragment mass.

In the past decade, the strength of the multi coincidence technique has been demonstrated in the study of the photostability of numerous biomolecules in the gas phase.[177–184] Here, we take the example of the photoexcitation of $TrpH^+$ which leads to C_α-C_β bond breakage and production of ionic fragments with m/z 130, among other fragmentation channels. The latter ionic fragment was long considered as resulting solely from a two-step mechanism following H loss. The discrimination of fragmentation events occurring on different fragmentation time scales allowed to evidence the existence of two distinct deactivation pathways (see Figure 6) leading to the same m/z 130 ionic fragments. This fragment is produced either in a sequential or binary fragmentation as indicated in the schemes below:

Scheme (a): Step 1: m/z 205 → m/z 204 + H; Step 2: m/z 204 → m/z 130 + 74

Scheme (b): m/z 205 → m/z 130 + 75

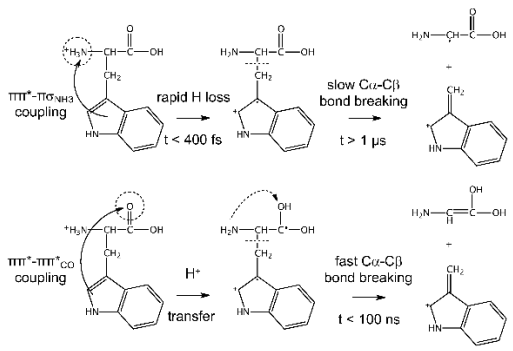

Figure 6. Two mechanisms associated to the m/z 130 photoproduct of $TrpH^+$ based on the ion/neutral coincidence experiment: (a) slow C_α-C_β bond breakage subsequent to H-loss and (b) fast C_α-C_β bond breakage subsequent to proton transfer to CO group of the carboxylic acid moiety.

In scheme (a), the coupling of the optically excited ππ* state and the πσ* state induces an electron transfer from the aromatic chromophore to the NH_3^+ group, as described earlier in the text. Rapid H atom loss leads to the formation of the m/z 204 radical cation, which produces m/z 130 with a decay time constant > 1 µs. In scheme (b), the coupling of the optically excited ππ* state and the $\pi\pi_{CO}$* state induces a proton transfer to the CO group, which triggers a fast binary fragmentation (C_α-C_β bond rupture), as corroborated by the VV plot (correlation between the speeds of the neutral and ionic fragments) of rapid m/z 130 fragment ions.[177] The interpretation of the fast C_α-C_β bond breakage was supported by calculations as due to the dissociation in the excited state after a concerted electron-proton transfer toward the carbonyl group in a comparative study of protonated tryptophan with tryptamine and protonated tyrosine with tyramine, *i.e.* in the presence or absence of the -COOH group, respectively (see Figure 7).[178] Events in the bottom right side of the two-dimensional plots of Figure 7 (a-d) are related to binary fragmentation occurring in less than 150 ns and are denoted as fast fragmentation. The striking point is that no fast fragmentation is observed for the decarboxylated amino acids.

Thus, UV photofragmentation studies with multi-coincidence detection of fragments resulting from C_α-C_β bond breakage unraveled the role of the -COOH group in the fast fragmentation process.

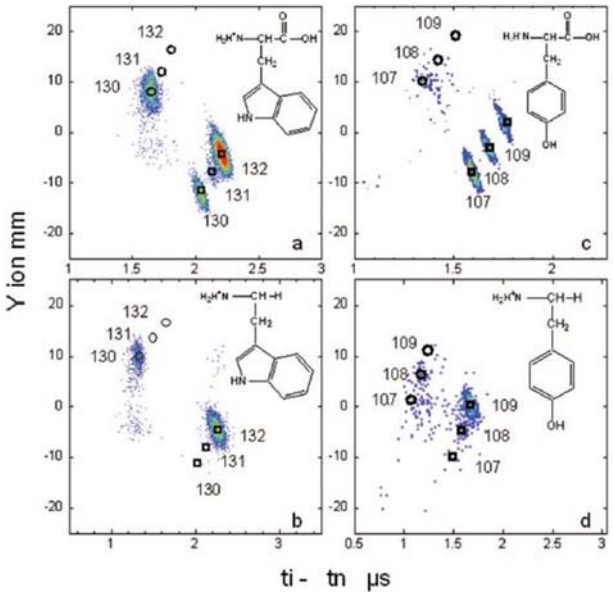

Figure 7. Two dimensional plots $N(t_i\text{-}t_n,y_i)$ for the four protonated molecules: (a) tryptophan, (b) tryptamine, (c) tyrosine, and (d) tyramine. The open squares indicate the calculated positions of the fragment ions issued from a fast fragmentation process. Only the m/z 130 are produced by a slow fragmentation (open circle) following secondary fragmentation of the tryptophan (a) and tryptamine (b) radical cations. Reproduced with permission from ref 178. Copyright 2008 American Institute of Physics.

The fragment at m/z 132, which was initially assigned to a secondary fragment of the immonium ion according to CID studies,[185] is in fact related to the proton transfer reaction from the ammonium group to the indole ring followed by the C_α-C_β bond cleavage. This ionic fragment, which had been unambiguously demonstrated to originate from the emission of a single neutral fragment of 73 Da,[177] is still present in the absence of the -COOH group. Hence,

regarding $TrpH^+$, one can conclude that the $\pi\pi_{CO}^*$ state is not involved in this fragmentation mechanism after photoexcitation. Regarding the mechanism, formation of m/z 132 fragments in $TrpH^+$ after C_α-C_β bond breakage in a binary fragmentation, has been rationalized as a hydrogen and proton transfer onto the indole chromophore moiety following UV excitation. Studies of supramolecular complexes with 18-crown-6 ethers can provide essential clues on proton driven fragmentation.[179,186] In such complexes, the crown ether is anchored onto the protonated ammonium group and prevents interaction between the latter group and the aromatic chromophore, as discussed further in this review article. The immediate effect is the absence of CID-like fragmentation after IC to the ground state, while C_α-C_β bond breakage is still observed but not through production of m/z 132 ions.

The excited state dynamics of $TrpH^+$ has been studying through the same pump-probe photodissociation scheme as for tryptamine.[187,188] A fast decay with two time constants of 400 fs and 15 ps are observed following excitation at 266 nm. The sub-picosecond lifetime suggests that the unresolved vibronic spectrum of $TrpH^+$ at the band origin (284 nm) may be due to lifetime broadening. This was rather surprising since the lifetime of the first excited state of neutral Trp is in the nanosecond range.[135] Although the presence of an excess proton barely shifts the band origin of the $^1\pi\pi^*$ excited state, it strongly affects the nonradiative deactivation process. Interestingly, the pump-probe photodissociation signals obviously change for each fragment (see Figure 8), i.e. the amplitude and sign of the pre exponential factors of the bi exponential decay function. In particular, the NH_3 loss channel is first depleted within the first 400 fs and then, its fragmentation yield increases during the second time scale of 15 ps.[188] This clearly evidences that one can control the fragmentation channels and branching ratio using suitable laser pulses (here at the femtosecond time scale) with the right delay between the pump and probe lasers. Besides, the fragment ion m/z 132 associated to the proton transfer to the ring and C_α-C_β bond break is the only channel insensitive to the probe laser. The absence of pump-

probe signal of one specific channel indicates that this latter fragmentation channel is not in competition with the other ones, neither in the excited state nor in the ground state.

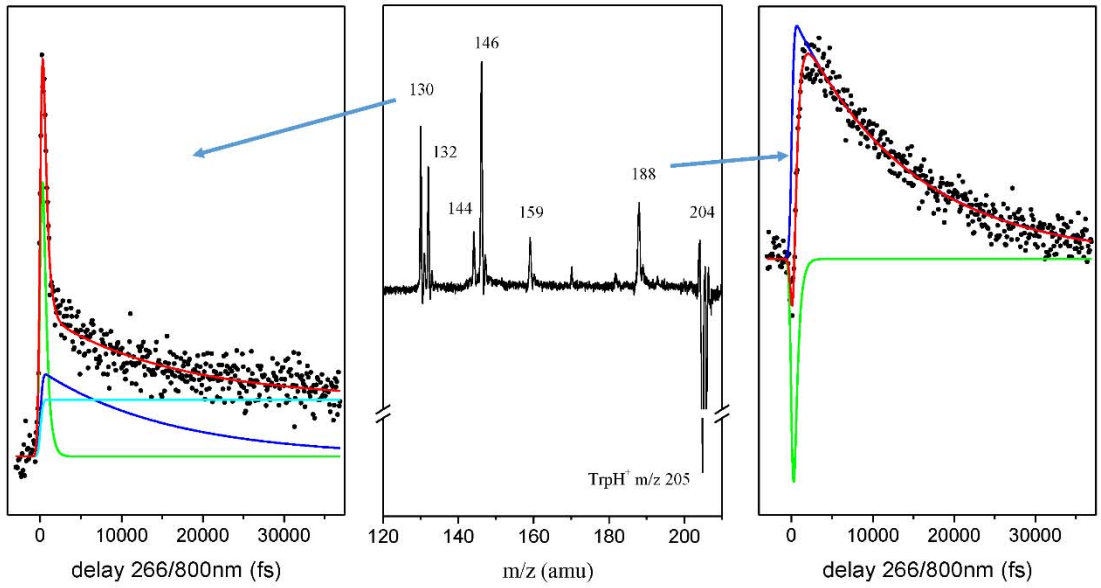

Figure 8. Time-resolved pump-probe photodissociation signals recorded on m/z 130 (C_α-C_β bond cleavage) and m/z 188 (NH_3 loss) fragment channels of $TrpH^+$ following 266 nm excitation. Both transients share the same time constant of τ_1 = 400 fs (green line) and τ_2 = 15 ps (blue line) assigned to different nonradiative deactivation process in $TrpH^+$ but with different pre exponential factors (sign and amplitude), reflecting the effect of the probe photon upon the fragmentation yield of each channel. Adapted with permission from ref 188. Copyright 2005 American Chemical Society.

Excited state calculations on $TrpH^+$ have shown that several low-lying excited states with π^*, σ^* and π_{CO}^* electronic configurations were present within 0.5 eV and their relative position changes according to the Trp rotamer.[140,189] The precise labelling of these states is somehow difficult due to lack of symmetry and the large mixing of the molecular orbitals. Ideally, the electronic structure of the excited states could be defined as two $\pi\pi^*$ states (L_b and L_a as for

indole) and two charge transfer states of $\pi\sigma_{NH3}$* and $\pi\pi_{CO}$* characters. While the relative position of the charge transfer states compared to the locally excited state depends on the conformation of the molecule, in any case, S_1 is the optically bright $\pi\pi$* state. It should be noted that the $\pi\sigma_{NH}$* state (where the σ symmetry refer to the indole plane) involved in the deactivation of the indole chromophore is not predicted to play a significant role in $TrpH^+$.

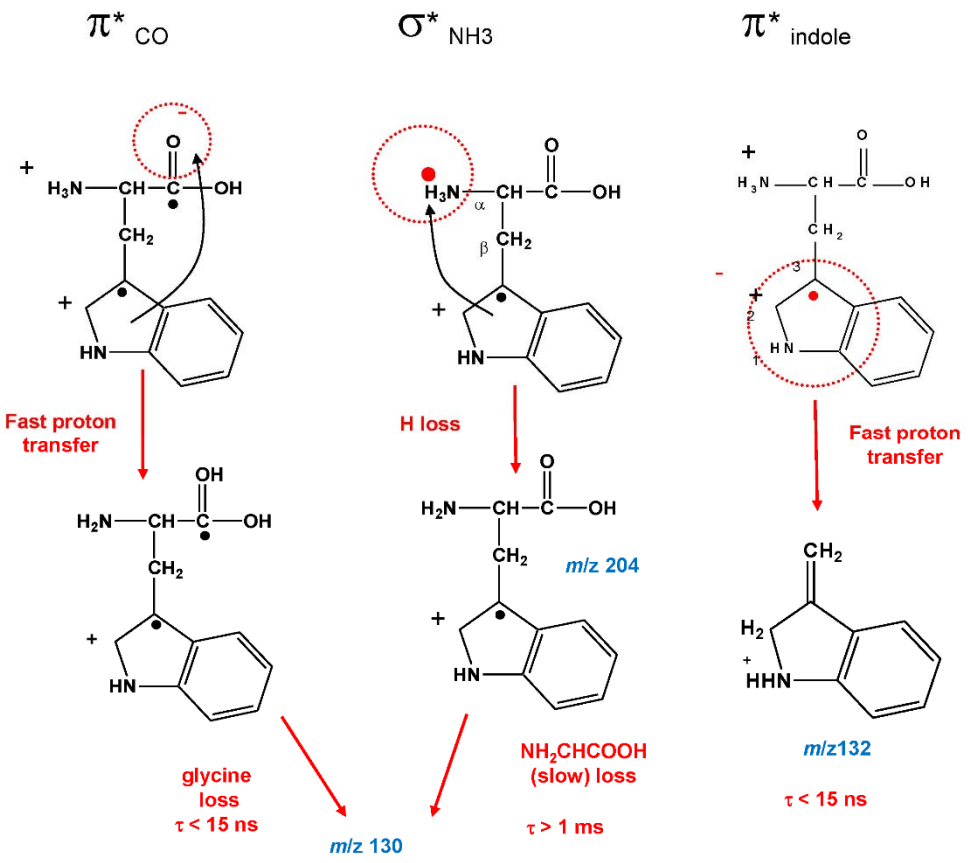

Figure 9. General scheme showing the connection between the electron localization (excited state) and the fragmentation channels in $TrpH^+$. Adapted with permission from ref 190. Copyright 2009 EDP Sciences.

Optimization of the S_1 $\pi\pi^*$ excited state leads for the four lowest energy conformers to an unexpected result in stark contrast to the other protonated aromatic molecules: a barrierless proton transfer reaction from the NH_3^+ group to the indole chromophore. The proton transfer reaction involves rather large nuclear displacements, an out-of-plane CH bend and a ring puckering at the proton accepting carbon atom, leading to a small S_1/S_0 energy gap and possible path for IC through a CI. It is thus believed that this deactivation process is responsible for the ultrafast excited state lifetime of $TrpH^+$. Hydrogen transfer to the ring (coupled proton and electron transfer) was previously proposed[124] to rationalize the fluorescence quenching of zwitterionic tryptophan.

The H loss fragment is related to the dynamics on the $\pi\sigma^*$ state that is dissociative along the N-H stretch coordinate. Experimentally, this channel opens with some excess energy in the S_1 state.[175] The MEP of the H loss reaction exhibits a small barrier of 0.2 eV, in qualitative agreement with the experimental finding.[189] Geometry optimization of the higher excited states ($\pi\sigma^*$ and $\pi\pi_{CO}^*$) leads to barrierless hydrogen transfer from the protonated ammonium to the carboxylic oxygen. The hydrogen transfer reaction can be viewed as an electron-driven proton transfer process triggered by an electron transfer from the indole ring to the carboxylic acid group and then a proton transfer from the ammonium to the negatively charged acidic group. The H atom transfer leads to a biradical ion with a positive hole on the indole ring and an unpaired electron on the aliphatic carbon. Minimum Energy Path along the C_α-C_β bond in $TrpH^+$ suggests that the hydrogenated carboxylic form leads to a barrierless C_α-C_β dissociation.[178] Finally, excited state calculations suggest that the H atom transfer is conformer dependent since it depends on the overlap of the π orbitals of the indole and carboxyl groups.[190] However, the unresolved vibronic spectrum of $TrpH^+$ precludes more definitive statements about the conformer selectivity. The overall picture of the excited state dissociation pathways in $TrpH^+$ is presented in Figure 9.

4.2.2. Protonated tyrosine and phenylalanine: conformer selectivity in the photofragmentation process

$TyrH^+$ and $PheH^+$ are very similar in essence to $TrpH^+$, with the same protonation site on the amino group and S_0-S_1 electronic transitions barely shifted from their neutral analogues. However, their excited state dynamics are drastically different from $TrpH^+$. Cold $TyrH^+$ and $PheH^+$ show well-resolved vibronic photodissociation spectra at the band origin.[191–194] Besides, the excited state lifetime of $TyrH^+$ has been measured as a function of the excess energy in the ππ* state,[195] from a few ns at the band origin (284 nm) down to 22 ps for room temperature ions with large excess energy in the S_1 state (266 nm).[187] While in $TrpH^+$ the coupling between the πσ* state and the locally excited state governs the excited state dynamics, the larger πσ*/ππ* energy gap in $TyrH^+$ and $PheH^+$ precludes an ultrafast deactivation process (see Figure 10), as confirmed by ab initio calculations.[189] It is also interesting to note that simple thermodynamics considerations (Ionization Potential and Proton Affinity of amino acids) used to estimate the asymptotic limit of the H loss reaction from the ammonium group of protonated aromatic amino acids (see Figure 5) provide a very satisfying qualitative picture of the excited state properties of these compounds.[187] This model considers that the electron removed from the aromatic part (IP of the neutral molecule) and added onto the NH_3^+ group (electron affinity of the ammonium group) leads to constant electron-binding energy of the ammonium group attached to the aromatic moiety of 3.2 eV.[196] This crude model allows estimating the relative energy of the πσ* and ππ* states as a function of the ionization potential of the aromatic amino acids, the πσ*/ππ* energy gap being smaller as the IP decreases.

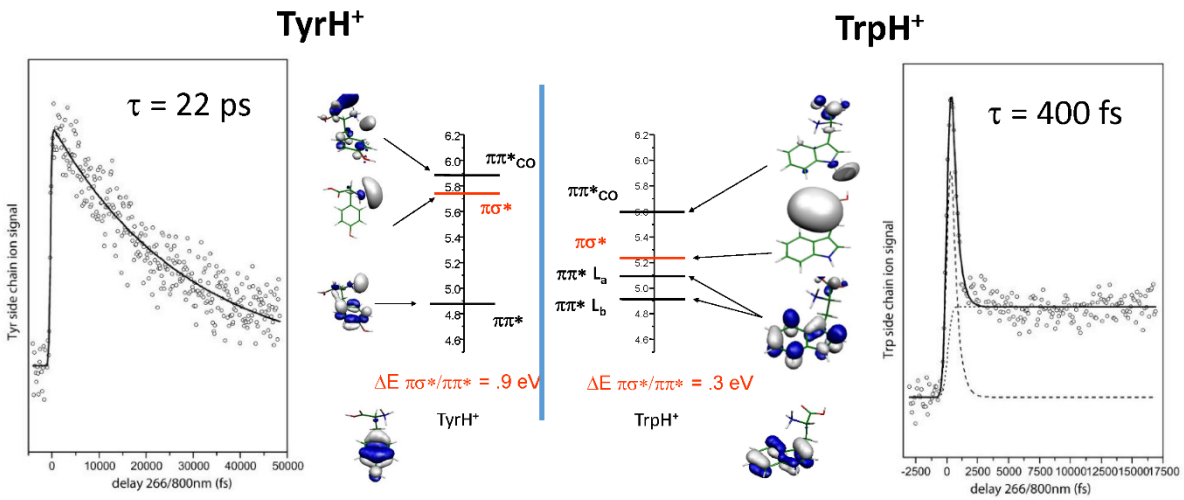

Figure 10. Comparison between protonated tyrosine (TyH^+) and protonated tryptophan ($TrpH^+$). CC2 vertical excited state energies along with the molecular orbital representation and pump-probe photodissociation transients at 266 nm recorded on the same fragment channel, the C_α-C_β bond break. The larger $\pi\sigma^*/\pi\pi^*$ energy gap in $TyrH^+$ explains the longer excited state lifetime (22 ps) than in $TrpH^+$ (400 fs). The constant signal at long delay in $TrpH^+$ reveals the formation of the radical cation following H-loss which further absorbs the probe photons leading to the C_α-C_β bond break. Adapted with permission from ref 187. Copyright 2005 The Royal Society of Chemistry.

The excited state properties of these two protonated aromatic amino acids have extensively been studied. Two main experimental findings were particularly interesting. First, the fragmentation branching ratio strongly evolves with the excess energy in the S_1 state, as already observed in protonated aromatic amines (see section 4.1). Second, a conformer-selectivity in the photodissociation spectroscopy has been observed, providing a direct link between gas phase structure and photo reactivity.[197]

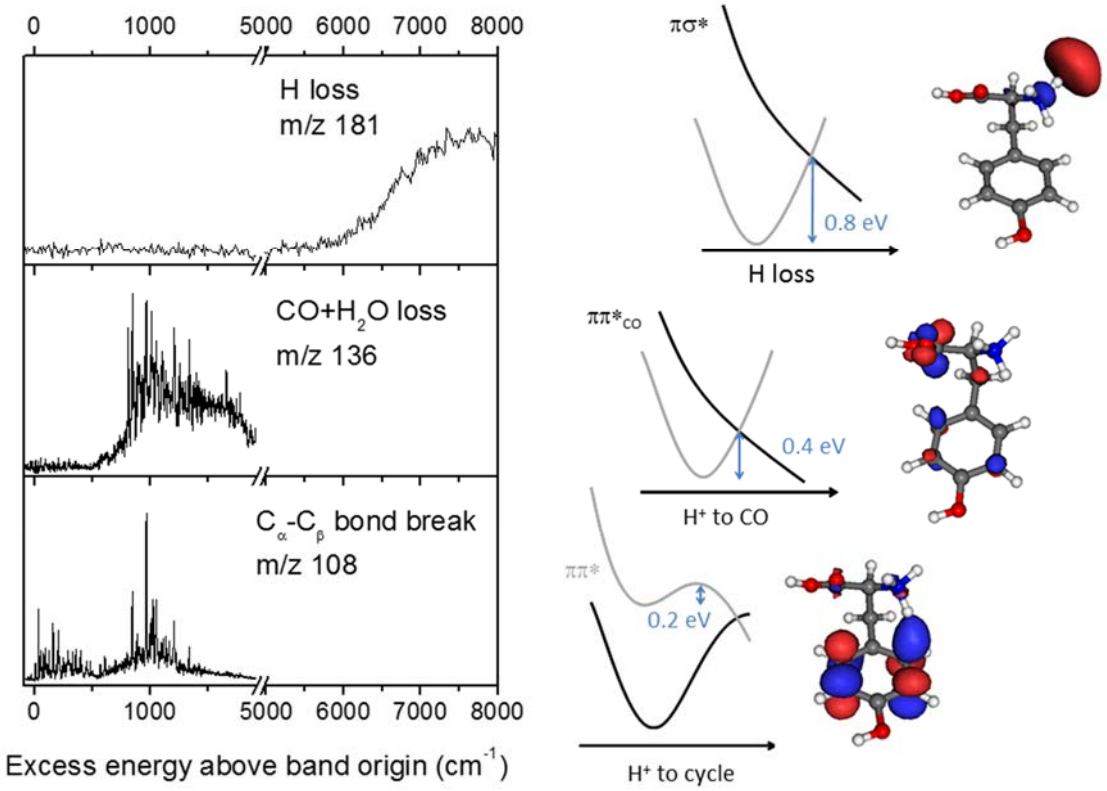

Figure 11. UV Photodissociation spectra of cold $TyrH^+$ recorded on different fragmentation channels depending on the excitation energy along with the nonradiative deactivation processes predicted from ab initio calculations.

In $PheH^+$, the C_α-C_β bond break is the unique fragmentation channel from the band origin to about 700 cm^{-1} above. From this excess energy, this pathway closes and the immonium ion at m/z 120 becomes the unique fragmentation channel. In $TyrH^+$, the situation is even more complicated, as reported in Figure 11. At the band origin, the main fragmentation channel (10-fold more intense than the others) is related to the C_α-C_β bond break. From 800 cm^{-1}, this reaction becomes in competition with the other fragmentation channels associated to the ammonia and water loses (m/z 147) and the immonium ion (m/z 136) but only for the rot conformer (*vide infra*). Finally, from 6000 cm^{-1} above the band origin, the H-loss channel

opens. Here again, as for the aromatic amines and tryptophan, the C_α-C_β bond break is related to the proton transfer from the ammonium to the aromatic ring. The corresponding ionic fragment bears an extra hydrogen (m/z 108) as compared to the mass of the aromatic chromophore cation. The MEP of the S_1 $\pi\pi^*$ state along the N-H stretch pointing to the ring confirms that this proton transfer reaction is energetically allowed, with a barrier of less than 0.15 eV and 0.25 eV for all conformers of tyrosine and phenylalanine, respectively.

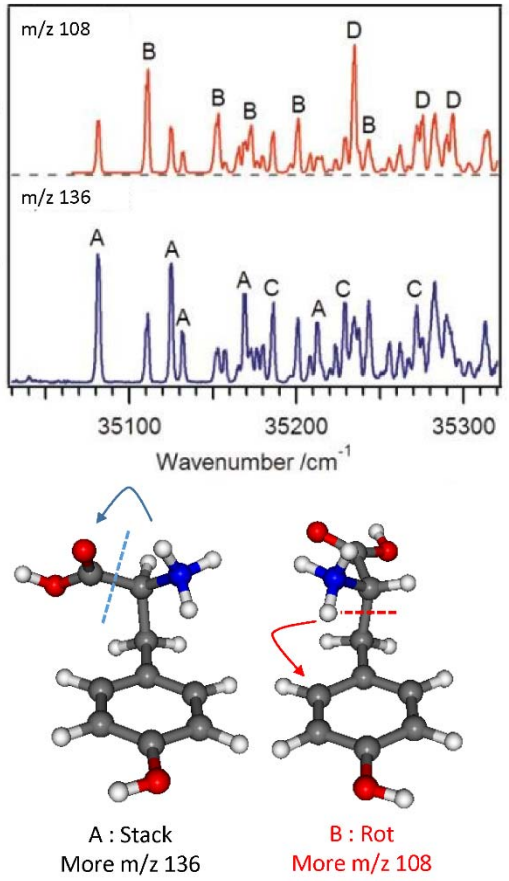

Figure 12. Conformation-selected photofragmentation spectra of $TyrH^+$. The stack conformer preferentially fragments through m/z 136 ionic fragment (CO + H_2O loss) following proton transfer to the carbonyl while excitation of the rot conformer leads mainly to the C_α-C_β bond cleavage following proton transfer to the ring. Adapted with permission from ref 191. Copyright 2007 American Chemical Society.

The most striking result is the strong conformer selectivity in the fragmentation of $TyrH^+$. Four low-lying conformers, which can be sorted in two main groups according to the backbone orientation (rotamer along the C_α-C_β bond), were assigned by Stearn et al.[191] through IR/UV hole burning photodissociation spectroscopy. In the first group, both ammonium and carboxylic acid lie above the π cloud (stack/gauche conformer) while in the rot/anti rotamer, only the ammonium is in direct interaction with the aromatic ring, the carboxylic acid group being in an anti-position to the ring. This latter one leads preferentially to the C_α-C_β bond breaking, as reported in Figure 12.

Geometry optimizations of the $\pi\pi_{CO}^*$ state of the stack and rot conformers have revealed that the $\pi\pi^*/\pi\pi_{CO}^*$ curve crossings occur at lower energy for the stack isomer (0.4 eV) than for the rot one (0.6 eV). The barrier for the charge transfer from the aromatic ring to the carboxylic group is thus conformer dependent, with an optimal π^*/π_{CO}^* orbital overlap in the stack conformer. For both conformers, the dynamics on the $\pi\pi_{CO}^*$ state leads to a proton transfer from the ammonium to the negatively charged carboxylic group.[197] Along the proton transfer coordinate, a second crossing with the ground state occurs leading to the immonium ion (loss of H_2O + CO).[198] Although two deactivation processes in the excited state are clearly in competition with different yields for the two rotamers, it should be reminded here that the excited state lifetimes of the two rotamers of $TyrH^+$ were almost identical and continuously decreased as a function of the excess energy in the S_1 state, from 1.5 ns at the band origin to few hundreds ps at 2000 cm^{-1} above.[195]

In conclusion, during the last ten years, a tremendous effort has been undertaken to decipher the excited state properties of single aromatic amino acids. Although being rather simple molecular systems, their photophysics and photochemistry are very rich and much more complicated than expected. In these model systems, following electronic excitation, several

deactivation pathways can be in competition, some of them leading to specific photofragments, i.e. not related to statistical type fragmentation as observed in low energy collision induced dissociation experiments. Besides, conformer selectivity has been documented, which paves the way for a better understanding of the photochemistry of small peptides for which structures can be assigned through laser spectroscopy.

5. Protonated peptides containing an aromatic amino acids

As for single aromatic amino acids, the photochemistry of protonated peptides is largely influenced by the coupling of the locally excited ππ* state with the πσ* and ππCO* charge transfer states localized on the peptide backbone. In small peptides, both the primary and secondary structures should impact the strength of the interaction between the aromatic ring with the ammonium and carbonyl groups. In order to establish a relationship between peptide conformations and specific photo reactivity, a very useful bottom-up approach is to consider the effect of local interactions on the aromatic chromophore. As it will be presented hereafter, the understanding of the photophysics of small peptides remains quite challenging due to inherent complexity and the difficulty of getting accurate theoretical supports.

5.1. The πσ*/ππ* coupling in peptides: NH_3^+ - π cloud interaction

5.1.1. Excited state dynamics of di- and tri-peptide

Excited state dynamics of small protonated peptides were studied on a very few systems. The short excited state lifetimes of isolated aromatics amino acids ($TrpH^+$ and $TyrH^+$) were attributed to the interaction of the protonated ammonium group with the aromatic ring, leading to the electronic πσ*/ππ* coupling larger in Trp than in Tyr. In dipeptides, depending on the primary sequence, one would expect that the position of the aromatic amino acid in N or C termini changes the interaction of the UV chromophore with the NH_3^+ moiety. Protonated $TrpLeuH^+$ indeed exhibits similar excited state lifetimes than $TrpH^+$, with two time constants

of 1 and 10 ps.[199] Interestingly, for the complementary peptide LeuTrpH$^+$ where the Trp is not directly linked to the protonated ammonium group, the excited state lifetimes were also very short, in the order of 0.5 and 10 ps, as for bare TrpH$^+$.[200] In a last example, Gregoire et al.[201] have investigated two glycine tripeptides containing a Trp or Tyr residues in the middle of the sequence. Here again, the excited state lifetimes were similar to the bare aromatic amino acids, in the order of 500 fs and 5 ps for GlyTrpGlyH$^+$ and GlyTyrGlyH$^+$, respectively. The excited state lifetime of GlyTyrGlyH$^+$ is ten times longer than for GlyTrpGlyH$^+$, which matches the ratio measured for the bare amino acids. It turns out that the $\pi\sigma^*/\pi\pi^*$ model initially proposed to explain the excited state lifetimes of bare aromatic amino acids can be applied to small protonated peptides, independently of the primary sequence. All these experiments were performed on room temperature ions at fixed excitation energy (266 nm), well above the band origin of the peptides. So one should consider that the measured transients were an average of the excited state lifetimes at large excess energy of all the possible conformers populated at this temperature. No direct correlation could thus be made between excited state properties and specific conformation of the peptides.

5.1.2. Statistical *vs* non statistical fragmentation process

Although the excited state dynamics seems to be independent of the peptide sequence, differences in their photochemistry were identified. First, in Trp containing peptides, the H loss reaction leading to the formation of radical Trp$^+$ was not detected following excitation at 266 nm, in stark contrast to bare Trp. However, in GlyTrpGlyH$^+$, one of the UV deactivation pathways leads to the formation of TrpGly$^{\bullet+}$ radical cation that further dissociates into specific secondary fragments. Such radicals are thought to be generated in the excited state since they are not observed in CID. More generally, the photofragmentation patterns can differ according to the localization of the aromatic amino acid. In C terminus, the photodissociation mass spectra resemble those obtained under CID conditions, suggesting that IC followed by statistical

fragmentation occurs. No mechanism for IC was proposed, but the absence of specific photofragments reveals the lack of direct dissociation in the excited state. However, when Trp is at the N terminal part, specific photofragmentation channels were observed and assigned to a non-statistical fragmentation directly from the excited state. In $TrpLeuH^+$, the m/z 130 fragment is the only one with a predominant short time component of 500 fs, which was interpreted as a direct dissociation in the excited state enhanced by the absorption of the probe photon.[199] It should be stressed here that in this case, the m/z 130 fragment is not issued from the Trp radical cation, because the H atom loss is not observed and the transient recorded on this specific channel does not exhibit a plateau as expected if a stable Trp^+ radical cation were formed and excited by the probe laser.[168] As previously explained in the case of bare aromatic amino acids, the m/z 130 fragment is also related to the coupling of the locally excited state with the $\pi\pi_{CO}^*$ state leading to the C_α-C_β bond cleavage. This reaction indeed happens quite often in peptides and will be further described in section 5.3.

The interaction between the ammonium group and the aromatic ring has also been studied through photodissociation spectroscopy of cold peptides ions for which structural assignments can be made. In Trp containing dipeptides, as for bare Trp, the electronic spectra of $AlaTrpH^+$ or $TrpGlyH^+$ are broad, whatever the position of the Trp residue. The main difference between the two species is the spectral shift of the absorption band towards longer wavelengths in $AlaTrpH^+$.[202] A similar trend was observed in $AlaTyrH^+$ dipeptides by Stearn et al.[203] This red shift has been interpreted as a stronger proton-π interaction due to higher flexibility of the peptide chain with a larger number of bonds between the chromophore and the ammonium group. However, for the two AlaX-H^+ (X=Trp, Tyr) dipeptides, there is no indication of excited state fragmentation which would be evidenced by photofragments different than those observed in CID. When the ammonium group gets closer to the aromatic ring, one has to suppose that the $\pi\sigma^*/\pi\pi^*$ coupling responsible for the non-statistical fragmentation is altered, with a higher

rate for IC. However, it is quite difficult to establish a direct link between the cation-π interaction and the increased flexibility of the ammonium group with the length of the peptide chain since in $AlaAlaTyrH^+$ tripeptide, the band origin is blue shifted by about 800 cm^{-1} as compared to bare tyrosine, but in $AlaAlaTyrAlaAlaH^+$, the spectral shift is less than few tens of wavenumbers.[204]

5.2. Impeding the interaction between NH_3^+ and the aromatic chromophore

In the small size peptides depicted so far, due to the strong proton-π interaction, the distance between the aromatic chromophore and the NH_3^+ terminal group remains quite short, even though the aromatic amino acids is not at the N terminal position. In larger peptides, the protonated ammonium could be involved in H-bond with the carbonyl group of the peptide bonds, preventing interaction with the π cloud.[205] It is thus expected that the secondary structure of the peptide would have an influence on the relaxation processes following the electronic excitation. Antoine et al.[206] reported the photodissociation of singly and doubly protonated AlaGlyTrpLeuLys pentapeptide which contains a Trp in the middle of the sequence. At 266 nm, the photoinduced dissociation mass spectrum of the singly protonated species is composed of b-type ions, as observed under CID, plus an ionic fragment corresponding to the loss of the Trp side chain (loss of 130 Da). At 220 nm, two main fragments are detected corresponding to the H loss channel along with the 130 Da loss channel. Both fragments are issued from a non-statistical dissociation occurring in the excited state. The most puzzling result has been obtained for the doubly charged peptide, which does not fragment following excitation at 260 nor 220 nm. The absorption is mainly due to a ππ-ππ∗ transition on the indole chromophore, which is not so sensitive to the environment, since the absorption band is barely shifted from isolated Trp to Trp containing proteins in solution.[113] So the absence of photofragmentation is likely

due to a predominant radiative deactivation process, emphasizing the weak electronic coupling of the locally excited ππ* state with charge transfer states in the unfolded structures.

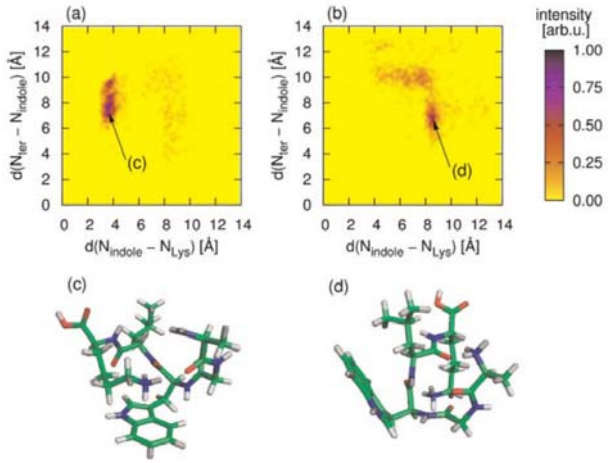

Figure 13. Statistical ensemble of the structures obtained for the singly (a) and doubly (b) protonated AlaGlyTrpLeuLys peptide obtained from the REM simulation at 300 K. Results are plotted as a function of the distance between the protonated ammonium group with the nitrogen of the indole chromophore. (c) and (d): representation structures and the mono and di protonated peptide. Reproduced with permission from ref 206. Copyright 2006 John Wiley & Sons.

Conformational searches were performed for the singly and doubly protonated peptide using Replica Exchange Method (REM)[207,208] using Amber96 force field.[209] For the singly protonated species, the most basic site is the amino group of the lysine side chain while for the doubly protonated peptides, the N terminal amino group bears the second proton. For the singly protonated peptide, the most stable structures are folded, in which the protonated ammonium group of the lysine residue stays in close interaction with the indole chromophore, with an average N_{Lys}-N_{indole} distance lower than 4 Å. In the doubly protonated species, due to coulombic repulsion between the two ammonium moieties, none of the charged groups are in contact with

the Trp side chain, but are mostly solvated by the carbonyl groups of the peptide chain (see Figure 13). According to the seminal photofragmentation mechanism, the coupling of the ππ* state with dissociative πσ* state, where the active electron is localized on the ammonium group triggers the non-radiative process. This electronic coupling strongly depends on the distance between the indole ring and the protonated group, a direct link between fragmentation efficiency and secondary structure could thus be made.

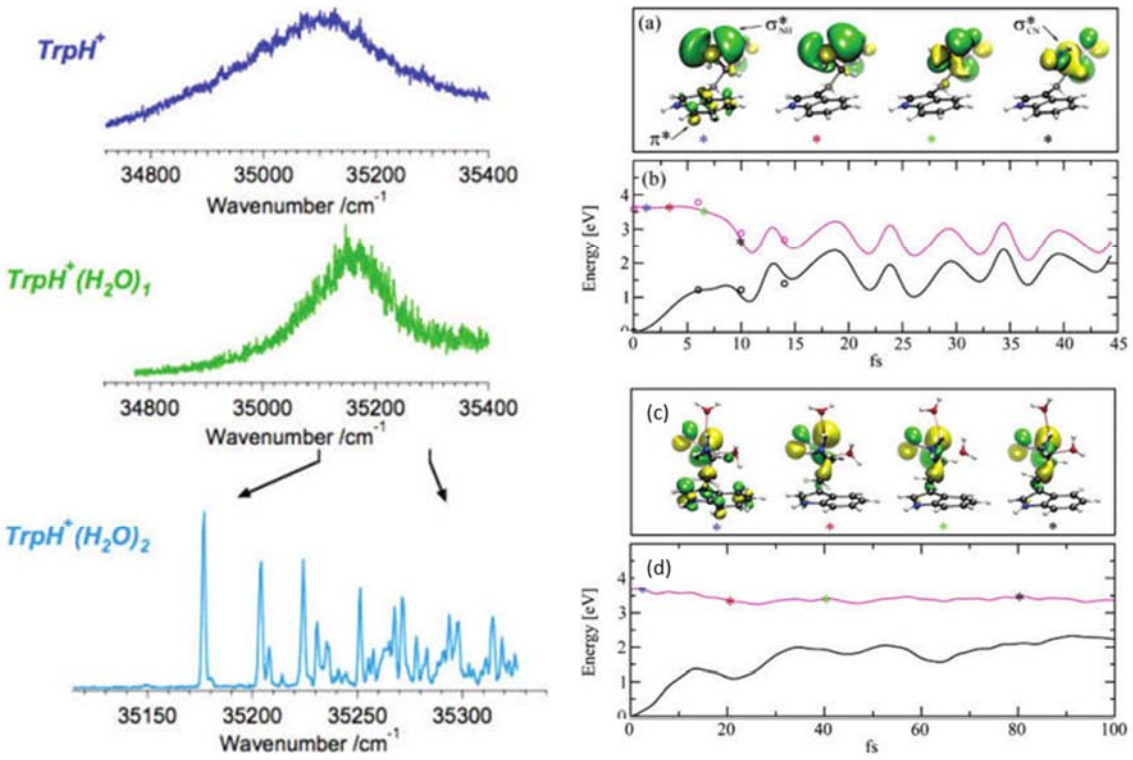

Figure 14. (Left) Electronic photofragmentation spectra of $TrpH^+$-$(H_2O)_{n=0-2}$. (Right) Time evolution of photoexcited $TrpH^+$ (a-b) and $TrpH^+$-$(H_2O)_2$ (c-d) during TDDFT dynamics. (b/d) Ground (black) and excited state energies (magenta). (a/c) dominant Kohn-Sham orbital contributions to excited state. Adapted with permission from ref 210. Copyright 2006 American Chemical Society.

The influence of the $\pi\sigma_{NH3}*$ state on the photophysics of the indole chromophore has been further confirmed in the case of water cluster containing $TrpH^+$. Mercier et al.[210] report the dramatic micro solvation effects on the photodissociation spectroscopy of $TrpH^+$. As reported in Figure 14, the vibronic spectrum of $TrpH^+$ gets narrower by adding one water molecule and becomes well-resolved upon addition of the second. This dramatic effect has been interpreted as an unexpected lengthening of the excited state lifetime of $TrpH^+$ embedded in small water clusters. In the 1-2 complex, the solvent molecules make two H-bonds with the protonated ammonium group, leaving the third hydrogen in interaction with the carbonyl oxygen. In such a structure, the proton-π interaction is strongly reduced and the σ^* orbital centered on the ammonium is largely destabilized, shifting the $\pi\sigma*$ state by up to 1.3 eV.

Finally, the complexes of protonated amino acids and dipeptides with crown ether (CE) provide another examples in which the photophysics is strongly affected by the lack of interaction between the protonated ammonium group and the aromatic ring.[211] In such complexes, the NH_3^+ is fully solvated in the crown ring which prevents the proton-π interaction normally occurring in bare protonated peptides. A series of photodissociation experiment has been conducted in the group of Steen B. Nielsen in Aarhus at the electrostatic ion storage ring ELISA.[186,212,213] Quite surprisingly, upon CE complexation, the CID-like fragments issued from IC to the ground state were mostly suppressed while the aromatic side chain loss following the C_α-C_β bond cleavage was still detected. This latter fragment cannot be assigned to the secondary fragmentation channel of the radical cation following H-loss because the $\pi\sigma*$ state is largely destabilized by more than 1 eV by the CE.[179] Therefore, one has to conclude that another excited state, probably the $\pi\pi_{CO}*$ charge transfer state, is involved in the non-statistical process leading to the specific C_α-C_β bond cleavage channel.

5.3. Specific photofragmentation channel: the C_α-C_β bond cleavage

Among the specific photofragmentation channels, the C_α-C_β bond cleavage is the one which is commonly detected in aromatic acids containing peptides. In isolated amino acids, several deactivation mechanisms account for this reaction which may also occur in peptides. First, the C_α-C_β bond break is the main secondary fragmentation channel of the radical cation formed after H loss. However, the H loss reaction is a very minor fragmentation channel of the peptides excited around the band origin,[214] so it is not thought to be relevant to the photophysics of peptides. The H loss channel is generally detected at much higher energy, typically under laser excitation at 220 nm[215,216] leading to direct excitation of the $\pi\sigma^*$ state repulsive along the N-H stretch. The second most likely process giving rise to the C_α-C_β bond cleavage implies the electronic coupling of the $\pi\pi^*$ state with the charge transfer $\pi\pi_{CO}^*$ state. Independently of the primary or secondary structure of the peptide, a carbonyl group will always be in the vicinity of the aromatic ring, making a through space or through bond electron transfer likely. However, Joly et al.[217] have shown that the rate of C_α-C_β tyrosyl side-chain cleavage is charge and sequence dependent. For the singly protonated peptides, it tends to decrease as the size of the peptide increases. In the doubly protonated species, the rate of aromatic side-chain loss generally vanishes.

In an attempt to clarify the role of the coupling between the locally excited $\pi\pi^*$ state and charge transfer states, *i.e.* $\pi\pi_{CO}^*$ and $\pi\sigma_{NH3}^*$, Dehon et al.[218] investigated, at 263 nm using multi-coincidence detection, the photofragmentation pathways in small peptides containing tyrosine as the UV chromophore: $GlyTyrH^+$, $TyrGlyH^+$, $GlyTyrGlyH^+$, $AlaTyrH^+$ and $TyrAlaH^+$. While the dominant fragmentation channels result from fragmentation of the vibrationally excited protonated species in the ground state, it has been shown that the UV photospecific channels, i.e. C_α-C_β bond breakage in $TyrGlyH^+$ and $TyrAlaH^+$ and direct z-type

bond breakage in $GlyTyrGlyH^+$, can be rationalized upon consideration of charge transfer states (CC2 calculations of vertical excitation energies) accessible after absorption of one UV photon. In both photo specific bond ruptures, the mechanism involves a $\pi\pi^*/\pi\pi_{CO}^*$ charge transfer to the CO group of the peptide bond adjacent to the tyrosyl chromophore, which is followed by a proton transfer from the NH_3^+ moiety. For $TyrGlyH^+$ and $TyrAlaH^+$, C_α-C_β bond breakage leads to neutral loss of the tyrosyl side chain residue. In $GlyTyrGlyH^+$, the photospecific z-type fragmentation mechanism leads to the formation of the same ionic fragment at m/z 222 as in CID experiments. The multi-coincidence detection approach allowed to disentangle the contributions of the two processes, because of the shorter fragmentation time of the binary (UV photospecific) mechanism compared with the multistep mechanism (CID). In all these studies, the secondary structure of the peptides was unknown and the excitation energy was set at 263 nm, which precludes a definitive understanding of the photophysics.

Several IR-UV double resonance spectroscopies of cold peptides ions were reported, which have pointed out conformation-specific photofragmentation.[219] $TyrAlaH^+$ dipeptide exhibits excited state fragmentation involving loss of the tyrosyl side chain radical, while the complementary $AlaTyrH^+$ does not.[203] This is a general trend observed in all tyrosine containing peptides, the C_α-C_β bond break occurs only when the aromatic residue is located at the N terminus. Two conformers were assigned, both having NH-π and NH-CO interactions through a C_5 type H-bond between the ammonium and, the π cloud and adjacent carbonyl, respectively. The two conformers differ by the rotation along the C_α-C_β bond such that the peptide bond is anti or gauche relative to the ring.[220] These two conformers have different photofragmentation mass spectra, with a larger rate of tyrosyl side chain loss for the anti than for the gauche conformer. Such selectivity was already observed in protonated tyrosine where the C_α-C_β bond break is prominent in the anti conformer (also noted rot). It is worth mentioning that in the latter case, a proton transfer from the ammonium to the cycle leads to the m/z 108 photofragment,

while for the peptides, the neutral tyrosyl side chain loss (107 Da) is observed. As explained above, the multi coincidence experiment has shown that in TyrX-H^+ dipeptides, the cleavage of the C_α-C_β bond is direct, leading to the tyrosyl side chain loss (107 Da) as unique neutral fragment. The neutral 107 Da loss is consistent with the higher ionization potential of the tyrosyl side chain residue than the peptide chain, thus promoting an electron transfer from the peptide chain back to the chromophore.

In larger tyrosine containing peptides, the loss of neutral tyrosyl side chain is also a usual photofragment. Kopysov et al.[221] investigated a series of tyrosine-phosphorylated peptides (Ac-$TyrAla_3SerLys$) through cold ion UV spectroscopy and observed that the most abundant photofragment corresponds to the cleavage of the C_α-C_β bond. Conformer selectivity also occurs in tyrosine containing pentapeptides, as pointed out by DeBlase et al.[222] The UV photodissociation mass spectra of the diastereomer $TyrAla^DProAlaAlaH^+$ peptides is conformer-specific with respect to the extent of tyrosyl side chain loss. However, for the two assigned conformers, the NH_3^+ forms three hydrogen bonds with the phenyl ring, a carbonyl and the carboxylic acid group, so the reason why one conformer exclusively fragments through C_α-C_β bond cleavage remains unclear. Gramicidin S, a decapeptide with two phenylalanine residues, provides another dramatic example of fragmentation selectivity for peptide conformation.[220] The conformers which exhibit a strong proton-π interaction between the NH_3^+ and the ring mostly fragment following IC. At contrary, when the aromatic ring is remote from the charged ammonium and free from the rest of the peptide, the main and unique fragmentation channel corresponds to the phenylalanine side chain loss.

The photodissociation mass spectrum of Leu Enkephalin (TyrGlyGlyPheLeu) in the spectral region of the tyrosine chromophore also comprises CID-type fragments along with 107 Da loss.[223] More fascinating is the increase in the rate of formation of this latter fragment at the expense of the CID-like fragments through the IR gain experiment. In such a scheme, the UV

laser is tuned to the red of the S_0-S_1 band origin while the IR, shined before the UV laser, is scanned in the 3μm region to induce photofragmentation as soon as it falls into resonance with a vibrational mode of the parent ion. Two tentative explanations can account for such results. First, the pre-heated ions through IR absorption undergo isomerization to high energy conformers more prone to dissociation through C_α-C_β bond cleavage. Because of the lack of UV selectivity in the IR gain spectroscopy, this hypothesis cannot be easily tested. One should nevertheless concede that in similar IR hole-filing experiments performed on neutral molecules streamed in a molecular beam,[224] in any case, the increase of the internal energy through IR excitation changes the relative population of the low-lying conformers already present at low temperature without isomerization to new, high-lying conformers. In a second hypothesis, the branching ratio between the tyrosyl side chain loss and the IC leading to CID-like fragments changes with the excess energy in the excited state. Such evolution of the fragmentation branching ratio with the excess energy has already been observed and explained in the photodissociation spectroscopy of single amino acids. To confirm this assumption, this would however require quantum chemistry calculations to localize the higher charge transfer states responsible for the curve crossing with the locally exited state of the peptides.[225]

By investigating larger and larger peptides through photodissociation spectroscopy, one might argue that within the observable time window of an ion trap experiment, according to a statistical-type of fragmentation, the energy brought by one UV photon would not be enough to induce the dissociation. In order to prevent this bottleneck, Rizzo et al.[204,226,227] have developed a spectroscopic technique in which the protonated peptides, first excited by the UV laser, undergo infrared multiple photon excitation (IRMPE) provided by a CO_2 laser. In such a scheme, a dramatic increase of the photofragmentation yield of two orders of magnitude was observed on several peptides that contain tyrosine, tryptophan and phenylalanine residues. In any case, the loss of the aromatic side chain through C_α-C_β bond cleavage is the main, if not

unique, fragmentation channel enhanced by CO_2 excitation. Since the C_α-C_β bond is not, by far, the weakest in the ground state of protonated peptides, the large increase of the rate associated with this reaction is incompatible with a dissociation in the ground state. In order to gain insight into the fragmentation mechanism of the IRMPE method, Zabuga et al.[228] performed time- and frequency-resolved excited state photofragmentation experiments (see Figure 15) on Phe and Tyr containing protonated peptides $(AcXAla_5LysH^+)_{X=Phe,Tyr}$ by replacing the CO_2 laser with a tunable IR OPO laser. They proposed a model involving the deactivation of the $\pi\pi^*$ excited state toward a triplet state which has an exit barrier to C_α-C_β dissociation. By measuring the IR power dependency upon the photofragmentation rate, they deduced an upper limit of 6800 cm^{-1} (2 photons excitation) for the C_α-C_β dissociation barrier in the triplet state. The triplet state lifetimes of 20 μs and 100 μs were reported for tyrosine and phenylalanine containing peptides, respectively. Besides, for $AcPheAla_5LysH^+$, a long time constant (more than 100 ms) is observed, which was attributed to collisional cooling of the vibrationally activated triplet state.

It should be mentioned here that in the ion/neutral coincidence experiment, the dynamics of fragmentation associated with the C_α-C_β bond cleavage reaction was investigated in smaller peptides.[183] Since the peptides were not cryogenically cooled and the UV excitation wavelength was set at 263 nm, a direct comparison of the time constants determined in the two experiments is not easy. The main outcome of the coincidence experiment is the evidence for ion-dipole interactions during the dissociation event between the incipient neutral and ionic fragments associated with the aromatic side chain loss, which results in the formation of a metastable ion-molecule complex thus controlling the observed fragmentation time. If the two experiments have definitively shown that long-lived species are in play during the specific C_α-C_β photofragmentation, the exact nature of the latter remains either the relaxation to the triplet state or the formation of metastable ion-molecule complex following the initial C_α-C_β bond cleavage.

More theoretical works are needed in particular to understand why the C_α-C_β bond would be so weakened in the triplet state.

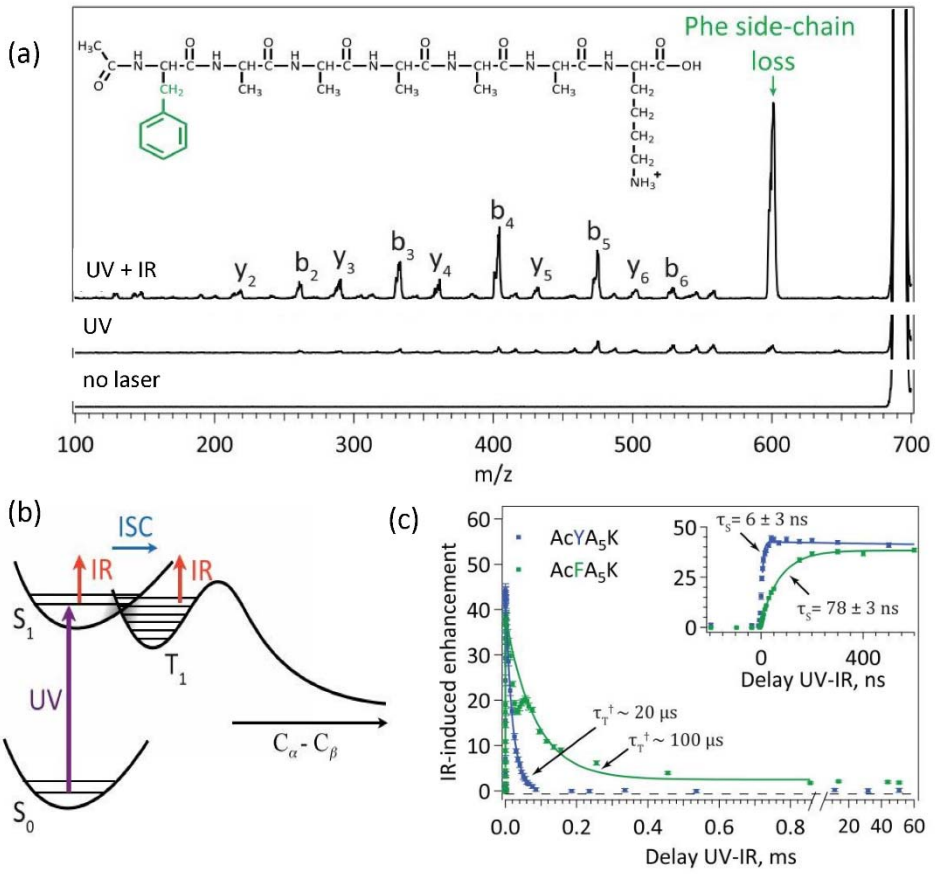

Figure 15. (a) Mass spectra of AcPheAla5LysH$^+$ without laser, with UV fixed at the band origin and with additional CO_2 laser at time delay of 1.2 µs. (b) Schematic model explaining the non-statistical photofragmentation in phenylalanine containing peptides. After ISC, the barrier to C_α-C_β bond dissociation can be overcome by absorption of IR photons (c) Time dependence of the infrared-induced enhancement of the C_α-C_β bond cleavage in AcXAla5LysH$^+$, (X=Tyr, Phe). Adapted with permission from ref 228. Copyright 2014 American Institute of Physics.

6. Photoinduced processes in bi-chromophore systems

Electronic energy transfer (EET) is another type of photoinduced process that can be used to probe the local interaction in peptides. EET requires two interacting subunits which are not generally chemically bonded in naturally occurring peptides. Instead, many applications of EET use semi-rigid linkers between the donor and acceptor chromophores to keep a well-defined structure and to maintain some properties of the isolated chromophores but are out of the scope of this review. Resonance Energy Transfer (RET) has been the subject of many review articles[229–232] and we only present few studies performed on gaseous peptides ions for which structural information is available.

6.1. Fluorescence quenching

Fluorescence-based method are widely developed in molecular biology, not only for imaging but also for going beyond pure photon detection, e.g. providing structural information of the proteins. The general principle is to follow the fluorescence emission of a probe in the presence of a quencher located somewhere in the peptide sequence. Trp-Cage protein is one of the simplest systems in which such fluorescence quenching has been extensively studied. Trp-cage is a small protein containing 20 residues with a single Trp close to the N terminal part.[233] A covalently attached dye at the C terminus is responsible for the fluorescence emission that is quenched when the Trp residue is in strong interaction through photoinduced electron transfer, leading to nonradiative decay of the excited dye.[234,235] In the native protein structure, the Trp residue is buried by three proline and as the protein is heated, unfolding occurs which releases Trp from its cage and becomes more exposed to intramolecular interactions with the dye.

Parks and co-workers[236] used fluorescence spectroscopy to monitor the temperature and charge effects on the conformational dynamics of isolated Trp-cage ions. They showed that the protein unfolds more readily at high temperature as the charge state increases from 2^+ to 3^+,

consistent with unfolding promoted by greater Coulombic repulsion in the higher charge state. Interestingly, the Trp-Cage mutant in which salt bridge between Lys_8^+, Asp_9^- and Arg_{16}^+ is suppressed behaves essentially the same,[237] suggesting that the strong salt bridge interaction is not critical for the stability of the protein in the gas phase, at odds with the conclusion drawn from the condensed phase.[238] They also studied a set of polyproline peptides of different lengths[239] and found that the fluorescence quenching was increased by the presence of a strong electrostatic field (charged Arginine residues) which in turns lowers the charge transfer state between the dye and the Trp side chain.[240,241] These seminal studies have clearly demonstrated the ability of fluorescence methods to probe the structure of peptides in which a strong coupling between a fluorescent dye and a quencher occurs at short distances. However, the precise mechanism by which quenching occurs at short dye-Trp distances still needs to be tackled through high-level quantum chemistry, in particular which singlet or triplet excited states are involved in the photophysics of the dimer.

6.2. Förster Resonance Energy Transfer (FRET)

Fluorescence (or Förster) resonance energy transfer (FRET) is one of the standard optical method used in condensed phase to probe the energy transfer and conformation of peptides and proteins. Single molecule fluorescence studies of protein folding and unfolding have been successfully developed in molecular biology the last fifteen years.[242–244] Unfortunately, in the gas phase, a very few groups have successfully developed such technique, mostly because of the inherent difficulty to collect the fluorescence emission of ionic peptides confined at low density in the ion trap.

FRET involves nonradiative transfer of electronic excitation from an excited donor, D* to a ground-state acceptor molecule A. The efficiency of this dipole–dipole interaction depends on the distance between the fluorophores, the spectral overlap of the donor emission and the acceptor absorption (the so-called overlap integral), the refractive index of the media (unity in

the gas phase), the donor quantum yield, and the relative orientation of the fluorophores.[245] The Förster radius R_0, distance at which the energy transfer efficiency E is divided by two, is typically 20-60 Å. Note that the Förster theory relies on the point dipole approximation which requires that the inter chromophore distance be long compared to the size of the chromophores. Experimentally, the FRET efficiency can be estimated by measuring the emission spectra or the fluorescence decays of the donor/acceptor pair. FRET is a strongly distance sensitive method, so-called "spectroscopic ruler",[246] used to obtain distance constraints of a molecule without a precise knowledge of its structure.

The Jockusch group in Toronto successfully developed gas phase FRET to explore the conformational changes of polyprolines as a function of the peptide length and charge state.[247] Such polyproline peptides were initially thought to form rigid helices in liquid,[248] while more recent works contradict this ideal picture.[249,250] The choice of the donor D and acceptor A fluorescent dyes, that are covalently bound to the N and C termini of the peptide, is crucial. A good spectral overlap between acceptor excitation and donor emission is required. FRET efficiency is monitored by recording the steady state emission spectra and lifetimes (of the donor) of the (A)-GlyGlyPro_nLys-(D)-NH_2 peptides, n=8, 14, 20. As depicted in Figure 16, the FRET efficiency, which is close to unity for the shortest peptide, decreases as a function of the peptide length and for higher charge state, suggesting a more extended structure. Surprisingly, the longer peptide with 20 prolines showed almost complete RET, which is not compatible with an extended helical structure but more likely suggests a hairpin-like structure that brings the two chromophores in close proximity.

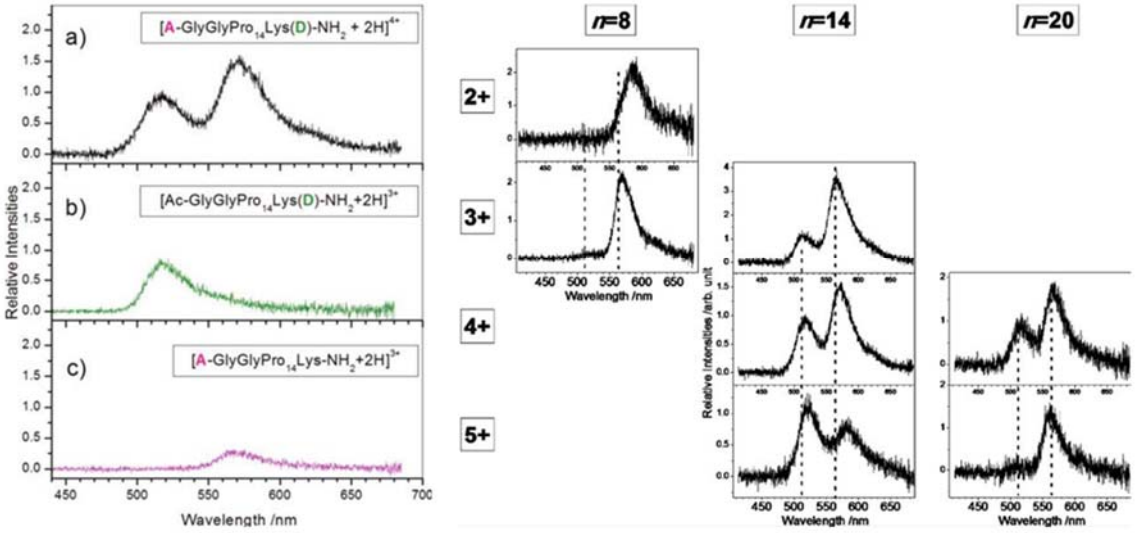

Figure 16. (Left) Fluorescence spectra of Pro_{14} based peptides excited at 470 nm containing (a) both donor (D) and acceptor (A), (b) only the donor and (c) only the acceptor. (Right) Influence of the charge state and peptide length on the emission of (A)-GlyGlyPro_nLys-(D) peptides. Adapted with permission from ref 247. Copyright 2010 American Chemical Society.

Application of FRET to a gaseous protein GB1 (59 residues) has showed that the native structure of the protein, which is retained over a broad pH range (1.5-11), is disturbed in the gas phase as the charge state increases, revealing a Coulombic driven unfolding and expansion of its structure.[251] Finally, a proof of concept of hybrid experimental setups interfacing laser-induced fluorescence detection with ion mobility spectrometry has been established on rhodamine dye, which has the potential to address still open questions such as to which extent gas phase peptides ions retain their native structures.[252,253]

6.3. Action-FRET

Despite the promising opportunity of gas-phase FRET to probe the conformation of mass-selected biomolecules, the inherent difficulty of collecting the fluorescence in an ion trap has

hindered its dissemination in many research labs. To circumvent this drawback, Dugourd and coworkers have proposed an elegant variant of gas-phase FRET, the so-called action-FRET based on photofragmentation (see Figure 17) rather than fluorescence detection.[254] As for FRET, action-FRET requires a good overlap of the donor emission and acceptor absorption spectra and RET must happen on a time scale shorter than the relaxation of the donor chromophore. The choice of a suitable fluorescent donor chromophore and a dark-quenching acceptor chromophore has been crucial for the successful achievement of action-FRET. The donor is rhodamine 575 (rh575) and the acceptor chromophore is N-succinimidyl ester (QSY7), a rhodamine derivative, which both possess a single positive charge. An additional criterion is however mandatory, that is the specific photofragmentation of the acceptor molecule, reflecting the electronic excitation of the acceptor followed by a non-statistical fragmentation process prior to energy redistribution in the ground state.[255] By recording the action spectra monitored on the specific acceptor photofragments, RET is directly evidenced if the donor absorption band is observed. The FRET efficiency is thus defined as the ratio of the area of the peaks in the action spectrum due to absorption of the donor and acceptor chromophores. Action-FRET was first tested on polyalanine peptides of different sizes for which collision cross sections were also measured independently in order to provide a direct link between the secondary structure and the FRET efficiency[254] and since then successfully applied to the study of the structural transition with charge state of amyloid-β peptide[256,257] $A\beta_{12-28}$ and its dimer[258] and finally recently combined with ion mobility spectrometry within the same experimental setup to investigate the unfolding of ubiquitin.[259]

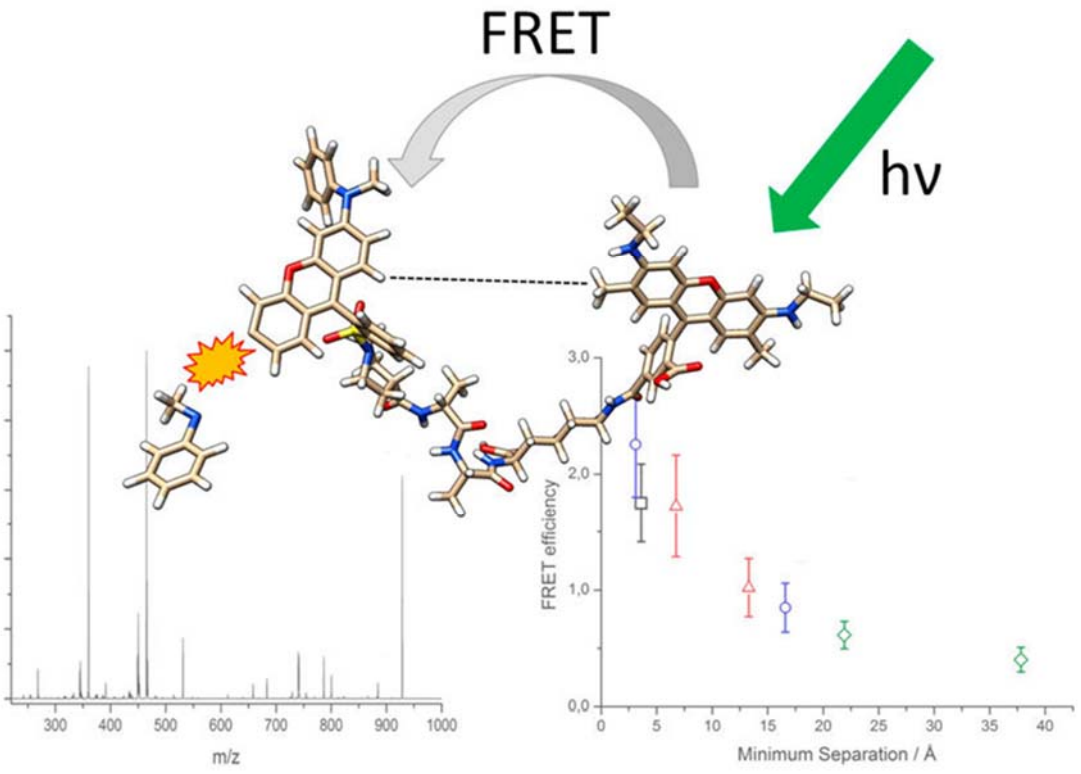

Figure 17. Principle of Action-FRET developed in the group of Ph. Dugourd. The specific photofragmentation yield of the acceptor chromophore is followed as a function of the donor distance for different alanine-based peptides which conformations are probed through ion mobility spectrometry. Reproduced with permission from ref 254. Copyright 2014 American Chemical Society.

RET can also be revealed through the change in photophysics of the chromophores upon homodimer formation, in systems where the donor and acceptor are the same species. It turns out that rhodamine fluorescence quantum yield drastically decreases at high concentrations,[260,261] a self-quenching which has been rationalized by short excited state lifetime (below 1 ps) and IC and ISC processes of the dimer.[262,263] Because self-quenching is extremely sensitive to small inter chromophore distance changes and only occurs at short-distance below 10 Å, it provides a complementary distance dependence to FRET experiments

which are devoted to larger conformational changes. Daly et al.[264] used action-self quenching to probe the conformational heterogeneity of doubly-grafted $A\beta_{12\text{-}28}^{3+}$ peptide. Its action spectra is composed of two bands which are assigned to the formation of a dimer (495 nm) and the monomer at 435 nm. Here again, specific photofragmentation channels related to bond cleavages of the chromophore moiety which are not observed in CID are used to evidence self-quenching.

6.4. Excitation energy transfer in naturally occurring peptides containing a methionine or disulfide bond

Among the amino acids, cysteine and methionine are two sulfur-containing biomolecules which deserve special attention as it is well established that such residues can be easily oxidized by various forms of reactive oxygen species to form sulfoxides, i.e. one of the post-translational modifications, which leads to significant changes in the behavior of these systems. Such oxidative modified species accumulate during aging and are responsible for a number of age-related diseases.[265] C_α-C_β bond breakage in selected methionine-containing dipeptides and their sulfoxide analogs with, tyrosine and tryptophan as UV chromophores, has been investigated by Kumar et al.[266] It is shown that methionine-containing dipeptides with tryptophan and tyrosine undergo photospecific C_α-C_β bond breakage. Neutral side chain production is enhanced with sulfoxidation when the UV chromophore is on the N-terminus. Based on the relative abundance of fragment ions produced by C_α-C_β bond breakage, it is suggested that the presence of oxygen on the methionyl-sulfur enhances proton transfer from the side chain to the sulfoxide, which facilitates the loss of the neutral side chain. Also, no ionic side chain loss is observed with tyrosine-containing dipeptides.

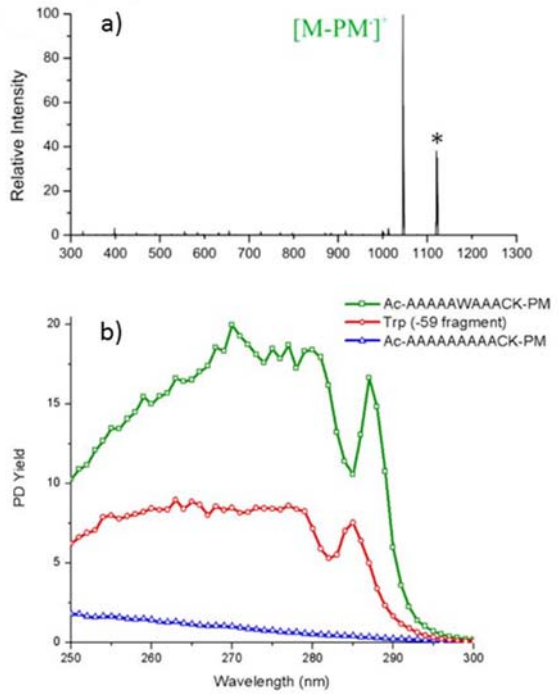

Figure 18. (a) Photodissociation mass spectrum of protonated $AcAla_5TrpAla_3CysLys$-PM, * precursor ion, with its main photofragment associated to the loss of propyl mercaptan (PM). (b) Action spectra of the peptide (green line), Trp (red line) and the peptide without Trp residue (blue). Adapted from ref 267. Copyright 2014 American Chemical Society.

While resonant energy transfer between designed, synthetic donor and acceptor chromophores grafted to peptides has been widely used to probe the peptide structures both in the condensed phase and the gas phase, excitation energy transfer (EET) is also expected to occur between naturally occurring amino acids with excitation bands in the near UV such as aromatic and disulfide chromophores. The smaller size of these chromophores, compared to the dye molecules commonly used in the FRET experiments, should not disrupt too much the secondary structure of the peptides if site-directed mutagenesis is employed to incorporate such residues in a peptide sequence. As for action-FRET, energy transfer would be identified by specific photofragment channels of the acceptor chromophore following donor excitation.

Hendricks et al.[267] have developed an action-EET based on excitation of Trp/Tyr donors and direct dissociation of proximal disulfide bond. They tested this method on cysteine containing polyalanine and Trp-Cage peptides, in which the disulfide bond is formed with propyl mercaptan (PM). EET is clearly evidenced in the action spectra of the peptides showing the excitation bands of the aromatic chromophore while monitoring the homolytic fragmentation of the disulfide bond (see Figure 18). Without aromatic chromophore, the photodissociation yield of cysteine containing polyalanine is low and slightly increases at shorter excitation wavelength around 250 nm. In the presence of Tyr or Trp, the spectrum closely resembles those of bare protonated Tyr and Trp, consistent with fragmentation following EET.

The distance dependence of the excitation energy transfer between Trp and the disulfide bond has been qualitatively evaluated in a series of alanine containing peptides. The fact that the photodissociation yield drops significantly within 15 Å suggest that EET is likely due to a Dexter exchange transfer,[268] which depends exponentially on the inter chromophore distance, rather than a Förster mechanism. With tyrosine as donor chromophore, the distance dependence is even more pronounced with energy transfer occurring only at distances lower than 6 Å. The short distance range of EET with tyrosine provides severe structural constraints that are complementary to information gained through ion mobility measurements.[269] Finally, the Julian group demonstrated a sequential two-step energy transfer from phenylalanine to tyrosine and to a disulfide, leading to its homolytic cleavage. It is worth mentioning that EET is only observed in the presence of tyrosine and at distances shorter than 6 Å.[270] This two-step energy transfer of Phe has been tentatively explained by the poor overlap of Phe emission with the absorption band of the disulfide, thus requiring Tyr to bridge the gap. EET between Phe and Tyr has indeed been recently studied via cryogenic cold ion spectroscopy in the groups of Boyarkin and Rizzo in Lausanne.

6.5. Energy transfer between Phe and Tyr in conformer-selected peptides

Kopysov et al.[271] employed UV fragmentation spectroscopy of cold ions to measure the conformer-specific resonant energy transfer efficiencies in Leu-Enk. These short peptides naturally contains Tyr and Phe while the high spectral resolution of the cryogenic spectroscopy provides conformer selectivity. The excitation spectra were generated by monitoring the Tyr side chain loss fragment, corresponding to the specific C_α-C_β bond cleavage, as already emphasized in section 5.3. The fact that UV excitation of Phe generates the specific photofragment of Tyr residues clearly suggests that RET has occurred. The RET efficiency can be evaluated by measuring the yield of the specific Tyr photofragment channel arising from excitation of Phe. According to the Förster formalism, the authors conclude that the distance between the Phe and Tyr chromophore is significantly shorter in the (DD) $TyrAla^{D}GlyPheLeu^{D}H^+$ stereoisomer than in the (LL) $TyrAla^{L}GlyPheLeu^{L}H^+$ and $Leu\text{-}EnkH^+$. However, although the averaged inter chromophore distances in Enk and (LL) stereoisomer pentapeptide fit within the lower limit of the dipole-point approximation of the Förster theory (about 10 Å), the Phe-Tyr distance in DD stereoisomer of less than 6 Å indicates that the Dexter formalism is more appropriate for estimate the RET efficiency, as suggested in the previous studies of Hendricks et al.[270] It should also be stressed here that the Förster approximation assumes that the donor and acceptor chromophores sample orientation space isotropically, such that $\langle \kappa^2 \rangle = 2/3$, κ being the orientation factor. In conformer selected peptides, the donor and acceptor are obviously limited in their orientation freedom, so the orientation factor should be explicitly calculated.[272]

Finally, Scutelnic et al.[273] have investigated EET in conformer-selected peptides containing a Phe and Tyr residues through double-resonance UV-IR spectroscopy of cryogenically cooled $Ac\text{-}PheAlaTyrLysH^+$ peptides. In such a scheme, an IR laser probes the electronic excited peptides, giving the spectral fingerprint of the electronic state. The evolution of the IR spectra

as the function of the delay time between the pump (UV) and the probe (IR) pulses then provides a direct measurement of the excited state lifetime that can be related to the EET rate. At short delays (5 ns), the IR spectrum of the excited state of each conformer mostly differs from the corresponding ground state spectrum by a single transition. Excitation of phenylalanine shifts the Phe NH stretch by -39 cm^{-1} and excitation of the tyrosine chromophore induces a red-shift of -71 cm^{-1} of the hydroxyl OH stretch along with a -32 cm^{-1} red-shift of the vicinal Lys NH stretch. This indicates that within 5 ns, the electronic energy stays localized on the initially excited chromophore, independently of the probed conformer. Resonant energy transfer is monitored by looking at the emergence of transitions assigned to the excited state of tyrosine upon excitation of the Phe chromophore as the function of the delay between the pump UV and the probe IR. Interestingly, while the two conformers only differ by the relative orientation of the two chromophores which are virtually at the same distances (about 11 Å), their EET rate changes by a factor of two. Besides, the EET is nearly complete between Phe to Tyr, since the photo specific C_α-C_β bond cleavage of the Phe residues is not observed.

7. Summary and outlook

Gas phase UV spectroscopy is a powerful tool to study the dynamics of nonradiative processes in conformer-selected aromatic amino acids and peptides. During the last decade, thanks to the fruitful combination of mass spectrometry with laser spectroscopy, a wealth of data that shed light on the nonradiative deactivation processes of protonated species has been collected. With the advent of cryogenic ion spectroscopy, all the spectroscopic tools developed for neutrals have been transferred to protonated, mass- and conformer-selected peptides. UV photofragmentation has clearly emerged as a new spectroscopic technique, providing complementary, nonradiative information as compared to fluorescence which remains particularly difficult to setup in ionic trap. Excited state dynamics of single protonated aromatic

amino acids are indeed quite rich and complex, with conformer selectivity in the photofragment channels in case of tyrosine or a large range of dynamical processes ranging from fs (for the excited state lifetime of the locally excited state) to seconds for secondary fragmentation channels in tryptophan. Competition between statistical fragmentation following IC to the ground state, versus direct dissociation triggered by a charge or energy transfer in the excited state reveals a particular importance. Charge transfer and triplet states have been invoked to play a fundamental role in these nonradiative deactivation mechanisms. It is noteworthy that through photofragmentation, these optically dark states, which cannot be directly accessed through one-color excitation from the ground state, can be spectroscopically characterized through IR, visible or UV excitation thanks to their specific photofragmentation channels, for instance the C_α-C_β bond cleavage. Moreover, the unique ability to store ions in the ion trap for a long time, compared to the radiative fluorescence (ns) and phosphorescence (ms) lifetimes, allows deciphering the entire deactivation dynamics over ten decades or more until final IC to the ground state and fragmentation. This is clearly a major improvement as compared to gas phase laser spectroscopy of neutral molecules cooled and streamed in molecular beam. First, due to the higher ionization potential from these dark states, much shorter probe wavelengths that may fall outside the spectral range of commercial tabletop lasers are required to perform pump-probe photo ionization spectroscopy on neutrals.[274] Second, excited state dynamics of neutral molecules cannot be probed for more than 1 μs or so due to the velocity of the incoming molecules streamed in the jet. Such multiscale time dynamics have indeed been recently demonstrated in which long-lived charge transfer and triplet states have been probed up to tens of millisecond in the case protonated DNA bases[275] and related compounds,[276,277] in small peptides containing a tyrosine and phenylalanine residues[228,273] and in metal containing peptides[278] where a sequential proton coupled electron transfer dynamics has been deciphered over 8 orders of magnitude.

The ability to control the entrance and exit channels of the photoreaction through mass spectrometry, the deposited excess energy through laser excitation and the structure of the molecules through cryogenic ion spectroscopy offer unique opportunities to precisely investigate photophysical and photochemical processes of conformer-selected peptides. At the moment, most of the reported studies have been conducted on small molecular systems, from single aromatic amino acids to short peptide chains. These experimental data on rather small molecular sizes indeed provide a natural testing ground for future benchmarking of advanced theoretical calculations on the excited state properties of these ions. The analysis of well-resolved vibronic spectra recorded on the different photofragmentation channels that may be in competition as a function of a small amount of excess energy, typically few hundreds of wavenumbers, definitively requires high accuracy calculations of excited state PESs, which still represents a major theoretical challenge. As always, one has to find the good compromise between the accuracy of the quantum chemistry methods and its efficiency to treat the photochemical or photophysical process. It should be stressed here again that the electronic structure of the protonated species is exactly the same as the neutrals, i.e. closed shell electronic configuration. Therefore, all the recent advances in nonadiabatic quantum molecular dynamics[12–14,279,280] could be used to disentangle their excited state properties. Obviously, the description of the whole deactivation process, starting for the initial excitation of the $^1\pi\pi^*$ state until the final fragmentation events requires multiscale dynamics that are still most challenging. Machine learning algorithms could offer great opportunities to predict excited state energies, forces and couplings at virtually no computational cost,[281–285] as already demonstrated for simulations of infrared spectra of peptides.[286]

While the photophysics of neutral and protonated aromatic amino acids and peptides have been investigated both experimentally and theoretically, studies on deprotonated aromatic species remain rather scarce and so mostly to be explored. Such studies are generally based on

photoelectron spectroscopy using time-of-flight or velocity map imaging methods that cannot be directly performed with anions stored in an ion trap. Besides, the cross sections for photodetachment of electrons near threshold are usually low,[287] which requires high efficiency detection. Deprotonated species readily lose an electron following electronic excitation,[37] with photoelectron spectra specific of the deprotonation site, as evidenced in case of $[Tyr\ -H]^-$ which consists of a mixture of phenoxide and carboxylate anion[288] while the latter is the only tautomer for $[Trp\ -H]^-$.[289] In the GFP model chromophore, p-hydroxybenzylidene-2-3dimethylimidazolone anion ($HBDI^-$), competition between photodetachment and photofragmentation occurs at the band origin,[290] emphasizing that the $S_1\ ^1\pi\pi^*$ is a bound state in the Franck-Condon region of the anion[291] with a sub-picosecond dynamics followed by IC.[292,293] Neutral reaction dynamics studied through photoelectron spectroscopy and photoelectron-photoion coincidence experiments of small anionic molecules and clusters have been well documented.[294,295] Nevertheless, fundamental questions regarding the neutral radical issued from photodetachment of deprotonated aromatic amino acids and related compounds remain mostly unanswered to date,[296] although a few studies have been devoted to the formation and fragmentation of radical peptides anions.[297–299] Finally, radical peptide cations, which are of prime importance in catalysis in biological systems, show a rich fragmentation chemistry through collision activation, involving radical migration and electron transfer, sharing similarity with the specific photofragmentation channel observed for the protonated species, such as C_α-N and C_α-C_β bond cleavages.[300–303] Pump-probe photodissociation experiments would certainly reveal the excited state dynamics of these radical aromatic peptides.

ACKNOWLEDGMENT

The authors thank financial supports from the ANR Research grants ANR-2010-BLANC-040501 and ANR-17-CE05-0005-01, the RTRA "Triangle de la Physique" (COMOVA and COMOVA II), the University Paris Sud, Aix-Marseille University, GDR EMIE and LUMAT federation (LUMAT FR 2764). The authors acknowledge discussions with C. Dedonder-Lardeux and M. Broquier.

Authors Information

* Corresponding author: E-mail: gilles.gregoire@u-psud.fr

ORCID

Satchin Soorkia: 0000-0003-4635-2864

Christophe Jouvet: 0000-0002-4071-6455

Gilles Grégoire: 0000-0002-8577-3621

Biographies

Satchin Soorkia is Associate Professor in the department of Chemistry at Université Paris-Sud. He received his PhD degree in Chemical Physics from Université Paris-Sud - Laboratoire Francis Perrin CEA/DSM/IRAMIS/SPAM (2005-2008). He, then, continued as a postdoctoral fellow at University of California, Berkeley, to conduct laboratory research for planetary atmospheres at the Advanced Light Source Synchrotron, before joining the faculty at Université Paris-Sud and Institut des Sciences Moléculaires d'Orsay in 2010. His research is focused on photoinduced processes in charged molecular species of biological interest such as DNA/RNA bases and small peptides.

Christophe Jouvet earned a PhD (electronic relaxation of glyoxal in a supersonic jet) at the University Paris-Sud in Orsay, then spent one year in 1981 as a post-doctoral fellow at the

University of Chicago with Prof. S. A. Rice. He completed his "thèse d'état" (reactivity and electronic relaxation in mercury van der Waals complexes) in 1985. He got a permanent position as CNRS Researcher in the Photophysics Lab in Orsay. He became Research Director in 1994 and move to Aix Marseille University in 2012. He is director of the International French-Argentina Laboratory LEMIR. His first researches were focused on the reactivity of small molecular clusters. Since 20 years, his research is devoted to unravel the excited state properties of protonated molecules.

Gilles Grégoire got his PhD in Physics in 1999 at the University Pierre and Marie Curie in Paris. He spent a first post doc at the University of Paris Sud, Orsay, with Pr. Christophe Jouvet and a second one at the University of Georgia, USA, in the group of Mike Duncan. In 2001, he got a permanent research position at the French National Scientific Research Center (CNRS) at the Laser Physics Lab. in University Paris North. In 2013, he became a senior scientist and moved in 2015 to the Institute of Molecular Science of Orsay at University Paris Sud. His research focusses on spectroscopy, photophysics and photochemistry of molecules of biological interest in the gas phase and in particular on fundamental properties and dynamical processes in molecular excited states.

REFERENCES

(1) Chalfie, M.; Tu, Y.; Euskirchen, G.; Ward, W.; Prasher, D. Green Fluorescent Protein as a Marker for Gene Expression. *Science.* **1994**, *263*, 802–805.

(2) Tsien, R. Y. The Green Fluorescent Protein. *Annu. Rev. Biochem.* **1998**, *67*, 509–544.

(3) Betzig, E.; Patterson, G. H.; Sougrat, R.; Lindwasser, O. W.; Olenych, S.; Bonifacino, J. S.; Davidson, M. W.; Lippincott-Schwartz, J.; Hess, H. F. Imaging Intracellular Fluorescent Proteins at Nanometer Resolution. *Science.* **2006**, *313*, 1642–1645.

(4) Giepmans, B. N. G.; Adams, S. R.; Ellisman, M. H.; Tsien, R. Y. The Fluorescent Toolbox for Assessing Protein Location and Function. *Science.* **2006**, *312*, 217–224.

(5) Day, R. N.; Davidson, M. W. The Fluorescent Protein Palette: Tools for Cellular Imaging. *Chem. Soc. Rev.* **2009**, *38*, 2887.

(6) Zimmer, M. GFP: From Jellyfish to the Nobel Prize and Beyond. *Chem. Soc. Rev.* **2009**, *38*, 2823.

(7) Meech, S. R. Excited State Reactions in Fluorescent Proteins. *Chem. Soc. Rev.* **2009**, *38*, 2922.

(8) Wachter, R. M.; Watkins, J. L.; Kim, H. Mechanistic Diversity of Red Fluorescence Acquisition by GFP-like Proteins. *Biochemistry* **2010**, *49*, 7417–7427.

(9) Dedecker, P.; De Schryver, F. C.; Hofkens, J. Fluorescent Proteins: Shine on, You Crazy Diamond. *J. Am. Chem. Soc.* **2013**, *135*, 2387–2402.

(10) Mishin, A. S.; Belousov, V. V; Solntsev, K. M.; Lukyanov, K. A. Novel Uses of Fluorescent Proteins. *Curr. Opin. Chem. Biol.* **2015**, *27*, 1–9.

(11) Acharya, A.; Bogdanov, A. M.; Grigorenko, B. L.; Bravaya, K. B.; Nemukhin, A. V.; Lukyanov, K. A.; Krylov, A. I. Photoinduced Chemistry in Fluorescent Proteins: Curse or Blessing? *Chem. Rev.* **2017**, *117*, 758–795.

(12) Curchod, B. F. E.; Martínez, T. J. Ab Initio Nonadiabatic Quantum Molecular Dynamics. *Chem. Rev.* **2018**, *118*, 3305–3336.

(13) Crespo-Otero, R.; Barbatti, M. Recent Advances and Perspectives on Nonadiabatic Mixed Quantum–Classical Dynamics. *Chem. Rev.* **2018**, *118*, 7026–7068.

(14) Lischka, H.; Nachtigallová, D.; Aquino, A. J. A.; Szalay, P. G.; Plasser, F.; Machado, F. B. C.; Barbatti, M. Multireference Approaches for Excited States of Molecules. *Chem. Rev.* **2018**, *118*, 7293–7361.

(15) Barbatti, M.; Borin, A. C.; Ullrich, S. *Photoinduced Phenomena in Nucleic Acids I: Nucleobases in the Gas Phase and in Solvents*; 2015; Vol. 355.

(16) Barbatti, M.; Borin, A. C.; Ullrich, S. *Photoinduced Phenomena in Nucleic Acids II: DNA Fragments and Phenomenological Aspects*; 2015; Vol. 356.

(17) Improta, R.; Santoro, F.; Blancafort, L. Quantum Mechanical Studies on the Photophysics and the Photochemistry of Nucleic Acids and Nucleobases. *Chem. Rev.* **2016**, *116*, 3540–3593.

(18) Tanaka, K. The Origin of Macromolecule Ionization by Laser Irradiation (Nobel Lecture). *Angew. Chemie Int. Ed.* **2003**, *42*, 3860–3870.

(19) Fenn, J. B. Electrospray Wings for Molecular Elephants (Nobel Lecture). *Angew. Chemie Int. Ed.* **2003**, *42*, 3871–3894.

(20) Zhang, Z.; Smith, D. L. Determination of Amide Hydrogen Exchange by Mass Spectrometry: A New Tool for Protein Structure Elucidation. *Protein Sci.* **1993**, *2*, 522–531.

(21) Engen, J. R.; Smith, D. L. Peer Reviewed: Investigating Protein Structure and Dynamics by Hydrogen Exchange MS. *Anal. Chem.* **2008**, *73*, 256 A-265 A.

(22) Konermann, L.; Pan, J.; Liu, Y.-H. Hydrogen Exchange Mass Spectrometry for Studying Protein Structure and Dynamics. *Chem. Soc. Rev.* **2011**, *40*, 1224–1234.

(23) Sharp, J. S.; Becker, J. M.; Hettich, R. L. Analysis of Protein Solvent Accessible Surfaces by Photochemical Oxidation and Mass Spectrometry. *Anal. Chem.* **2004**, *76*, 672–683.

(24) Mendoza, V. L.; Vachet, R. W. Probing Protein Structure by Amino Acid-Specific Covalent Labeling and Mass Spectrometry. *Mass Spectrom. Rev.* **2009**, *28*, 785–815.

(25) Jarrold, M. F. Peptides and Proteins in the Vapor Phase. *Annu. Rev. Phys. Chem.* **2000**, *51*, 179–207.

(26) Kanu, A. B.; Dwivedi, P.; Tam, M.; Matz, L.; Hill, H. H. Ion Mobility-Mass Spectrometry. *J. Mass Spectrom.* **2008**, *43*, 1–22.

(27) Bernstein, S. L.; Dupuis, N. F.; Lazo, N. D.; Wyttenbach, T.; Condron, M. M.; Bitan, G.; Teplow, D. B.; Shea, J.-E.; Ruotolo, B. T.; Robinson, C. V.; et al. Amyloid-β Protein Oligomerization and the Importance of Tetramers and Dodecamers in the Aetiology of Alzheimer's Disease. *Nat. Chem.* **2009**, *1*, 326–331.

(28) Wysocki, V. H.; Tsaprailis, G.; Smith, L. L.; Breci, L. A. Mobile and Localized Protons: A Framework for Understanding Peptide Dissociation. *J. Mass Spectrom.* **2000**, *35*, 1399–1406.

(29) Paizs, B.; Suhai, S. Fragmentation Pathways of Protonated Peptides. *Mass Spectrom. Rev.* **2005**, *24*, 508–548.

(30) Zubarev, R. A. Electron-Capture Dissociation Tandem Mass Spectrometry. *Curr. Opin. Biotechnol.* **2004**, *15*, 12–16.

(31) Cooper, H. J.; Håkansson, K.; Marshall, A. G. The Role of Electron Capture Dissociation in Biomolecular Analysis. *Mass Spectrom. Rev.* **2005**, *24*, 201–222.

(32) Syrstad, E. A.; Turecček, F. Toward a General Mechanism of Electron Capture Dissociation. *J. Am. Soc. Mass Spectrom.* **2005**, *16*, 208–224.

(33) Grégoire, G.; Gaigeot, M. P.; Marinica, D. C.; Lemaire, J.; Schermann, J. P.; Desfrançois, C. Resonant Infrared Multiphoton Dissociation Spectroscopy of Gas-Phase

Protonated Peptides. Experiments and Car–Parrinello Dynamics at 300 K. *Phys. Chem. Chem. Phys.* **2007**, *9*, 3082–3097.

(34) Polfer, N. C.; Oomens, J.; Dunbar, R. C. Alkali Metal Complexes of the Dipeptides PheAla and AlaPhe: IRMPD Spectroscopy. *ChemPhysChem* **2008**, *9*, 579–589.

(35) Brodbelt, J. S.; Wilson, J. J. Infrared Multiphoton Dissociation in Quadrupole Ion Traps. *Mass Spectrom. Rev.* **2009**, *28*, 390–424.

(36) Reilly, J. P. Ultraviolet Photofragmentation of Biomolecular Ions. *Mass Spectrom. Rev.* **2009**, *28*, 425–447.

(37) Antoine, R.; Dugourd, P. Visible and Ultraviolet Spectroscopy of Gas Phase Protein Ions. *Phys. Chem. Chem. Phys.* **2011**, *13*, 16494–16509.

(38) Dedonder, C.; Féraud, G.; Jouvet, C. Excited-State Dynamics of Protonated Aromatic Amino Acids. In *Photophysics of Ionic Biochromophores*; Brøndsted Nielsen, S., Wyer, J. A., Eds.; Springer, Berlin, Heidelberg, 2013; pp 155–180.

(39) Staniforth, M.; Stavros, V. G. Recent Advances in Experimental Techniques to Probe Fast Excited-State Dynamics in Biological Molecules in the Gas Phase: Dynamics in Nucleotides, Amino Acids and Beyond. *Proc. R. Soc. A Math. Phys. Eng. Sci.* **2013**, *469*, 20130458–20130458.

(40) Sobolewski, A. L.; Domcke, W.; Dedonder-Lardeux, C.; Jouvet, C. Excited-State Hydrogen Detachment and Hydrogen Transfer Driven by Repulsive 1πσ* States: A New Paradigm for Nonradiative Decay in Aromatic Biomolecules. *Phys. Chem. Chem. Phys.* **2002**, *4*, 1093–1100.

(41) Pino, G. A.; Oldani, A. N.; Marceca, E.; Fujii, M.; Ishiuchi, S.-I.; Miyazaki, M.;

Broquier, M.; Dedonder, C.; Jouvet, C. Excited State Hydrogen Transfer Dynamics in Substituted Phenols and Their Complexes with Ammonia: ππ∗-πσ∗ Energy Gap Propensity and Ortho -Substitution Effect. *J. Chem. Phys.* **2010**, *133*, 124313.

(42) Roberts, G. M.; Chatterley, A. S.; Young, J. D.; Stavros, V. G. Direct Observation of Hydrogen Tunneling Dynamics in Photoexcited Phenol. *J. Phys. Chem. Lett.* **2012**, *3*, 348–352.

(43) Sur, A.; Johnson, P. M. Radiationless Transitions in Gas Phase Phenol and the Effects of Hydrogen Bonding. *J. Chem. Phys.* **1986**, *84*, 1206–1209.

(44) Lipert, R. J.; Colson, S. D. Deuterium Isotope Effects on S1 Radiationless Decay in Phenol and on Intermolecular Vibrations in the Phenol-Water Complex. *J. Phys. Chem.* **1989**, *93*, 135–139.

(45) Lan, Z.; Domcke, W.; Vallet, V.; Sobolewski, A. L.; Mahapatra, S. Time-Dependent Quantum Wave-Packet Description of the $^1\pi\sigma^*$ Photochemistry of Phenol. *J. Chem. Phys.* **2005**, *122*, 224315.

(46) Vieuxmaire, O. P. J.; Lan, Z.; Sobolewski, A. L.; Domcke, W. Ab Initio Characterization of the Conical Intersections Involved in the Photochemistry of Phenol. *J. Chem. Phys.* **2008**, *129*, 224307.

(47) King, G. A.; Oliver, T. A. A.; Nix, M. G. D.; Ashfold, M. N. R. High Resolution Photofragment Translational Spectroscopy Studies of the Ultraviolet Photolysis of Phenol- d_5. *J. Phys. Chem. A* **2009**, *113*, 7984–7993.

(48) Yang, K. R.; Xu, X.; Zheng, J.; Truhlar, D. G. Full-Dimensional Potentials and State Couplings and Multidimensional Tunneling Calculations for the Photodissociation of Phenol. *Chem. Sci.* **2014**, *5*, 4661–4680.

(49) Xu, X.; Zheng, J.; Yang, K. R.; Truhlar, D. G. Photodissociation Dynamics of Phenol: Multistate Trajectory Simulations Including Tunneling. *J. Am. Chem. Soc.* **2014**, *136*, 16378–16386.

(50) Nix, M. G. D.; Devine, A. L.; Cronin, B.; Dixon, R. N.; Ashfold, M. N. R. High Resolution Photofragment Translational Spectroscopy Studies of the near Ultraviolet Photolysis of Phenol. *J. Chem. Phys.* **2006**, *125*, 133318.

(51) Ashfold, M. N. R.; Devine, A. L.; Dixon, R. N.; King, G. A.; Nix, M. G. D.; Oliver, T. A. A. Exploring Nuclear Motion through Conical Intersections in the UV Photodissociation of Phenols and Thiophenol. *Proc. Natl. Acad. Sci. U. S. A.* **2008**, *105*, 12701–12706.

(52) Dixon, R. N.; Oliver, T. A. A.; Ashfold, M. N. R. Tunnelling under a Conical Intersection: Application to the Product Vibrational State Distributions in the UV Photodissociation of Phenols. *J. Chem. Phys.* **2011**, *134*, 194303.

(53) Tseng, C. M.; Lee, Y. T.; Ni, C. K. H Atom Elimination from the πσ* State in the Photodissociation of Phenol. *J. Chem. Phys.* **2004**, *121*, 2459–2461.

(54) Woo, K. C.; Kim, S. K. Multidimensional H Atom Tunneling Dynamics of Phenol: Interplay between Vibrations and Tunneling. *J. Phys. Chem. A* **2019**, *123*, 1529–1537.

(55) Lai, H. Y.; Jhang, W. R.; Tseng, C.-M. Communication: Mode-Dependent Excited-State Lifetime of Phenol under the S_1/S_2 Conical Intersection. *J. Chem. Phys.* **2018**, *149*, 031104.

(56) Schick, C. P.; Carpenter, S. D.; Weber, P. M. Femtosecond Multiphoton Ionization Photoelectron Spectroscopy of the S 2 State of Phenol. *J. Phys. Chem. A* **1999**, *103*, 10470–10476.

(57) Livingstone, R. A.; Thompson, J. O. F.; Iljina, M.; Donaldson, R. J.; Sussman, B. J.;

Paterson, M. J.; Townsend, D. Time-Resolved Photoelectron Imaging of Excited State Relaxation Dynamics in Phenol, Catechol, Resorcinol, and Hydroquinone. *J. Chem. Phys.* **2012**, *137*, 184304.

(58) Ashfold, M. N. R. The Role of πσ* Excited States in the Photodissociation of Heteroaromatic Molecules. *Science.* **2006**, *312*, 1637–1640.

(59) Solgadi, D.; Jouvet, C.; Tramer, A. Resonance-Enhanced Multiphoton Ionization Spectra and Ionization Thresholds of Phenol-(Ammonia)n Clusters. *J. Phys. Chem.* **1988**, *92*, 3313–3315.

(60) Syage, J. A.; Steadman, J. Picosecond Measurements of Phenol Excited-state Proton Transfer in Clusters. I. Solvent Basicity and Cluster Size Effects. *J. Chem. Phys.* **1991**, *95*, 2497–2510.

(61) Syage, J. A. Ultrafast Measurements of Chemistry in Clusters: Excited-State Proton Transfer. *J. Phys. Chem.* **1995**, *99*, 5772–5786.

(62) Schmitt, M.; Jacoby, C.; Gerhards, M.; Unterberg, C.; Roth, W.; Kleinermanns, K. Structures and Vibrations of Phenol$(NH_3)_{2–4}$ Clusters. *J. Chem. Phys.* **2000**, *113*, 2995–3001.

(63) Grégoire, G.; Dedonder-Lardeux, C.; Jouvet, C.; Martrenchard, S.; Solgadi, D. Has the Excited State Proton Transfer Ever Been Observed in Phenol−$(NH_3)_n$ Molecular Clusters? *J. Phys. Chem. A* **2001**, *105*, 5971–5976.

(64) Pino, G. A.; Dedonder-Lardeux, C.; Grégoire, G.; Jouvet, C.; Martrenchard, S.; Solgadi, D. Intracluster Hydrogen Transfer Followed by Dissociation in the Phenol–$(NH_3)_3$ Excited State: $PhOH(S_1)–(NH_3)_3 \rightarrow PhO^{\bullet+}(NH_4)(NH_3)_2$. *J. Chem. Phys.* **1999**, *111*, 10747–10749.

(65) Ishiuchi, S. I.; Daigoku, K.; Saeki, M.; Sakai, M.; Hashimoto, K.; Fujii, M. Hydrogen

Transfer in Photoexcited Phenol/Ammonia Clusters by UV-IR-UV Ion Dip Spectroscopy and Ab Initio Molecular Orbital Calculations. I. Electronic Transitions. *J. Chem. Phys.* **2002**, *117*, 7077–7082.

(66) Ishiuchi, S.; Daigoku, K.; Saeki, M.; Sakai, M.; Hashimoto, K.; Fujii, M. Hydrogen Transfer in Photo-Excited Phenol/Ammonia Clusters by UV–IR–UV Ion Dip Spectroscopy and Ab Initio Molecular Orbital Calculations. II. Vibrational Transitions. *J. Chem. Phys.* **2002**, *117*, 7083–7093.

(67) Sobolewski, A. L.; Domcke, W. Photoinduced Electron and Proton Transfer in Phenol and Its Clusters with Water and Ammonia. *J. Phys. Chem. A* **2001**, *105*, 9275–9283.

(68) Miyazaki, M.; Ohara, R.; Daigoku, K.; Hashimoto, K.; Woodward, J. R.; Dedonder, C.; Jouvet, C.; Fujii, M. Electron-Proton Decoupling in Excited-State Hydrogen Atom Transfer in the Gas Phase. *Angew. Chemie Int. Ed.* **2015**, *54*, 15089–15093.

(69) Miyazaki, M.; Ohara, R.; Dedonder, C.; Jouvet, C.; Fujii, M. Electron-Proton Transfer Mechanism of Excited-State Hydrogen Transfer in Phenol-$(NH_3)_n$ (n= 3 and 5). *Chem. - A Eur. J.* **2018**, *24*, 881–890.

(70) Hause, M. L.; Heidi Yoon, Y.; Case, A. S.; Crim, F. F. Dynamics at Conical Intersections: The Influence of O–H Stretching Vibrations on the Photodissociation of Phenol. *J. Chem. Phys.* **2008**, *128*, 104307.

(71) An, H.; Baeck, K. K. Quantum Wave Packet Propagation Study of the Photochemistry of Phenol: Isotope Effects (Ph-OD) and the Direct Excitation to the $^1\pi\sigma^*$ State. *J. Phys. Chem. A* **2011**, *115*, 13309–13315.

(72) Lin, Y.-C.; Lee, C.; Lee, S.-H.; Lee, Y.-Y.; Lee, Y. T.; Tseng, C.-M.; Ni, C.-K. Excited-

State Dissociation Dynamics of Phenol Studied by a New Time-Resolved Technique. *J. Chem. Phys.* **2018**, *148*, 074306.

(73) Tseng, C.-M.; Lee, Y. T.; Lin, M.-F.; Ni, C.-K.; Liu, S.-Y.; Lee, Y.-P.; Xu, Z. F.; Lin, M. C. Photodissociation Dynamics of Phenol. *J. Phys. Chem. A* **2007**, *111*, 9463–9470.

(74) Tseng, C.-M.; Lin, M.-F.; Yang, Y. L.; Ho, Y. C.; Ni, C.-K.; Chang, J.-L. Photostability of Amino Acids: Photodissociation Dynamics of Phenylalanine Chromophores. *Phys. Chem. Chem. Phys.* **2010**, *12*, 4989.

(75) Duncan, M. A.; Dietz, T. G.; Liverman, M. G.; Smalley, R. E. Photoionization Measurement of the Triplet Lifetime of Benzene. *J. Phys. Chem.* **1981**, *85*, 7–9.

(76) Stephenson, T. A.; Rice, S. A. Vibrational State Dependence of Radiationless Processes in $^1B_{2u}$ Benzene. *J. Chem. Phys.* **1984**, *81*, 1073–1082.

(77) Sekreta, E.; Reilly, J. P. Direct Observation of Intersystem Crossing in Benzene by Laser Photoelectron Spectroscopy. *Chem. Phys. Lett.* **1988**, *149*, 482–486.

(78) Callomon, J. H.; Parkin, J. E.; Lopez-Delgado, R. Non-Radiative Relaxation of the Excited Ã 1B2u State of Benzene. *Chem. Phys. Lett.* **1972**, *13*, 125–131.

(79) Féraud, G.; Pino, T.; Falvo, C.; Parneix, P.; Combriat, T.; Bréchignac, P. Intramolecular Processes Revealed Using UV-Laser-Induced IR-Fluorescence: A New Perspective on the "Channel Three" of Benzene. *J. Phys. Chem. Lett.* **2014**, *5*, 1083–1090.

(80) Radloff, W.; Stert, V.; Freudenberg, T.; Hertel, I. .; Jouvet, C.; Dedonder-Lardeux, C.; Solgadi, D. Internal Conversion in Highly Excited Benzene and Benzene Dimer: Femtosecond Time-Resolved Photoelectron Spectroscopy. *Chem. Phys. Lett.* **1997**, *281*, 20–26.

(81) Minns, R. S.; Parker, D. S. N.; Penfold, T. J.; Worth, G. A.; Fielding, H. H. Competing

Ultrafast Intersystem Crossing and Internal Conversion in the “Channel 3” Region of Benzene. *Phys. Chem. Chem. Phys.* **2010**, *12*, 15607.

(82) Palmer, I. J.; Ragazos, I. N.; Bernardi, F.; Olivucci, M.; Robb, M. A. An MC-SCF Study of the S1 and S2 Photochemical Reactions of Benzene. *J. Am. Chem. Soc.* **1993**, *115*, 673–682.

(83) Sobolewski, A. L.; Woywod, C.; Domcke, W. Ab Initio Investigation of Potential-Energy Surfaces Involved in the Photophysics of Benzene and Pyrazine. *J. Chem. Phys.* **1993**, *98*, 5627–5641.

(84) Huang, C.-L.; Jiang, J.-C.; Lee, Y. T.; Ni, C.-K. Photodissociation of Ethylbenzene and n -Propylbenzene in a Molecular Beam. *J. Chem. Phys.* **2002**, *117*, 7034–7040.

(85) Chen, Y.; Barkley, M. D. Toward Understanding Tryptophan Fluorescence in Proteins. *Biochemistry* **1998**, *37*, 9976–9982.

(86) Vivian, J. T.; Callis, P. R. Mechanisms of Tryptophan Fluorescence Shifts in Proteins. *Biophys. J.* **2001**, *80*, 2093–2109.

(87) Callis, P. R.; Liu, T. Quantitative Prediction of Fluorescence Quantum Yields for Tryptophan in Proteins. *J. Phys. Chem. B* **2004**, *108*, 4248–4259.

(88) Callis, P. R.; Petrenko, A.; Muiño, P. L.; Tusell, J. R. Ab Initio Prediction of Tryptophan Fluorescence Quenching by Protein Electric Field Enabled Electron Transfer. *J. Phys. Chem. B* **2007**, *111*, 10335–10339.

(89) Platt, J. R. Classification of Spectra of Cata-Condensed Hydrocarbons. *J. Chem. Phys.* **1949**, *17*, 484–495.

(90) Giussani, A.; Merchán, M.; Roca-Sanjuán, D.; Lindh, R. Essential on the Photophysics and Photochemistry of the Indole Chromophore by Using a Totally Unconstrained Theoretical

Approach. *J. Chem. Theory Comput.* **2011**, *7*, 4088–4096.

(91) Bersohn, R.; Even, U.; Jortner, J. Fluorescence Excitation Spectra of Indole, 3-methyl Indole, and 3-indole Acetic Acid in Supersonic Jets. *J. Chem. Phys.* **1984**, *80*, 1050–1058.

(92) Hager, J. W.; Demmer, D. R.; Wallace, S. C. Electronic Spectra of Jet-Cooled Indoles: Evidence for the ^1L_a State. *J. Phys. Chem.* **1987**, *91*, 1375–1382.

(93) Arnold, S.; Sulkes, M. Spectroscopy of Solvent Complexes with Indoles: Induction of ^1L_a-^1L_b State Coupling. *J. Phys. Chem.* **1992**, *96*, 4768–4778.

(94) Zwier, T. S. The Spectroscopy of Solvation in Hydrogen-Bonded Aromatic Clusters. *Annu. Rev. Phys. Chem.* **1996**, *47*, 205–241.

(95) Dian, B. C.; Longarte, A.; Zwier, T. S. Hydride Stretch Infrared Spectra in the Excited Electronic States of Indole and Its Derivatives: Direct Evidence for the $^1\pi\sigma^*$ State. *J. Chem. Phys.* **2003**, *118*, 2696.

(96) Küpper, J.; Pratt, D. W.; Meerts, W. L.; Brand, C.; Tatchen, J.; Schmitt, M. Vibronic Coupling in Indole: II. Investigation of the ^1L_a–^1L_b Interaction Using Rotationally Resolved Electronic. *Phys. Chem. Chem. Phys.* **2010**, *12*, 4980–4988.

(97) Brand, C.; Küpper, J.; Pratt, D. W.; Meerts, W. L.; Krügler, D.; Tatchen, J.; Schmitt, M. Molecular Mechanisms of the Photostability of Life. *Phys. Chem. Chem. Phys.* **2010**, *12*, 4897.

(98) Iqbal, A.; Stavros, V. G. Exploring the Time Scales of H-Atom Elimination from Photoexcited Indole. *J. Phys. Chem. A* **2010**, *114*, 68–72.

(99) Livingstone, R.; Schalk, O.; Boguslavskiy, A. E.; Wu, G.; Bergendahl, L. T.; Stolow, A.; Paterson, M. J.; Townsend, D. Following the Excited State Relaxation Dynamics of Indole and 5-Hydroxyindole Using Time-Resolved Photoelectron Spectroscopy. *J. Chem. Phys.* **2011**,

135, 194307.

(100) Serrano-Andrés, L.; Roos, B. O. Theoretical Study of the Absorption and Emission Spectra of Indole in the Gas Phase and in a Solvent. *J. Am. Chem. Soc.* **1996**, *118*, 185–195.

(101) Sobolewski, A. L.; Domcke, W. Ab Initio Investigations on the Photophysics of Indole. *Chem. Phys. Lett.* **1999**, *315*, 293–298.

(102) Borin, A. C.; Serrano-Andrés, L. A Theoretical Study of the Absorption Spectra of Indole and Its Analogs: Indene, Benzimidazole, and 7-Azaindole. *Chem. Phys.* **2000**, *262*, 253–265.

(103) Brisker-Klaiman, D.; Dreuw, A. Explaining Level Inversion of the L_a and L_b States of Indole and Indole Derivatives in Polar Solvents. *ChemPhysChem* **2015**, *16*, 1695–1702.

(104) Montero, R.; Conde, Á. P.; Ovejas, V.; Castaño, F.; Longarte, A. Ultrafast Photophysics of the Isolated Indole Molecule. *J. Phys. Chem. A* **2012**, *116*, 2698–2703.

(105) Dedonder-Lardeux, C.; Grosswasser, D.; Jouvet, C.; Martrenchard, S. Dissociative Hydrogen Transfer in Indole–$(NH_3)_n$ Clusters. *PhysChemComm* **2001**, *4*, 21–23.

(106) Lippert, H.; Stert, V.; Hesse, L.; Schulz, C. P.; Hertel, I. V.; Radloff, W. Ultrafast Photoinduced Processes in Indole–Water Clusters. *Chem. Phys. Lett.* **2003**, *376*, 40–48.

(107) Nix, M. G. D.; Devine, A. L.; Cronin, B.; Ashfold, M. N. R. High Resolution Photofragment Translational Spectroscopy of the near UV Photolysis of Indole: Dissociation via the $^1\pi\sigma^*$ State. *Phys. Chem. Chem. Phys.* **2006**, *8*, 2610–2618.

(108) Oliver, T. a a; King, G. a; Ashfold, M. N. R. Position Matters: Competing O-H and N-H Photodissociation Pathways in Hydroxy- and Methoxy-Substituted Indoles. *Phys. Chem. Chem. Phys.* **2011**, *13*, 14646–14662.

(109) Eftink, M. R. The Use of Fluorescence Methods to Monitor Unfolding Transitions in Proteins. *Biophys. J.* **1994**, *66*, 482–501.

(110) Eftink, M. R. Fluorescence Techniques for Studying Protein Structure. In *Methods of Biochemical Analysis*; John Wiley & Sons, Ltd, 2006; pp 127–205.

(111) Lakowicz, J. R. On Spectral Relaxation in Proteins. *Photochem. Photobiol.* **2000**, *72*, 421.

(112) Engelborghs, Y. The Analysis of Time Resolved Protein Fluorescence in Multi-Tryptophan Proteins. *Spectrochim. Acta Part A Mol. Biomol. Spectrosc.* **2001**, *57*, 2255–2270.

(113) *Principles of Fluorescence Spectroscopy*; Lakowicz, J. R., Ed.; Springer US: Boston, MA, 2006.

(114) Broos, J.; Tveen-Jensen, K.; de Waal, E.; Hesp, B. H.; Jackson, J. B.; Canters, G. W.; Callis, P. R. The Emitting State of Tryptophan in Proteins with Highly Blue-Shifted Fluorescence. *Angew. Chemie Int. Ed.* **2007**, *46*, 5137–5139.

(115) Alston, R. W.; Lasagna, M.; Grimsley, G. R.; Scholtz, J. M.; Reinhart, G. D.; Pace, C. N. Peptide Sequence and Conformation Strongly Influence Tryptophan Fluorescence. *Biophys. J.* **2008**, *94*, 2280–2287.

(116) Pan, C.-P.; Muiño, P. L.; Barkley, M. D.; Callis, P. R. Correlation of Tryptophan Fluorescence Spectral Shifts and Lifetimes Arising Directly from Heterogeneous Environment. *J. Phys. Chem. B* **2011**, *115*, 3245–3253.

(117) Callis, P. R. Binding Phenomena and Fluorescence Quenching. I: Descriptive Quantum Principles of Fluorescence Quenching Using a Supermolecule Approach. *J. Mol. Struct.* **2014**, *1077*, 14–21.

(118) Callis, P. R. Binding Phenomena and Fluorescence Quenching. II: Photophysics of Aromatic Residues and Dependence of Fluorescence Spectra on Protein Conformation. *J. Mol. Struct.* **2014**, *1077*, 22–29.

(119) Eftink, M. R. Fluorescence Techniques for Studying Protein Structure; John Wiley & Sons, Ltd, 1991; pp 127–205.

(120) Callis, P. R.; Vivian, J. T. Understanding the Variable Fluorescence Quantum Yield of Tryptophan in Proteins Using QM-MM Simulations. Quenching by Charge Transfer to the Peptide Backbone. *Chem. Phys. Lett.* **2003**, *369*, 409–414.

(121) Chen, Y.; Liu, B.; Yu, H.-T.; Barkley, M. D. The Peptide Bond Quenches Indole Fluorescence. *J. Am. Chem. Soc.* **1996**, *118*, 9271–9278.

(122) McMahon, L. P.; Colucci, W. J.; McLaughlin, M. L.; Barkley, M. D. Deuterium Isotope Effects in Constrained Tryptophan Derivatives: Implications for Tryptophan Photophysics. *J. Am. Chem. Soc.* **1992**, *114*, 8442–8448.

(123) Yu, H. T.; Colucci, W. J.; McLaughlin, M. L.; Barkley, M. D. Fluorescence Quenching in Indoles by Excited-State Proton Transfer. *J. Am. Chem. Soc.* **1992**, *114*, 8449–8454.

(124) Blancafort, L.; González, D.; Olivucci, M.; Michael A. Robb. Quenching of Tryptophan $^{1}(\pi,\pi^*)$ Fluorescence Induced by Intramolecular Hydrogen Abstraction via an Aborted Decarboxylation Mechanism. *J. Am. Chem. Soc.* **2002**, *124*, 6398–6406.

(125) Sharma, D.; Léonard, J.; Haacke, S. Ultrafast Excited-State Dynamics of Tryptophan in Water Observed by Transient Absorption Spectroscopy. *Chem. Phys. Lett.* **2010**, *489*, 99–102.

(126) Pan, C.-P.; Barkley, M. D. Conformational Effects on Tryptophan Fluorescence in Cyclic Hexapeptides. *Biophys. J.* **2004**, *86*, 3828–3835.

(127) Szabo, A. G.; Rayner, D. M. Fluorescence Decay of Tryptophan Conformers in Aqueous Solution. *J. Am. Chem. Soc.* **1980**, *102*, 554–563.

(128) Adams, P. D.; Chen, Y.; Ma, K.; Zagorski, M. G.; Sönnichsen, F. D.; McLaughlin, M. L.; Barkley, M. D. Intramolecular Quenching of Tryptophan Fluorescence by the Peptide Bond in Cyclic Hexapeptides. *J. Am. Chem. Soc.* **2002**, *124*, 9278–9286.

(129) Cable, J. R.; Tubergen, M. J.; Levy, D. H. Electronic Spectroscopy of Small Tryptophan Peptides in Supersonic Molecular Beams. *J. Am. Chem. Soc.* **1988**, *110*, 7349–7355.

(130) Meijer, G.; de Vries, M. S.; Hunziker, H. E.; Wendt, H. R. Laser Desorption Jet-Cooling of Organic Molecules. *Appl. Phys. B* **1990**, *51*, 395–403.

(131) Piuzzi, F.; Dimicoli, I.; Mons, M.; Tardivel, B.; Zhao, Q. A Simple Laser Vaporization Source for Thermally Fragile Molecules Coupled to a Supersonic Expansion: Application to the Spectroscopy of Tryptophan. *Chem. Phys. Lett.* **2000**, *320*, 282–288.

(132) Abo-Riziq, A.; Bushnell, J. E.; Crews, B.; Callahan, M.; Grace, L.; de Vries, M. S. Gas Phase Spectroscopy of the Pentapeptide FDASV. *Chem. Phys. Lett.* **2006**, *431*, 227–230.

(133) Abo-Riziq, A.; Crews, B. O.; Callahan, M. P.; Grace, L.; de Vries, M. S. Spectroscopy of Isolated Gramicidin Peptides. *Angew. Chemie Int. Ed.* **2006**, *45*, 5166–5169.

(134) Rizzo, T. R.; Park, Y. D.; Levy, D. H. Dispersed Fluorescence of Jet-cooled Tryptophan: Excited State Conformers and Intramolecular Exciplex Formation. *J. Chem. Phys.* **1986**, *85*, 6945–6951.

(135) Philips, L. A.; Webb, S. P.; Martinez, S. J.; Fleming, G. R.; Levy, D. H. Time-Resolved Spectroscopy of Tryptophan Conformers in a Supersonic Jet. *J. Am. Chem. Soc.* **1988**, *110*, 1352–1355.

(136) Park, Y. D.; Rizzo, T. R.; Peteanu, L. A.; Levy, D. H. Electronic Spectroscopy of Tryptophan Analogs in Supersonic Jets: 3-Indole Acetic Acid, 3-indole Propionic Acid, Tryptamine, and *N* -acetyl Tryptophan Ethyl Ester. *J. Chem. Phys.* **1986**, *84*, 6539–6549.

(137) Sipior, J.; Sulkes, M. Spectroscopy of Tryptophan Derivatives in Supersonic Expansions: Addition of Solvent Molecules. *J. Chem. Phys.* **1988**, *88*, 6146–6156.

(138) Tubergen, M. J.; Cable, J. R.; Levy, D. H. Substituent Effects on the Electronic Spectroscopy of Tryptophan Derivatives in Jet Expansions. *J. Chem. Phys.* **1990**, *92*, 51–60.

(139) Snoek, L. C.; Kroemer, R. T.; Hockridge, M. R.; Simons, J. P. Conformational Landscapes of Aromatic Amino Acids in the Gas Phase: Infrared and Ultraviolet Ion Dip Spectroscopy of Tryptophan. *Phys. Chem. Chem. Phys.* **2001**, *3*, 1819–1826.

(140) Nolting, D.; Marian, C.; Weinkauf, R. Protonation Effect on the Electronic Spectrum of Tryptophan in the Gas Phase. *Phys. Chem. Chem. Phys.* **2004**, *6*, 2633.

(141) Gindensperger, E.; Haegy, A.; Daniel, C.; Marquardt, R. Ab Initio Study of the Electronic Singlet Excited-State Properties of Tryptophan in the Gas Phase: The Role of Alanyl Side-Chain Conformations. *Chem. Phys.* **2010**, *374*, 104–110.

(142) Nguyen, T. V.; Pratt, D. W. Permanent Electric Dipole Moments of Four Tryptamine Conformers in the Gas Phase: A New Diagnostic of Structure and Dynamics. *J. Chem. Phys.* **2006**, *124*, 054317.

(143) Schmitt, M.; Brause, R.; Marian, C. M.; Salzmann, S.; Meerts, W. L. Electronically Excited States of Tryptamine and Its Microhydrated Complex. *J. Chem. Phys.* **2006**, *125*, 124309.

(144) Böhm, M.; Tatchen, J.; Krügler, D.; Kleinermanns, K.; Nix, M. G. D.; LeGreve, T. A.;

Zwier, T. S.; Schmitt, M. High-Resolution and Dispersed Fluorescence Examination of Vibronic Bands of Tryptamine: Spectroscopic Signatures for L_a/L_b Mixing near a Conical Intersection. *J. Phys. Chem. A* **2009**, *113*, 2456–2466.

(145) Carney, J. R.; Zwier, T. S. The Infrared and Ultraviolet Spectra of Individual Conformational Isomers of Biomolecules: Tryptamine. *J. Phys. Chem. A* **2000**, *104*, 8677–8688.

(146) Grace, L. I.; Cohen, R.; Dunn, T. .; Lubman, D. M.; de Vries, M. S. The R2PI Spectroscopy of Tyrosine: A Vibronic Analysis. *J. Mol. Spectrosc.* **2002**, *215*, 204–219.

(147) Iqbal, A.; Stavros, V. G. Active Participation of $^1\pi\sigma^*$ States in the Photodissociation of Tyrosine and Its Subunits. *J. Phys. Chem. Lett.* **2010**, *1*, 2274–2278.

(148) Ovejas, V.; Fernández-Fernández, M.; Montero, R.; Castaño, F.; Longarte, A. Ultrafast Nonradiative Relaxation Channels of Tryptophan. *J. Phys. Chem. Lett.* **2013**, *4*, 1928–1932.

(149) Zwier, T. S. Laser Probes of Conformational Isomerization in Flexible Molecules and Complexes. *J. Phys. Chem. A* **2006**, *110*, 4133–4150.

(150) Dian, B. C.; Longarte, A.; Mercier, S.; Evans, D. A.; Wales, D. J.; Zwier, T. S. The Infrared and Ultraviolet Spectra of Single Conformations of Methyl-Capped Dipeptides: N-Acetyl Tryptophan Amide and N-Acetyl Tryptophan Methyl Amide. *J. Chem. Phys.* **2002**, *117*, 10688–10702.

(151) Chin, W.; Piuzzi, F.; Dimicoli, I.; Mons, M. Probing the Competition between Secondary Structures and Local Preferences in Gas Phase Isolated Peptide Backbones. *Phys. Chem. Chem. Phys.* **2006**, *8*, 1033–1048.

(152) Sobolewski, A. L.; Domcke, W. Relevance of Electron-Driven Proton-Transfer

Processes for the Photostability of Proteins. *ChemPhysChem* **2006**, *7*, 561–564.

(153) Marazzi, M.; Sancho, U.; Castaño, O.; Domcke, W.; Frutos, L. M. Photoinduced Proton Transfer as a Possible Mechanism for Highly Efficient Excited-State Deactivation in Proteins. *J. Phys. Chem. Lett.* **2010**, *1*, 425–428.

(154) Shemesh, D.; Sobolewski, A. L.; Domcke, W. Role of Excited-State Hydrogen Detachment and Hydrogen-Transfer Processes for the Excited-State Deactivation of an Aromatic Dipeptide: N-Acetyl Tryptophan Methyl Amide. *Phys. Chem. Chem. Phys.* **2010**, *12*, 4899.

(155) Hünig, I.; Kleinermanns, K. Conformers of the Peptides Glycine-Tryptophan, Tryptophan-Glycine and Tryptophan-Glycine-Glycine as Revealed by Double Resonance Laser Spectroscopy. *Phys. Chem. Chem. Phys.* **2004**, *6*, 2650–2658.

(156) Řeha, D.; Valdés, H.; Vondrášek, J.; Hobza, P.; Abu-Riziq, A.; Crews, B.; de Vries, M. S. Structure and IR Spectrum of Phenylalanyl-Glycyl-Glycine Tripetide in the Gas-Phase: IR/UV Experiments, Ab Initio Quantum Chemical Calculations, and Molecular Dynamic Simulations. *Chem. - A Eur. J.* **2005**, *11*, 6803–6817.

(157) Valdes, H.; Spiwok, V.; Rezac, J.; Reha, D.; Abo-Riziq, A. G.; de Vries, M. S.; Hobza, P. Potential-Energy and Free-Energy Surfaces of Glycyl-Phenylalanyl-Alanine (GFA) Tripeptide: Experiment and Theory. *Chem. - A Eur. J.* **2008**, *14*, 4886–4898.

(158) Mons, M.; Piuzzi, F.; Dimicoli, I.; Gorb, L.; Leszczynski, J. Near-UV Resonant Two-Photon Ionization Spectroscopy of Gas Phase Guanine: Evidence for the Observation of Three Rare Tautomers. *J. Phys. Chem. A* **2006**, *110*, 10921–10924.

(159) Marian, C. M. The Guanine Tautomer Puzzle: Quantum Chemical Investigation of

Ground and Excited States. *J. Phys. Chem. A* **2007**, *111*, 1545–1553.

(160) Sobolewski, A. L.; Domcke, W.; Hättig, C. Tautomeric Selectivity of the Excited-State Lifetime of Guanine/Cytosine Base Pairs: The Role of Electron-Driven Proton-Transfer Processes. *Proc. Natl. Acad. Sci. U. S. A.* **2005**, *102*, 17903–17906.

(161) Shemesh, D.; Sobolewski, A. L.; Domcke, W. Efficient Excited-State Deactivation of the Gly-Phe-Ala Tripeptide via an Electron-Driven Proton-Transfer Process. *J. Am. Chem. Soc.* **2009**, *131*, 1374–1375.

(162) Mališ, M.; Loquais, Y.; Gloaguen, E.; Biswal, H. S.; Piuzzi, F.; Tardivel, B.; Brenner, V.; Broquier, M.; Jouvet, C.; Mons, M.; et al. Unraveling the Mechanisms of Nonradiative Deactivation in Model Peptides Following Photoexcitation of a Phenylalanine Residue. *J. Am. Chem. Soc.* **2012**, *134*, 20340–20351.

(163) Dŏslić, N.; Kovăcević, G.; Ljubić, I. Signature of the Conformational Preferences of Small Peptides: A Theoretical Investigation. *J. Phys. Chem. A* **2007**, *111*, 8650–8658.

(164) Mališ, M.; Loquais, Y.; Gloaguen, E.; Jouvet, C.; Brenner, V.; Mons, M.; Ljubić, I.; Došlić, N. Non-Radiative Relaxation of UV Photoexcited Phenylalanine Residues: Probing the Role of Conical Intersections by Chemical Substitution. *Phys. Chem. Chem. Phys.* **2014**, *16*, 2285.

(165) Loquais, Y.; Gloaguen, E.; Alauddin, M.; Brenner, V.; Tardivel, B.; Mons, M. On the near UV Photophysics of a Phenylalanine Residue: Conformation-Dependent ππ* State Deactivation Revealed by Laser Spectroscopy of Isolated Neutral Dipeptides. *Phys. Chem. Chem. Phys.* **2014**, *16*, 22192–22200.

(166) Mališ, M.; Došlić, N. Nonradiative Relaxation Mechanisms of UV Excited

Phenylalanine Residues: A Comparative Computational Study. *Molecules* **2017**, *22*, 493.

(167) Domcke, W.; Sobolewski, A. L. Spectroscopy Meets Theory. *Nat. Chem.* **2013**, *5*, 257–258.

(168) Kang, H.; Jouvet, C.; Dedonder-Lardeux, C.; Martrenchard, S.; Charrière, C.; Grégoire, G.; Desfrançois, C.; Schermann, J. P.; Barat, M.; Fayeton, J. A. Photoinduced Processes in Protonated Tryptamine. *J. Chem. Phys.* **2005**, *122*, 84307.

(169) Grégoire, G.; Jouvet, C.; Dedonder, C.; Sobolewski, A. L. On the Role of Dissociative πσ* States in the Photochemistry of Protonated Tryptamine and Tryptophan: An Ab Initio Study. *Chem. Phys.* **2006**, *324*, 398–404.

(170) Féraud, G.; Broquier, M.; Dedonder-Lardeux, C.; Grégoire, G.; Soorkia, S.; Jouvet, C. Photofragmentation Spectroscopy of Cold Protonated Aromatic Amines in the Gas Phase. *Phys. Chem. Chem. Phys.* **2014**, *16*, 5250–5259.

(171) Broquier, M.; Soorkia, S.; Grégoire, G. A Comprehensive Study of Cold Protonated Tyramine: UV Photodissociation Experiments and Ab Initio Calculations. *Phys. Chem. Chem. Phys.* **2015**, *17*, 25854–25862.

(172) Simons, J. P. Bio-Active Molecules in the Gas Phase. *Phys. Chem. Chem. Phys.* **2004**, *6*, E7.

(173) Andersen, J. U.; Cederquist, H.; Forster, J. S.; Huber, B. A.; Hvelplund, P.; Jensen, J.; Liu, B.; Manil, B.; Maunoury, L.; Brøndsted Nielsen, S.; et al. Photodissociation of Protonated Amino Acids and Peptides in an Ion Storage Ring. Determination of Arrhenius Parameters in the High-Temperature Limit. *Phys. Chem. Chem. Phys.* **2004**, *6*, 2676–2681.

(174) Kang, H.; Dedonder-Lardeux, C.; Jouvet, C.; Martrenchard, S.; Grégoire, G.;

Desfrançois, C.; Schermann, J.-P.; Barat, M.; Fayeton, J. A. Photo-Induced Dissociation of Protonated Tryptophan $TrpH^+$: A Direct Dissociation Channel in the Excited States Controls the Hydrogen Atom Loss. *Phys. Chem. Chem. Phys.* **2004**, *6*, 2628–2632.

(175) Talbot, F. O.; Tabarin, T.; Antoine, R.; Broyer, M.; Dugourd, P. Photodissociation Spectroscopy of Trapped Protonated Tryptophan. *J. Chem. Phys.* **2005**, *122*, 074310.

(176) Boyarkin, O. V; Mercier, S. R.; Kamariotis, A.; Rizzo, T. R. Electronic Spectroscopy of Cold, Protonated Tryptophan and Tyrosine. *J. Am. Chem. Soc.* **2006**, *128*, 2816–2817.

(177) Lepère, V.; Lucas, B.; Barat, M.; Fayeton, J. A.; Picard, Y. J.; Jouvet, C.; Çarçabal, P.; Nielsen, I.; Dedonder-Lardeux, C.; Grégoire, G.; et al. Characterization of Neutral Fragments Issued from the Photodissociation of Protonated Tryptophane. *Phys. Chem. Chem. Phys.* **2007**, *9*, 5330.

(178) Lucas, B.; Barat, M.; Fayeton, J. A.; Perot, M.; Jouvet, C.; Grégoire, G.; Brondsted Nielsen, S. Mechanisms of Photoinduced C_α-C_β Bond Breakage in Protonated Aromatic Amino Acids. *J. Chem. Phys.* **2008**, *128*, 164302.

(179) Kadhane, U.; Pérot, M.; Lucas, B.; Barat, M.; Fayeton, J. A.; Jouvet, C.; Ehlerding, A.; Kirketerp, M.-B. S.; Nielsen, S. B.; Wyer, J. A.; et al. Photodissociation of Protonated Tryptamine and Its Supramolecular Complex with 18-Crown-6 Ether: Dissociation Times and Channels, Absorption Spectra, and Excited States Calculations. *Chem. Phys. Lett.* **2009**, *480*, 57–61.

(180) Sunil Kumar, S.; Pérot-Taillandier, M.; Lucas, B.; Soorkia, S.; Barat, M.; Fayeton, J. A. UV Photodissociation Dynamics of Deprotonated 2′-Deoxyadenosine 5′-Monophosphate [5′-DAMP–H]$^-$. *J. Phys. Chem. A* **2011**, *115*, 10383–10390.

(181) Cheong, N. R.; Nam, S. H.; Park, H. S.; Ryu, S.; Song, J. K.; Park, S. M.; Pérot, M.; Lucas, B.; Barat, M.; Fayeton, J. A.; et al. Photofragmentation in Selected Tautomers of Protonated Adenine. *Phys. Chem. Chem. Phys.* **2011**, *13*, 291–295.

(182) Soorkia, S.; Dehon, C.; Kumar, S. S.; Pedrazzani, M.; Frantzen, E.; Lucas, B.; Barat, M.; Fayeton, J. A.; Jouvet, C. UV Photofragmentation Dynamics of Protonated Cystine: Disulfide Bond Rupture. *J. Phys. Chem. Lett.* **2014**, *5*, 1110–1116.

(183) Soorkia, S.; Dehon, C.; S, S. K.; Pérot-Taillandier, M.; Lucas, B.; Jouvet, C.; Barat, M.; Fayeton, J. A. Ion-Induced Dipole Interactions and Fragmentation Times: C_α-C_β Chromophore Bond Dissociation Channel. *J. Phys. Chem. Lett.* **2015**, *6*, 2070–2074.

(184) Kumar, S.; Lucas, B.; Fayeton, J.; Scuderi, D.; Alata, I.; Broquier, M.; Barbu-Debus, K. Le; Lepère, V.; Zehnacker, A. Photofragmentation Mechanisms in Protonated Chiral Cinchona Alkaloids. *Phys. Chem. Chem. Phys.* **2016**, *18*, 22668–22677.

(185) El Aribi, H.; Orlova, G.; Hopkinson, A. C.; Siu, K. W. M. Gas-Phase Fragmentation Reactions of Protonated Aromatic Amino Acids: Concomitant and Consecutive Neutral Eliminations and Radical Cation Formations. *J. Phys. Chem. A* **2004**, *108*, 3844–3853.

(186) Kadhane, U.; Andersen, J. U.; Ehlerding, A.; Hvelplund, P.; Kirketerp, M. B. S.; Lykkegaard, M. K.; Nielsen, S. B.; Panja, S.; Wyer, J. A.; Zettergren, H. Photodissociation of Protonated Tryptophan and Alteration of Dissociation Pathways by Complexation with Crown Ether. *J. Chem. Phys.* **2008**, *129*, 1–6.

(187) Kang, H.; Jouvet, C.; Dedonder-Lardeux, C.; Martrenchard, S.; Grégoire, G.; Desfrançois, C.; Schermann, J.-P.; Barat, M.; Fayeton, J. A. Ultrafast Deactivation Mechanisms of Protonated Aromatic Amino Acids Following UV Excitation. *Phys. Chem. Chem. Phys.* **2005**, *7*, 394.

(188) Kang, H.; Dedonder-Lardeux, C.; Jouvet, C.; Grégoire, G.; Desfrançois, C.; Schermann, J.-P.; Barat, M.; Fayeton, J. A. Control of Bond-Cleaving Reactions of Free Protonated Tryptophan Ion by Femtosecond Laser Pulses. *J. Phys. Chem. A* **2005**, *109*, 2417–2420.

(189) Grégoire, G.; Jouvet, C.; Dedonder, C.; Sobolewski, A. L. Ab Initio Study of the Excited-State Deactivation Pathways of Protonated Tryptophan and Tyrosine. *J. Am. Chem. Soc.* **2007**, *129*, 6223–6231.

(190) Grégoire, G.; Lucas, B.; Barat, M.; Fayeton, J. A.; Dedonder-Lardeux, C.; Jouvet, C. UV Photoinduced Dynamics in Protonated Aromatic Amino Acid. *Eur. Phys. J. D* **2009**, *51*, 109–116.

(191) Stearns, J. A.; Mercier, S.; Seaiby, C.; Guidi, M.; Boyarkin, O. V.; Rizzo, T. R. Conformation-Specific Spectroscopy and Photodissociation of Cold, Protonated Tyrosine and Phenylalanine. *J. Am. Chem. Soc.* **2007**, *129*, 11814–11820.

(192) Choi, C. M.; Choi, D. H.; Kim, N. J.; Heo, J. Effective Temperature of Protonated Tyrosine Ions in a Cold Quadrupole Ion Trap. *Int. J. Mass Spectrom.* **2012**, *314*, 18–21.

(193) Redwine, J. G.; Davis, Z. a.; Burke, N. L.; Oglesbee, R. a.; McLuckey, S. a.; Zwier, T. S. A Novel Ion Trap Based Tandem Mass Spectrometer for the Spectroscopic Study of Cold Gas Phase Polyatomic Ions. *Int. J. Mass Spectrom.* **2013**, *348*, 9–14.

(194) Ishiuchi, S.; Wako, H.; Kato, D.; Fujii, M. High-Cooling-Efficiency Cryogenic Quadrupole Ion Trap and UV-UV Hole Burning Spectroscopy of Protonated Tyrosine. *J. Mol. Spectrosc.* **2017**, *332*, 45–51.

(195) Soorkia, S.; Broquier, M.; Grégoire, G. Conformer- and Mode-Specific Excited State Lifetimes of Cold Protonated Tyrosine Ions. *J. Phys. Chem. Lett.* **2014**, *5*, 4349–4355.

(196) Noble, J. A.; Dedonder-Lardeux, C.; Mascetti, J.; Jouvet, C. Electronic Spectroscopy of Protonated 1-Aminopyrene in a Cold Ion Trap. *Chem. - An Asian J.* **2017**, *12*, 1523–1531.

(197) Féraud, G.; Broquier, M.; Dedonder, C.; Jouvet, C.; Grégoire, G.; Soorkia, S. Excited State Dynamics of Protonated Phenylalanine and Tyrosine: Photo-Induced Reactions Following Electronic Excitation. *J. Phys. Chem. A* **2015**, *119*, 5914–5924.

(198) O'Hair, R. a; Broughton, P. S.; Styles, M. L.; Frink, B. T.; Hadad, C. M. The Fragmentation Pathways of Protonated Glycine: A Computational Study. *J. Am. Soc. Mass Spectrom.* **2000**, *11*, 687–696.

(199) Grégoire, G.; Kang, H.; Dedonder-Lardeux, C.; Jouvet, C.; Desfrançois, C.; Onidas, D.; Lepere, V.; Fayeton, J. A. Statistical vs. Non-Statistical Deactivation Pathways in the UV Photo-Fragmentation of Protonated Tryptophan–Leucinedipeptide. *Phys. Chem. Chem. Phys.* **2006**, *8*, 122–128.

(200) Nolting, D.; Schultz, T.; Hertel, I. V.; Weinkauf, R. Excited State Dynamics and Fragmentation Channels of the Protonated Dipeptide H_2N-Leu-Trp-COOH. *Phys. Chem. Chem. Phys.* **2006**, *8*, 5247.

(201) Grégoire, G.; Dedonder-Lardeux, C.; Jouvet, C.; Desfrançois, C.; Fayeton, J. A. Ultrafast Excited State Dynamics in Protonated GWG and GYG Tripeptides. *Phys. Chem. Chem. Phys.* **2007**, *9*, 78–82.

(202) Fujihara, A.; Matsumoto, H.; Shibata, Y.; Ishikawa, H.; Fuke, K. Photodissociation and Spectroscopic Study of Cold Protonated Dipeptides. *J. Phys. Chem. A* **2008**, *112*, 1457–1463.

(203) Stearns, J. A.; Guidi, M.; Boyarkin, O. V.; Rizzo, T. R. Conformation-Specific Infrared and Ultraviolet Spectroscopy of Tyrosine-Based Protonated Dipeptides. *J. Chem. Phys.* **2007**,

127, 154322.

(204) Rizzo, T. R.; Stearns, J. A.; Boyarkin, O. V. Spectroscopic Studies of Cold, Gas-Phase Biomolecular Ions. *Int. Rev. Phys. Chem.* **2009**, *28*, 481–515.

(205) Stearns, J. a; Seaiby, C.; Boyarkin, O. V; Rizzo, T. R. Spectroscopy and Conformational Preferences of Gas-Phase Helices. *Phys. Chem. Chem. Phys.* **2009**, *11*, 125–132.

(206) Antoine, R.; Broyer, M.; Chamot-Rooke, J.; Dedonder, C.; Desfrançois, C.; Dugourd, P.; Grégoire, G.; Jouvet, C.; Onidas, D.; Poulain, P.; et al. Comparison of the Fragmentation Pattern Induced by Collisions, Laser Excitation and Electron Capture. Influence of the Initial Excitation. *Rapid Commun. Mass Spectrom.* **2006**, *20*, 1648–1652.

(207) Swendsen, R. H.; Wang, J. S. Replica Monte Carlo Simulation of Spin-Glasses. *Phys. Rev. Lett.* **1986**, *57*, 2607–2609.

(208) Hansmann, U. H. E. Parallel Tempering Algorithm for Conformational Studies of Biological Molecules. *Chem. Phys. Lett.* **1997**, *281*, 140–150.

(209) Cornell, W. D.; Cieplak, P.; Bayly, C. I.; Gould, I. R.; Merz, K. M.; Ferguson, D. M.; Spellmeyer, D. C.; Fox, T.; Caldwell, J. W.; Kollman, P. A. A Second Generation Force Field for the Simulation of Proteins, Nucleic Acids, and Organic Molecules. *J. Am. Chem. Soc.* **1995**, *117*, 5179–5197.

(210) Mercier, S. R.; Boyarkin, O. V.; Kamariotis, A.; Guglielmi, M.; Tavernelli, I.; Cascella, M.; Rothlisberger, U.; Rizzo, T. R. Microsolvation Effects on the Excited-State Dynamics of Protonated Tryptophan. *J. Am. Chem. Soc.* **2006**, *128*, 16938–16943.

(211) Fujihara, A.; Sato, T.; Hayakawa, S. Enantiomer-Selective Ultraviolet Photolysis of Temperature-Controlled Protonated Tryptophan on a Chiral Crown Ether in the Gas Phase.

Chem. Phys. Lett. **2014**, *610–611*, 228–233.

(212) Wyer, J. A.; Ehlerding, A.; Zettergren, H.; Kirketerp, M.-B. S.; Brøndsted Nielsen, S. Tagging of Protonated Ala-Tyr and Tyr-Ala by Crown Ether Prevents Direct Hydrogen Loss and Proton Mobility after Photoexcitation: Importance for Gas-Phase Absorption Spectra, Dissociation Lifetimes, and Channels. *J. Phys. Chem. A* **2009**, *113*, 9277–9285.

(213) Ehlerding, A.; Wyer, J. A.; Zettergren, H.; Kirketerp, M.-B. S.; Nielsen, S. B. UV Photodissociation of Protonated Gly-Trp and Trp-Gly Dipeptides and Their Complexes with Crown Ether in an Electrostatic Ion Storage Ring. *J. Phys. Chem. A* **2010**, *114*, 299–303.

(214) Park, S.; Ahn, W.-K.; Lee, S.; Han, S. Y.; Rhee, B. K.; Oh, H. Bin. Ultraviolet Photodissociation at 266 Nm of Phosphorylated Peptide Cations. *Rapid Commun. Mass Spectrom.* **2009**, *23*, 3609–3620.

(215) Tabarin, T.; Antoine, R.; Broyer, M.; Dugourd, P. Specific Photodissociation of Peptides with Multi-Stage Mass Spectrometry. *Rapid Commun. Mass Spectrom.* **2005**, *19*, 2883–2892.

(216) Lemoine, J.; Tabarin, T.; Antoine, R.; Broyer, M.; Dugourd, P. UV Photodissociation of Phospho-Seryl-Containing Peptides: Laser Stabilization of the Phospho-Seryl Bond with Multistage Mass Spectrometry. *Rapid Commun. Mass Spectrom.* **2006**, *20*, 507–511.

(217) Joly, L.; Antoine, R.; Broyer, M.; Dugourd, P.; Lemoine, J. Specific UV Photodissociation of Tyrosyl-Containing Peptides in Multistage Mass Spectrometry. *J. Mass Spectrom.* **2007**, *42*, 818–824.

(218) Dehon, C.; Soorkia, S.; Pedrazzani, M.; Jouvet, C.; Barat, M.; Fayeton, J. A.; Lucas, B. Photofragmentation at 263 Nm of Small Peptides Containing Tyrosine: The Role of the Charge

Transfer on CO. *Phys. Chem. Chem. Phys.* **2013**, *15*, 8779.

(219) Stearns, J. A.; Boyarkin, O. V.; Rizzo, T. R. Effects of N-Terminus Substitution on the Structure and Spectroscopy of Gas-Phase Helices. *Chim. Int. J. Chem.* **2008**, *62*, 240–243.

(220) Kopysov, V.; Makarov, A.; Boyarkin, O. V. Nonstatistical UV Fragmentation of Gas-Phase Peptides Reveals Conformers and Their Structural Features. *J. Phys. Chem. Lett.* **2016**, *7*, 1067–1071.

(221) Kopysov, V.; Nagornova, N. S.; Boyarkin, O. V. Identification of Tyrosine-Phosphorylated Peptides Using Cold Ion Spectroscopy. *J. Am. Chem. Soc.* **2014**, *136*, 9288–9291.

(222) DeBlase, A. F.; Harrilal, C. P.; Lawler, J. T.; Burke, N. L.; McLuckey, S. A.; Zwier, T. S. Conformation-Specific Infrared and Ultraviolet Spectroscopy of Cold $[YAPAA+H]^+$ and $[YGPAA+H]^+$ Ions: A Stereochemical "Twist" on the β-Hairpin Turn. *J. Am. Chem. Soc.* **2017**, *139*, 5481–5493.

(223) Burke, N. L.; Redwine, J. G.; Dean, J. C.; McLuckey, S. A.; Zwier, T. S. UV and IR Spectroscopy of Cold Protonated Leucine Enkephalin. *Int. J. Mass Spectrom.* **2015**, *378*, 196–205.

(224) Dian, B. C.; Longarte, A.; Zwier, T. S. Conformational Dynamics in a Dipeptide after Single-Mode Vibrational Excitation. *Science.* **2002**, *296*, 2369–2373.

(225) Guglielmi, M.; Doemer, M.; Tavernelli, I.; Rothlisberger, U. Photodynamics of Lys^+-Trp Protein Motifs: Hydrogen Bonds Ensure Photostability. *Faraday Discuss.* **2013**, *163*, 189–203.

(226) Guidi, M.; Lorenz, U. J.; Papadopoulos, G.; Boyarkin, O. V; Rizzo, T. R. Spectroscopy

of Protonated Peptides Assisted by Infrared Multiple Photon Excitation. *J. Phys. Chem. A* **2009**, *113*, 797–799.

(227) Papadopoulos, G.; Svendsen, A.; Boyarkin, O. V; Rizzo, T. R. Conformational Distribution of Bradykinin [Bk + 2H]$^{2+}$ Revealed by Cold Ion Spectroscopy Coupled with FAIMS. *J. Am. Soc. Mass Spectrom.* **2012**, *23*, 1173–1181.

(228) Zabuga, A. V.; Kamrath, M. Z.; Boyarkin, O. V.; Rizzo, T. R. Fragmentation Mechanism of UV-Excited Peptides in the Gas Phase. *J. Chem. Phys.* **2014**, *141*, 154309.

(229) Scholes, G. D. Long Range Resonance Energy Transfer in Molecular Systems. *Annu. Rev. Phys. Chem.* **2003**, *54*, 57–87.

(230) Medintz, I. L.; Mattoussi, H. Quantum Dot-Based Resonance Energy Transfer and Its Growing Application in Biology. *Phys. Chem. Chem. Phys.* **2009**, *11*, 17–45.

(231) Andrews, D. L.; Curutchet, C.; Scholes, G. D. Resonance Energy Transfer: Beyond the Limits. *Laser Photon. Rev.* **2011**, *5*, 114–123.

(232) Curutchet, C.; Mennucci, B. Quantum Chemical Studies of Light Harvesting. *Chem. Rev.* **2017**, *117*, 294–343.

(233) Neidigh, J. W.; Fesinmeyer, R. M.; Andersen, N. H. Designing a 20-Residue Protein. *Nat. Struct. Biol.* **2002**, *9*, 425–430.

(234) Hudgins, R. R.; Huang, F.; Gramlich, G.; Nau, W. M. A Fluorescence-Based Method for Direct Measurement of Submicrosecond Intramolecular Contact Formation in Biopolymers: An Exploratory Study with Polypeptides. *J. Am. Chem. Soc.* **2002**, *124*, 556–564.

(235) Vaiana, A. C.; Neuweiler, H.; Schulz, A.; Wolfrum, J.; Sauer, M.; Smith, J. C. Fluorescence Quenching of Dyes by Tryptophan: Interactions at Atomic Detail from

Combination of Experiment and Computer Simulation. *J. Am. Chem. Soc.* **2003**, *125*, 14564–14572.

(236) Iavarone, A. T.; Parks, J. H. Conformational Change in Unsolvated Trp-Cage Protein Probed by Fluorescence. *J. Am. Chem. Soc.* **2005**, *127*, 8606–8607.

(237) Iavarone, A. T.; Duft, D.; Parks, J. H. Shedding Light on Biomolecule Conformational Dynamics Using Fluorescence Measurements of Trapped Ions. *J. Phys. Chem. A* **2006**, *110*, 12714–12727.

(238) Zhou, R. Trp-Cage: Folding Free Energy Landscape in Explicit Water. *Proc. Natl. Acad. Sci. U. S. A.* **2003**, *100*, 13280–13285.

(239) Iavarone, A. T.; Meinen, J.; Schulze, S.; Parks, J. H. Fluorescence Probe of Polypeptide Conformational Dynamics in Gas Phase and in Solution. *Int. J. Mass Spectrom.* **2006**, *253*, 172–180.

(240) Shi, X.; Duft, D.; Parks, J. H. Fluorescence Quenching Induced by Conformational Fluctuations in Unsolvated Polypeptides. *J. Phys. Chem. B* **2008**, *112*, 12801–12815.

(241) Shi, X.; Parks, J. H. Fluorescence Lifetime Probe of Biomolecular Conformations. *J. Am. Soc. Mass Spectrom.* **2010**, *21*, 707–718.

(242) Tinnefeld, P.; Sauer, M. Branching Out of Single-Molecule Fluorescence Spectroscopy: Challenges for Chemistry and Influence on Biology. *Angew. Chemie Int. Ed.* **2005**, *44*, 2642–2671.

(243) Michalet, X.; Weiss, S.; Jäger, M. Single-Molecule Fluorescence Studies of Protein Folding and Conformational Dynamics. *Chem. Rev.* **2006**, *106*, 1785–1813.

(244) Schuler, B.; Eaton, W. A. Protein Folding Studied by Single-Molecule FRET. *Curr.*

Opin. Struct. Biol. **2008**, *18*, 16–26.

(245) Förster, T. Zwischenmolekulare Energiewanderung Und Fluoreszenz. *Ann. Phys.* **1948**, *437*, 55–75.

(246) Stryer, L.; Haugland, R. P. Energy Transfer: A Spectroscopic Ruler. *Proc. Natl. Acad. Sci. U. S. A.* **1967**, *58*, 719–726.

(247) Talbot, F. O.; Rullo, A.; Yao, H.; Jockusch, R. A. Fluorescence Resonance Energy Transfer in Gaseous, Mass-Selected Polyproline Peptides. *J. Am. Chem. Soc.* **2010**, *132*, 16156–16164.

(248) Stryer, L. Fluorescence Energy Transfer as a Spectroscopic Ruler. *Annu. Rev. Biochem.* **1978**, *47*, 819–846.

(249) Schuler, B.; Lipman, E. A.; Steinbach, P. J.; Kumke, M.; Eaton, W. A. Polyproline and the "Spectroscopic Ruler" Revisited with Single-Molecule Fluorescence. *Proc. Natl. Acad. Sci.* **2005**, *102*, 2754–2759.

(250) Kuemin, M.; Schweizer, S.; Ochsenfeld, C.; Wennemers, H. Effects of Terminal Functional Groups on the Stability of the Polyproline II Structure: A Combined Experimental and Theoretical Study. *J. Am. Chem. Soc.* **2009**, *131*, 15474–15482.

(251) Czar, M. F.; Jockusch, R. A. Sensitive Probes of Protein Structure and Dynamics in Well-Controlled Environments: Combining Mass Spectrometry with Fluorescence Spectroscopy. *Curr. Opin. Struct. Biol.* **2015**, *34*, 123–134.

(252) Frankevich, V.; Martinez-Lozano Sinues, P.; Barylyuk, K.; Zenobi, R. Ion Mobility Spectrometry Coupled to Laser-Induced Fluorescence. *Anal. Chem.* **2013**, *85*, 39–43.

(253) Uteschil, F.; Kuklya, A.; Kerpen, K.; Marks, R.; Telgheder, U. Time-of-Flight Ion

Mobility Spectrometry in Combination with Laser-Induced Fluorescence Detection System. *Anal. Bioanal. Chem.* **2017**, *409*, 6279–6286.

(254) Daly, S.; Poussigue, F.; Simon, A.-L.; MacAleese, L.; Bertorelle, F.; Chirot, F.; Antoine, R.; Dugourd, P. Action-FRET: Probing the Molecular Conformation of Mass-Selected Gas-Phase Peptides with Förster Resonance Energy Transfer Detected by Acceptor-Specific Fragmentation. *Anal. Chem.* **2014**, *86*, 8798–8804.

(255) Bouakil, M.; Kulesza, A.; Daly, S.; MacAleese, L.; Antoine, R.; Dugourd, P. Visible Multiphoton Dissociation of Chromophore-Tagged Peptides. *J. Am. Soc. Mass Spectrom.* **2017**, *28*, 2181–2188.

(256) Daly, S.; Kulesza, A.; Poussigue, F.; Simon, A.-L.; Choi, C. M.; Knight, G.; Chirot, F.; MacAleese, L.; Antoine, R.; Dugourd, P. Conformational Changes in Amyloid-Beta$_{(12–28)}$ Alloforms Studied Using Action-FRET, IMS and Molecular Dynamics Simulations. *Chem. Sci.* **2015**, *6*, 5040–5047.

(257) Kulesza, A.; Daly, S.; MacAleese, L.; Antoine, R.; Dugourd, P. Structural Exploration and Förster Theory Modeling for the Interpretation of Gas-Phase FRET Measurements: Chromophore-Grafted Amyloid-*β* Peptides. *J. Chem. Phys.* **2015**, *143*, 025101.

(258) Kulesza, A.; Daly, S.; Choi, C. M.; Simon, A.-L.; Chirot, F.; MacAleese, L.; Antoine, R.; Dugourd, P. The Structure of Chromophore-Grafted Amyloid-$\beta_{12–28}$ Dimers in the Gas-Phase: FRET-Experiment Guided Modelling. *Phys. Chem. Chem. Phys.* **2016**, *18*, 9061–9069.

(259) Daly, S.; MacAleese, L.; Dugourd, P.; Chirot, F. Combining Structural Probes in the Gas Phase - Ion Mobility-Resolved Action-FRET. *J. Am. Soc. Mass Spectrom.* **2018**, *29*, 133–139.

(260) Penzkofer, A.; Lu, Y. Fluorescence Quenching of Rhodamine 6G in Methanol at High Concentration. *Chem. Phys.* **1986**, *103*, 399–405.

(261) Bindhu, C. V.; Harilal, S. S. Effect of the Excitation Source on the Quantum-Yield Measurements of Rhodamine B Laser Dye Studied Using Thermal-Lens Technique. *Anal. Sci.* **2001**, *17*, 141–144.

(262) Valdes-Aguilera, O.; Neckers, D. C. Aggregation Phenomena in Xanthene Dyes. *Acc. Chem. Res.* **1989**, *22*, 171–177.

(263) Setiawan, D.; Kazaryan, A.; Martoprawiro, M. A.; Filatov, M. A First Principles Study of Fluorescence Quenching in Rhodamine B Dimers: How Can Quenching Occur in Dimeric Species? *Phys. Chem. Chem. Phys.* **2010**, *12*, 11238.

(264) Daly, S.; Choi, C. M.; Chirot, F.; MacAleese, L.; Antoine, R.; Dugourd, P. Action-Self Quenching: Dimer-Induced Fluorescence Quenching of Chromophores as a Probe for Biomolecular Structure. *Anal. Chem.* **2017**, *89*, 4604–4610.

(265) Stadtman, E. R.; Van Remmen, H.; Richardson, A.; Wehr, N. B.; Levine, R. L. Methionine Oxidation and Aging. *Biochim. Biophys. Acta - Proteins Proteomics* **2005**, *1703*, 135–140.

(266) Kumar, S. S.; Lucas, B.; Soorkia, S.; Barat, M.; Fayeton, J. A. Cα–Cβ Chromophore Bond Dissociation in Protonated Tyrosine-Methionine, Methionine-Tyrosine, Tryptophan-Methionine, Methionine-Tryptophan and Their Sulfoxide Analogs. *Phys. Chem. Chem. Phys.* **2012**, *14*, 10225.

(267) Hendricks, N. G.; Lareau, N. M.; Stow, S. M.; McLean, J. A.; Julian, R. R. Bond-Specific Dissociation Following Excitation Energy Transfer for Distance Constraint

Determination in the Gas Phase. *J. Am. Chem. Soc.* **2014**, *136*, 13363–13370.

(268) Dexter, D. L. A Theory of Sensitized Luminescence in Solids. *J. Chem. Phys.* **1953**, *21*, 836–850.

(269) Hendricks, N. G.; Julian, R. R. Characterizing Gaseous Peptide Structure with Action-EET and Simulated Annealing. *Phys. Chem. Chem. Phys.* **2015**, *17*, 25822–25827.

(270) Hendricks, N. G.; Julian, R. R. Two-Step Energy Transfer Enables Use of Phenylalanine in Action-EET for Distance Constraint Determination in Gaseous Biomolecules. *Chem. Commun.* **2015**, *51*, 12720–12723.

(271) Kopysov, V.; Boyarkin, O. V. Resonance Energy Transfer Relates the Gas-Phase Structure and Pharmacological Activity of Opioid Peptides. *Angew. Chemie Int. Ed.* **2016**, *55*, 689–692.

(272) Muñoz-Losa, A.; Curutchet, C.; Krueger, B. P.; Hartsell, L. R.; Mennucci, B. Fretting about FRET: Failure of the Ideal Dipole Approximation. *Biophys. J.* **2009**, *96*, 4779–4788.

(273) Scutelnic, V.; Prlj, A.; Zabuga, A.; Corminboeuf, C.; Rizzo, T. R. Infrared Spectroscopy as a Probe of Electronic Energy Transfer. *J. Phys. Chem. Lett.* **2018**, *9*, 3217–3223.

(274) Lobsiger, S.; Etinski, M.; Blaser, S.; Frey, H.-M.; Marian, C.; Leutwyler, S. Intersystem Crossing Rates of S 1 State Keto-Amino Cytosine at Low Excess Energy. *J. Chem. Phys.* **2015**, *143*, 234301.

(275) Broquier, M.; Soorkia, S.; Pino, G.; Dedonder-Lardeux, C.; Jouvet, C.; Grégoire, G. Excited State Dynamics of Cold Protonated Cytosine Tautomers: Characterization of Charge Transfer, Intersystem Crossing, and Internal Conversion Processes. *J. Phys. Chem. A* **2017**, *121*, 6429–6439.

(276) Broquier, M.; Soorkia, S.; Dedonder-Lardeux, C.; Jouvet, C.; Theulé, P.; Grégoire, G. Twisted Intramolecular Charge Transfer in Protonated Amino Pyridine. *J. Phys. Chem. A* **2016**, *120*, 3797–3809.

(277) Soorkia, S.; Broquier, M.; Grégoire, G. Multiscale Excited State Lifetimes of Protonated Dimethyl Aminopyridines. *Phys. Chem. Chem. Phys.* **2016**, *18*, 23785–23794.

(278) MacAleese, L.; Hermelin, S.; Hage, K. El; Chouzenoux, P.; Kulesza, A.; Antoine, R.; Bonacina, L.; Meuwly, M.; Wolf, J.-P.; Dugourd, P. Sequential Proton Coupled Electron Transfer (PCET): Dynamics Observed over 8 Orders of Magnitude in Time. *J. Am. Chem. Soc.* **2016**, *138*, 4401–4407.

(279) Meng, Q.; Meyer, H. D. A Multilayer MCTDH Study on the Full Dimensional Vibronic Dynamics of Naphthalene and Anthracene Cations. *J. Chem. Phys.* **2013**, *138*, 014313.

(280) Huix-Rotllant, M.; Burghardt, I.; Ferré, N. Population of Triplet States in Acetophenone: A Quantum Dynamics Perspective. *Comptes Rendus Chim.* **2016**, *19*, 50–56.

(281) Montavon, G.; Rupp, M.; Gobre, V.; Vazquez-Mayagoitia, A.; Hansen, K.; Tkatchenko, A.; Müller, K. R.; Anatole Von Lilienfeld, O. Machine Learning of Molecular Electronic Properties in Chemical Compound Space. *New J. Phys.* **2013**, *15*, 095003.

(282) Häse, F.; Kreisbeck, C.; Aspuru-Guzik, A. Machine Learning for Quantum Dynamics: Deep Learning of Excitation Energy Transfer Properties. *Chem. Sci.* **2017**, *8*, 8419–8426.

(283) Hu, D.; Xie, Y.; Li, X.; Li, L.; Lan, Z. Inclusion of Machine Learning Kernel Ridge Regression Potential Energy Surfaces in On-the-Fly Nonadiabatic Molecular Dynamics Simulation. *J. Phys. Chem. Lett.* **2018**, *9*, 2725–2732.

(284) Chen, W. K.; Liu, X. Y.; Fang, W. H.; Dral, P. O.; Cui, G. Deep Learning for

Nonadiabatic Excited-State Dynamics. *J. Phys. Chem. Lett.* **2018**, *9*, 6702–6708.

(285) Dral, P. O.; Barbatti, M.; Thiel, W. Nonadiabatic Excited-State Dynamics with Machine Learning. *J. Phys. Chem. Lett.* **2018**, *9*, 5660–5663.

(286) Gastegger, M.; Behler, J.; Marquetand, P. Machine Learning Molecular Dynamics for the Simulation of Infrared Spectra. *Chem. Sci.* **2017**, *8*, 6924–6935.

(287) Reed, K. J.; Zimmerman, A. H.; Andersen, H. C.; Brauman, J. I. Cross Sections for Photodetachment of Electrons from Negative Ions near Threshold. *J. Chem. Phys.* **1976**, *64*, 1368–1375.

(288) Tian, Z.; Wang, X. Bin; Wang, L. S.; Kass, S. R. Are Carboxyl Groups the Most Acidic Sites in Amino Acids? Gas-Phase Acidities, Photoelectron Spectra, and Computations on Tyrosine, p-Hydroxybenzoic Acid, and Their Conjugate Bases. *J. Am. Chem. Soc.* **2009**, *131*, 1174–1181.

(289) Compagnon, I.; Allouche, A. R.; Bertorelle, F.; Antoine, R.; Dugourd, P. Photodetachment of Tryptophan Anion: An Optical Probe of Remote Electron. *Phys. Chem. Chem. Phys.* **2010**, *12*, 3399–3403.

(290) Forbes, M. W.; Jockusch, R. A. Deactivation Pathways of an Isolated Green Fluorescent Protein Model Chromophore Studied by Electronic Action Spectroscopy. *J. Am. Chem. Soc.* **2009**, *131*, 17038–17039.

(291) Deng, S. H. M.; Kong, X. Y.; Zhang, G.; Yang, Y.; Zheng, W. J.; Sun, Z. R.; Zhang, D. Q.; Wang, X. Bin. Vibrationally Resolved Photoelectron Spectroscopy of the Model GFP Chromophore Anion Revealing the Photoexcited S_1 state Being Both Vertically and Adiabatically Bound against the Photodetached D_0 continuum. *J. Phys. Chem. Lett.* **2014**, *5*,

2155–2159.

(292) Mooney, C. R. S.; Horke, D. A.; Chatterley, A. S.; Simperler, A.; Fielding, H. H.; Verlet, J. R. R. Taking the Green Fluorescence out of the Protein: Dynamics of the Isolated GFP Chromophore Anion. *Chem. Sci.* **2013**, *4*, 921–927.

(293) Henley, A.; Fielding, H. H. Anion Photoelectron Spectroscopy of Protein Chromophores. *Int. Rev. Phys. Chem.* **2019**, *38*, 1–34.

(294) Stolow, A.; Bragg, A. E.; Neumark, D. M. Femtosecond Time-Resolved Photoelectron Spectroscopy. *Chem. Rev.* **2004**, *104*, 1719–1758.

(295) Continetti, R. E.; Guo, H. Dynamics of Transient Species via Anion Photodetachment. *Chem. Soc. Rev.* **2017**, *46*, 7650–7667.

(296) Pino, G. A.; Jara-Toro, R. A.; Aranguren-Abrate, J. P.; Dedonder-Lardeux, C.; Jouvet, C. Dissociative Photodetachment: Vs. Photodissociation of Aromatic Carboxylates: The Benzoate and Naphthoate Anions. *Phys. Chem. Chem. Phys.* **2019**, *21*, 1797–1804.

(297) Joly, L.; Antoine, R.; Allouche, A. R.; Dugourd, P. Formation and Spectroscopy of a Tryptophan Radical Containing Peptide in the Gas Phase. *J. Am. Chem. Soc.* **2008**, *130*, 13832–13833.

(298) Antoine, R.; Joly, L.; Allouche, a. R.; Broyer, M.; Lemoine, J.; Dugourd, P. Electron Photodetachment of Trapped Doubly Deprotonated Angiotensin Peptides. UV Spectroscopy and Radical Recombination. *Eur. Phys. J. D* **2009**, *51*, 117–124.

(299) Brunet, C.; Antoine, R.; Dugourd, P.; Canon, F.; Giuliani, A.; Nahon, L. Formation and Fragmentation of Radical Peptide Anions: Insights from Vacuum Ultra Violet Spectroscopy. *J. Am. Soc. Mass Spectrom.* **2012**, *23*, 274–281.

(300) Bagheri-Majdi, E.; Ke, Y.; Orlova, G.; Chu, I. K.; Hopkinson, A. C.; Siu, K. W. M. Copper-Mediated Peptide Radical Ions in the Gas Phase. *J. Phys. Chem. B* **2004**, *108*, 11170–11181.

(301) Cordes, M.; Köttgen, A.; Jasper, C.; Jacques, O.; Boudebous, H.; Giese, B. Influence of Amino Acid Side Chains on Long-Distance Electron Transfer in Peptides: Electron Hopping via "Stepping Stones." *Angew. Chemie - Int. Ed.* **2008**, *47*, 3461–3463.

(302) Lam, A. K. Y.; Ryzhov, V.; O'Hair, R. A. J. Mobile Protons versus Mobile Radicals: Gas-Phase Unimolecular Chemistry of Radical Cations of Cysteine-Containing Peptides. *J. Am. Soc. Mass Spectrom.* **2010**, *21*, 1296–1312.

(303) Laskin, J.; Yang, Z.; Ng, C. M. D.; Chu, I. K. Fragmentation of α-Radical Cations of Arginine-Containing Peptides. *J. Am. Soc. Mass Spectrom.* **2010**, *21*, 511–521.

TOC Graphic